



U R T Ę C I G A N Ę

**DEVELOPMENT AND
INVESTIGATION OF
TECHNOLOGY FOR THE
NANOSTRUCTURED
MEMBRANES
FABRICATION APPLIED
IN BIOENGINEERING**

DOCTORAL DISSERTATION

K a u n a s
2 0 2 4

KAUNAS UNIVERSITY OF TECHNOLOGY

URTE CIGANE

DEVELOPMENT AND INVESTIGATION OF
TECHNOLOGY FOR THE
NANOSTRUCTURED MEMBRANES
FABRICATION APPLIED IN
BIOENGINEERING

Doctoral dissertation
Technological Sciences, Mechanical Engineering (T 009)

2024, Kaunas

This doctoral dissertation was prepared at Kaunas University of Technology, Faculty of Mechanical Engineering and Design, Department of Mechanical Engineering during the period of 2020–2024. The studies were supported by the Research Council of Lithuania.

The doctoral right has been granted to Kaunas University of Technology together with Vytautas Magnus University.

Scientific Supervisor

Prof. Dr. Hab. Arvydas PALEVIČIUS (Kaunas University of Technology, Technological Sciences, Mechanical Engineering, T 009).

Scientific Advisor

Prof. Dr. Vytautas JŪRĖNAS (Kaunas University of Technology, Technological Sciences, Mechanical Engineering, T 009).

Edited by: English language editor Dr. Armandas Rumšas (Publishing House *Technologija*), Lithuanian language editor Aurelija Gražina Rukšaitė (Publishing House *Technologija*).

Dissertation Defence Board of the Mechanical Engineering Science Field:

Prof. Dr. Hab. Vytautas OSTAŠEVIČIUS (Kaunas University of Technology, Technological Sciences, Mechanical Engineering, T 009) – **chairperson**;

Prof. Dr. Regita BENDIKIENĖ (Kaunas University of Technology, Technological Sciences, Mechanical Engineering, T 009);

Prof. Dr. Vytenis JANKAUSKAS (Vytautas Magnus University, Technological Sciences, Mechanical Engineering, T 009);

Prof. Dr. Sergei KRUCHININ (National Academy of Sciences of Ukraine, Ukraine, Natural Sciences, Physics, N 002);

Dr. Sigita URBAITĖ (Kaunas University of Technology, Technological Sciences, Mechanical Engineering, T 009).

The public defence of the dissertation will be held at 12 on 7 June 2024 at the public meeting of the Dissertation Defence Board of Mechanical Engineering Science Field in Rectorate Hall at Kaunas University of Technology.

Address: K. Donelaičio 73-402, Kaunas, LT-44249, Lithuania.

Phone (+370) 608 28 527; email doktorantura@ktu.lt

The doctoral dissertation was sent out on 7 May 2024.

The doctoral dissertation is available on the internet at <http://ktu.edu> and at the library of Kaunas University of Technology (Gedimino 50, Kaunas, LT-44239, Lithuania) and at the library of Vytautas Magnus University (K. Donelaičio 52, Kaunas, LT-44244, Lithuania).

KAUNO TECHNOLOGIJOS UNIVERSITETAS

URTĖ CIGANĖ

BIOINŽINERIOJE NAUDOJAMŲ
NANOSTRUKTŪRIZUOTŲ MEMBRANŲ
GAMYBOS TECHNOLOGIJOS KŪRIMAS IR
TYRIMAS

Daktaro disertacija
Technologijos mokslai, mechanikos inžinerija (T 009)

2024, Kaunas

Disertacija rengta 2020–2024 metais Kauno technologijos universiteto Mechanikos inžinerijos ir dizaino fakultete, Mechanikos inžinerijos katedroje. Mokslinius tyrimus rėmė Lietuvos mokslo taryba.

Doktorantūros teisė Kauno technologijos universitetui suteikta kartu su Vytauto Didžiojo universitetu.

Mokslinis vadovas

prof. habil. dr. Arvydas PALEVIČIUS (Kauno technologijos universitetas, technologijos mokslai, mechanikos inžinerija, T 009).

Mokslinis konsultantas

prof. dr. Vytautas JŪRĖNAS (Kauno technologijos universitetas, technologijos mokslai, mechanikos inžinerija, T 009).

Redagavo: anglų kalbos redaktorius dr. Armandas Rumšas (leidykla „Technologija“), lietuvių kalbos redaktorė Aurelija Gražina Rukšaitė (leidykla „Technologija“).

Mechanikos inžinerijos mokslo krypties disertacijos gynimo taryba:

prof. habil. dr. Vytautas OSTAŠEVIČIUS (Kauno technologijos universitetas, technologijos mokslai, mechanikos inžinerija, T 009) – **pirmininkas**;

prof. dr. Regita BENDIKIENĖ (Kauno technologijos universitetas, technologijos mokslai, mechanikos inžinerija, T 009);

prof. dr. Vytenis JANKAUSKAS (Vytauto Didžiojo universitetas, technologijos mokslai, mechanikos inžinerija, T 009);

prof. dr. Sergei KRUCHININ (Ukrainos nacionalinė mokslo akademija, Ukraina, gamtos mokslai, fizika, N 002);

dr. Sigita URBAITĖ (Kauno technologijos universitetas, technologijos mokslai, mechanikos inžinerija, T 009).

Disertacija bus ginama viešame Mechanikos inžinerijos mokslo krypties disertacijos gynimo tarybos posėdyje 2024 m. birželio 7 d. 12 val. Kauno technologijos universiteto Rektorato salėje.

Adresas: K. Donelaičio g. 73-402, Kaunas, LT-44249, Lietuva.

Tel. (+370) 608 28 527; el. paštas doktorantura@ktu.lt

Disertacija išsiųsta 2024 m. gegužės 7 d.

Su disertacija galima susipažinti interneto svetainėje <http://ktu.edu>, Kauno technologijos universiteto bibliotekoje (Gedimino g. 50, Kaunas, LT-44239, Lietuva) ir Vytauto Didžiojo universiteto bibliotekoje (K. Donelaičio g. 52, Kaunas, LT-44244, Lietuva).

CONTENTS

LIST OF TABLES	6
LIST OF FIGURES.....	7
ABSTRACT	8
INTRODUCTION.....	9
1. LITERATURE REVIEW	16
1.1. Anodized Aluminum Oxide (AAO) Nanoporous Membranes.....	16
1.2. Electrochemical Anodization Process.....	17
1.3. Chitosan Membranes.....	18
1.4. Solvent Casting Method.....	19
1.5. Conclusions of the Chapter	19
2. REVIEW OF THE PUBLICATIONS.....	21
2.1. “Review of nanomembranes: materials, fabrications and applications in tissue engineering (bone and skin) and drug delivery systems” (scientific publication No. [A1]).....	21
2.2. “Development and Analysis of Electrochemical Reactor with Vibrating Functional Element for AAO Nanoporous Membranes Fabrication” (scientific publication No. [A2]).....	22
2.3. “Vibration-Assisted Synthesis of Nanoporous Anodic Aluminum Oxide (AAO) Membranes” (scientific publication No. [A3])	25
2.4. “A Free-Standing Chitosan Membrane Prepared by the Vibration-Assisted Solvent Casting Method” (scientific publication No. [A4]).....	27
3. CONCLUSIONS	30
4. SANTRAUKA	31
REFERENCES.....	40
PUBLICATION COPIES.....	50
CURRICULUM VITAE	110
ACKNOWLEDGMENTS.....	114
APPENDIX	115
Appendix 1. Copy of the Protocol 2023-06-22 No. ST16-T009-12.....	115
Appendix 2. Copy of the Protocol 2023-09-22 No. ST16-T009-14.....	117

LIST OF TABLES

Table 1. Contribution of the author and co-authors on the published scientific article No. [A1].....	13
Table 2. Contribution of the author and co-authors on the published scientific article No. [A2].....	13
Table 3. Contribution of the author and co-authors on the published scientific article No. [A3].....	14
Table 4. Contribution of the author and co-authors on the published scientific article No. [A4].....	14

LIST OF FIGURES

Fig. 1. Number of publications as a function of time obtained for the keyword ‘AAO membranes’	16
Fig. 2. Visual representation of the anodization process from the first publication <i>Review of nanomembranes: materials, fabrications and applications in tissue engineering (bone and skin) and drug delivery systems</i>	22
Fig. 3. Electrochemical reactor for fabrication of nanoporous AAO membranes: (a) drawing of the reactor; (b) construction of the novel design electrochemical reactor: 1 – housing of the reactor, 2 – cover of the reactor, 3 – Peltier element, 4 – gasket, 5 – aluminum sheet, 6 – vibrating element (piezoelectric ring), 7 – electrical insulating element (piezoceramic), 8 – nut M3, 9 – place for mixing device, 10 – screw M3x50, 11 – temperature sensor, 12 – hole for electrolyte filling, 13 – cooler.....	23
Fig. 4. Nanoporous AAO membranes after the two-step anodization process: (a) without frequency excitation; (b) when using 3.1 kHz frequency excitation; (c) when using 4.1 kHz frequency excitation.....	24
Fig. 5. Illustration of the two-step anodization process.....	25
Fig. 6. Images of the thickness of AAO membrane when the membranes were fabricated under different anodization conditions: (a) no frequency excitation; (b) excitation at 20 kHz; (c) excitation at 40 kHz.....	26
Fig. 7. Current-time curves recorded during the second step of anodization.....	26
Fig. 8. SEM images of: (a) chitosan membrane; (b) nanopillar of chitosan membrane (cross-section).....	28
Fig. 9. Free-standing chitosan membrane.....	29

ABSTRACT

This dissertation is based on four scientific publications. In the first article, the problem of biological incompatibility and insufficient mechanical strength of synthetic nanostructured membranes applied in the fields of bioengineering is presented. Classifications of synthetic nanomembrane materials, various technologies, and porosity are presented. Also, the application of synthetic membranes in the fields of skin and bone tissue engineering and drug delivery systems is outlined. In addition, the article is based on 143 scientific papers. It highlights the need to improve nanostructured membrane fabrication to obtain biocompatible membranes for bioengineering applications. After the analysis, the anodization technology and the solvent casting method were chosen to be improved. In the second scientific publication, a novel two-step anodization technology is presented. The anodization process is performed by using high-frequency vibrations during the first and second steps of anodization. Moreover, a novel design of the electrochemical reactor with a vibrating element for the fabrication of nanoporous anodized aluminum oxide (AAO) membranes is presented. After conducting experiments on temperature variation, reactor mixing process, and vibration, it is concluded that the electrochemical reactor meets the requirements for the anodization process. Moreover, a comparison of membranes is also presented when anodization was performed without vibration vs when the first and second modes of vibration of an aluminum plate were used. AAO membranes with 82.6 ± 10 nm pore diameters and 43% porosity using frequency excitation at 3.1 kHz and AAO membranes with 86.1 ± 10 nm pore diameters and 46% porosity using frequency excitation at 4.1 kHz were obtained. When anodization was performed without vibration, AAO membranes with a pore diameter of 55.0 ± 10 nm and a porosity of 19% were obtained. In the third publication, the anodization process, and the vibration application of 20 kHz and 40 kHz frequencies are presented. When applying 20 kHz and 40 kHz frequencies, the pore diameter, the interpore distance, and the porosity of AAO membranes were found to be constant. However, changes in the porous AAO membrane thickness were observed. A 53 μm thickness was obtained at a frequency of 20 kHz, and a membrane thickness of 59 μm was obtained at a frequency of 40 kHz. In addition, the article presents experimental results of current measurement during the anodization process. In the fourth article, an improved solvent casting method using high-frequency vibrations is described. Also, a nanopillared chitosan membrane as a template using a nanoporous AAO membrane is discussed. Three types of chitosan membranes were obtained, where the height of the nanopillars was 1007 nm, 665 nm, and 377 nm when using 1%, 2%, and 3% chitosan solutions, respectively. In addition, theoretical results of the flow speed of chitosan solutions of different concentrations into nanopores and the influence on the height of the formed nanopillars are presented. Additionally, the size of 10×10 mm of chitosan membrane mimicking the artificial skin barrier is presented. The surface areas of chitosan were obtained as 15.05 cm^2 , 10.28 cm^2 , and 6.26 cm^2 with nanopillar heights of 1007 nm, 665 nm, and 377 nm, respectively.

INTRODUCTION

Various nanostructured membranes attract immense attention because they are characterized by versatility, stability, and the ability to control the parameters, which leads to the creation of unique structures. Different nanostructured membranes are already widely used in various fields, such as water treatment, solar cells, pressure, temperature and biosensors, flexible optoelectronic devices, and medicine. Recently, a breakthrough has been observed in a number of fields of bioengineering, where nanostructured membranes were practically applied in bone and skin tissue engineering and drug delivery systems.

In terms of mechanical engineering, there is still a lack of knowledge on the mechanical strength and biocompatibility of nanostructured membranes. As the relationship between the mechanical strength and biocompatibility of nanostructured membranes depends on the material and the fabrication method, it is relevant to choose the right technology to produce these membranes and apply them commercially. When designing synthetic nanostructured membranes, it is also important to ensure an ordered internal structure, which determines the unique properties of each membrane. Various manufacturing methods are used for this purpose, such as lithography, 3D printing, chemical vapor deposition, electrospinning, etc. However, these production methods require complex and expensive equipment, and the processes themselves are difficult to control, and are often unpredictable. In this context, another well-known and commonly used alternative is the two-step aluminum anodization process, where metal oxide layers are formed electrochemically. Nanoporous AAO membrane is well known for its relatively low production cost, a large surface area, a well-ordered nanoscale structure, and the ability to change nanopore dimensions by controlling the anodization process parameters such as voltage, current, electrolyte concentration, pH, electrolyte type, and temperature. However, there are still challenges to control and ensure the same geometry parameters of membrane nanopores, as these depend not only on the fabrication technology, but also on the selected fabrication conditions. Furthermore, because strength and hardness are essential requirements for most engineering materials, AAO is classified as a ceramic with high hardness and strength. Thus, the application of nanoporous AAO for template fabrication faces another challenge – the problem of membrane brittleness. Therefore, when modelling the influence of fabrication parameters on the membrane pore geometry, it is important not only to control the membrane pore sizes, but also to produce a more flexible nanoporous membrane from brittle aluminum oxide. To fabricate a less brittle oxide, it is necessary to analyze different theoretical models which could explain the formation of AAO and provide insights into the dependence of the formation of the oxide structure on a range of parameters.

With an increasing emphasis on environmental friendliness, nanomaterial templates are attracting systematic attention, and they are one of the most promising methods for the synthesis of nanostructured membranes. Thus, the fabricated AAO membrane can be used as the template. However, there is another challenge: How to transfer the geometry of the created AAO membrane accurately and reproducibly to a

biocompatible material? For this purpose, chitosan was chosen, as it has been extensively studied and is a promising alternative for the development of biocompatible bactericidal skin barriers. In addition, chitosan is now being used in commercial wound dressings and patches. To improve the properties of chitosan membranes, the surface can be modified, or various composites can be created. Also, to use chitosan membranes to create skin bands and patches, it is important to ensure the largest possible membrane surface area. For this purpose, nanopillar surfaces, which can increase the surface area several or even dozens of times, become superior to the conventional flat surfaces. Since chitosan membranes with nanopillars are promising for the development of skin protection barriers, it is also relevant to develop a manufacturing technology which would involve control of the geometry of nanopillars.

Research related to nanostructured membranes has been receiving a lot of attention from scientists and businesspeople, which is why it is important to develop technologies and deepen knowledge about the chemical and physical processes that take place during fabrication to solve the challenges related to nanostructured membranes. This doctoral dissertation presents a novel fabrication technology of nanoporous AAO membranes using vibrations, including production processes, their parameters, and a description of the properties of the fabricated membranes. Moreover, the doctoral dissertation presents a technology for replicating the geometry of the AAO membrane in a biocompatible chitosan membrane, when nanopillars are formed on the surface of the chitosan membrane. It also presents the relationships and interactions studied between various parameters, which is achieved by presenting sets of experimental results.

The aim of the doctoral dissertation

The aim of the doctoral dissertation is to develop and investigate the fabrication technology for nanostructured membranes applied in bioengineering.

The objectives of the doctoral dissertation

In order to achieve the aim of the doctoral dissertation, the following objectives were formulated:

1. To develop a temperature-controlled vibroelectrochemical reactor for the fabrication of nanoporous AAO membranes using high-frequency excitation during the two-step electrochemical anodization process.

2. To produce nanoporous AAO membranes using high-frequency excitation during the two-step electrochemical anodization process and to evaluate the influence of vibration on the porosity, thickness, hardness, and chemical composition of the membrane.

3. To produce a chitosan membrane with nanopillars as a template using a nanoporous AAO membrane and to determine the flow rates of solutions with different concentrations of chitosan into the nanopores and the influence on the height of the formed nanopillars when vibrations are used during the solvent casting method.

4. To create a patch prototype which simulates an artificial skin barrier, characterized by biocompatibility and a larger surface area.

Research methods

A vibroelectrochemical reactor with controllable temperature was developed for the fabrication of nanoporous AAO membranes. Its working principle is based on applying vibrations during the two-step electrochemical anodization process in oxalic acid. The compatibility of the reactor temperature, the mixing process, and vibrations were evaluated by experimental studies. A *Hitachi S-3400N* scanning electron microscope (*Hitachi Ltd.*, Tokyo, Japan) with an integrated *Bruker* energy dispersive X-ray spectroscopy system was used to determine the pore geometry and surface chemical composition of the produced AAO membranes. The resulting images were analyzed using the *ImageJ* data processing program. The *Vickers* indentations with a diamond tip (*Micro Vickers Hardness Testing Machine: HM-200*, Mitutoyo, Japan) was used to measure the surface microhardness of AAO membranes. *Ansys 17.0* (*Ansys®*, Pennsylvania, United States) and *COMSOL Multiphysics 5.4* (*COMSOL®*, Burlington, United States) were used to determine the theoretical vibration modes of the AAO membrane. The precise real-time instrument for surface measurement (PRISM) holographic interferometric system (*Hytec*, Los Alamos, United States) was used to monitor the experimental vibration modes of the membranes.

As the next step, chitosan membranes were produced by solvent casting on the AAO template by using solutions of various concentrations. A developed vibrostand was used for fabrication. A *Hitachi S-3400N* (*Hitachi Ltd.*, Tokyo, Japan) scanning electron microscope and *ImageJ* image analysis software were used to determine the surface geometry of the produced chitosan membranes. *COMSOL Multiphysics 5.4* (*COMSOL®*, Burlington, United States) was used to evaluate the theoretical flow rates of chitosan solutions of different concentrations into the pores.

The research was carried out at the Faculty of Mechanical Engineering and Design (Kaunas University of Technology, Kaunas, Lithuania), Lithuanian Energy Institute (Kaunas, Lithuania), and UAB Hella Lithuania (Quality Laboratory, Karmėlava, Lithuania).

Scientific novelty of the doctoral dissertation

1 The impact of vibrations applied during fabrication on the porosity, thickness, hardness, and chemical composition of the AAO membranes has been evaluated during the two-step electrochemical anodization process.

2. The flow rates of solutions of various concentrations of chitosan into the nanopores and the influence of the concentration on the height of the formed nanopillars have been determined when vibrations were used during the solvent casting method.

Statements presented for the defense

1. The porosity, thickness, and hardness of the nanoporous AAO membrane can be controlled by using high-frequency excitation without changing the chemical composition of the membrane surface.

2. During the electrochemical anodization process, the use of high-frequency excitation ensures the electrolyte mixing process along the nanopore, which leads to

the renewal of the liquid flow within the pore. In this way, efficient and fast mixing of the electrolyte flow in the nanopore is ensured.

3. In the production of chitosan membranes with nanopillars, high-frequency vibrations are used to ensure a larger surface area of the membrane and to control the height of the nanopillars.

Practical value

1. A temperature-controlled vibroelectrochemical reactor has been developed for the fabrication of nanoporous AAO membranes. Furthermore, the manufactured reactor could be used for other processes, where control over the temperature, voltage, and liquid mixing process is required.

2. The technology of nanoporous AAO membranes has been developed and described, which allows the required geometry of nanopores to be ensured by controlling the values of temperature, voltage, or vibration frequency.

3. Theoretical models of membrane vibration modes, electrolyte flow into nanopore using vibrations, and flow of a chitosan solution of various concentrations into nanopores using vibrations have been developed, which provides valuable information and knowledge for the development of further technological processes.

4. A prototype of a patch which mimics an artificial skin barrier has been created. It has been characterized in terms of biocompatibility and a larger surface area.

Research approbation

The scientific results obtained during the current research have been presented in various publications, which indicates the significance and impact of the research conducted during the doctoral studies.

The results of the dissertation have been presented in 4 scientific articles published in international journals listed in the ISI *Web of Science* database and have an impact factor. All four articles were published in Quartile 2 journals. The list of publications is given below:

- [A1] **Ciganė, Urtė**; Palevičius, Arvydas; Janušas, Giedrius. Review of nanomembranes: materials, fabrications and applications in tissue engineering (bone and skin) and drug delivery systems // *Journal of Materials Science*. New York: Springer. ISSN 0022-2461. 2021, vol. 56, iss. 24, p. 13479–13498. DOI: 10.1007/s10853-021-06164-x. **Impact factor 4.682, Q2.**
- [A2] **Cigane, Urte**; Palevicius, Arvydas; Jurenas, Vytautas; Pilkauskas, Kestutis; Janusas, Giedrius. Development and analysis of electrochemical reactor with vibrating functional element for AAO nanoporous membranes fabrication // *Sensors*. Basel: MDPI. ISSN 1424-8220. 2022, vol. 22, iss. 22, art. No. 8856, p. 1–14. DOI: 10.3390/s22228856. **Impact factor 3.900, Q2.**
- [A3] **Cigane, Urte**; Palevicius, Arvydas; Janusas, Giedrius. Vibration-assisted synthesis of nanoporous anodic aluminum oxide (AAO) membranes // *Micromachines*. Basel: MDPI. ISSN 2072-666X. 2022, vol. 13, iss. 12, art. No. 2236, p. 1–13. DOI: 10.3390/mi13122236. **Impact factor 3.400, Q2.**

[A4] **Cigane, Urte**; Palevicius, Arvydas; Janusas, Giedrius. A free-standing chitosan membrane prepared by the vibration-assisted solvent casting method // *Micromachines*. Basel: MDPI. ISSN 2072-666X. 2023, vol. 14, iss. 7, art. No. 1419, p. 1–13. DOI: 10.3390/mi14071419. **Impact factor 3.400, Q2.**

The contribution of the author and co-authors to the published articles is presented in Tables 1–4.

Table 1. Contribution of the author and co-authors on the published scientific article No. [A1]

Contribution	Author(s)
Studies on the literature	Urtė Ciganė
Conceptualization of the research direction	Urtė Ciganė
Analysis of the results	Urtė Ciganė
Graphical visualization of the results	Urtė Ciganė
Writing – original draft preparation	Urtė Ciganė
Writing – review and editing	Arvydas Palevičius Giedrius Janušas Urtė Ciganė
Modification of the manuscript based on the reviewer’s comments	Urtė Ciganė

Table 2. Contribution of the author and co-authors on the published scientific article No. [A2]

Contribution	Author(s)
Studies on the literature	Urtė Ciganė
Conceptualization of the research direction	Urtė Ciganė
Proposal of methodologies	Urtė Ciganė Arvydas Palevičius
Planning of the experimental works	Urtė Ciganė Arvydas Palevičius
Conducting research	Urtė Ciganė Vytautas Jūrėnas Giedrius Janušas
Validation and analysis of the experimental results	Urtė Ciganė Arvydas Palevičius Giedrius Janušas Vytautas Jūrėnas Kęstutis Pilkauskas
Graphical visualization of the experimental results	Urtė Ciganė
Writing – original draft preparation	Urtė Ciganė Kęstutis Pilkauskas
Writing – review and editing	Arvydas Palevičius Vytautas Jūrėnas Kęstutis Pilkauskas Urtė Ciganė
Modification of the manuscript based on the reviewer’s comments	Urtė Ciganė

Table 3. Contribution of the author and co-authors on the published scientific article No. [A3]

Contribution	Author(s)
Studies on the literature	Urtė Ciganė
Conceptualization of the research direction	Urtė Ciganė
Proposal of methodologies	Urtė Ciganė Arvydas Palevičius
Planning of the experimental works	Urtė Ciganė
Conducting research	Urtė Ciganė Giedrius Janušas
Validation and analysis of the experimental results	Urtė Ciganė Arvydas Palevičius Giedrius Janušas
Graphical visualization of the experimental results	Urtė Ciganė
Writing – original draft preparation	Urtė Ciganė
Writing – review and editing	Arvydas Palevičius Giedrius Janušas Urtė Ciganė
Modification of the manuscript based on the reviewer’s comments	Urtė Ciganė

Table 4. Contribution of the author and co-authors on the published scientific article No. [A4]

Contribution	Author(s)
Studies on the literature	Urtė Ciganė
Conceptualization of the research direction	Urtė Ciganė
Proposal of the methodologies	Urtė Ciganė Arvydas Palevičius
Planning of the experimental works	Urtė Ciganė
Conducting research	Urtė Ciganė Arvydas Palevičius
Validation and analysis of the experimental results	Urtė Ciganė Giedrius Janušas
Graphical visualization of the experimental results	Urtė Ciganė
Writing – original draft preparation	Urtė Ciganė
Writing – review and editing	Arvydas Palevičius Giedrius Janušas
Modification of the manuscript based on the reviewer’s comments	Urtė Ciganė

The publications of Urtė Ciganė and co-authors have been approved by the joint doctoral committee of Kaunas University of Technology and Vytautas Magnus University as suitable for writing a dissertation based on articles (as stated in Kaunas University of Technology Senate’s resolution of 30 November 2020 No. V3-S-37, page 61). Copies of Protocols Nos. ST16-T009-12 and ST16-T009-14 are provided further in the thesis, in Appendix 1 and Appendix 2, respectively.

In addition, the results have been presented at 8 international conferences, 2 international scientific seminars, and 1 exhibition.

Structure of the dissertation

This dissertation consists of an abstract, introduction, literature review, the main part which is split into four chapters (review of the four publications), conclusions, summary, references, publication copies, curriculum vitae, acknowledgments, and 2 appendices. The volume of the dissertation is 120 pages, including 9 figures, 4 tables, 97 bibliographic references, and copies of 4 publications.

1. LITERATURE REVIEW

The incredible speed of the nanotechnology revolution is particularly noticeable in Europe, China, and America, where billions of dollars and euros have been spent on nanotechnology in the last decade to exploit the enormous potential of this new science [1]. The rapid development of nanoscience is evidence that nanoscale manufacturing will soon be included in almost all fields of science and technology, which will subsequently require further industry development and investment in nanotechnology [2]. The scientific community develops technologies and products that are relatively cheaper, safer, and cleaner than the previous technologies [3]; as a result, research related to various nanostructured membranes has been attracting attention because these membranes can be characterized by versatility and the ability to control the parameters, which leads to the creation of unique structures [4, 5]. Therefore, this chapter provides general information on nanoporous AAO membranes as well as on the theory and capabilities of the electrochemical anodization process. In addition, chitosan membranes and details of the solvent casting method are introduced.

1.1. Anodized Aluminum Oxide (AAO) Nanoporous Membranes

Recently, nanoporous membrane technologies have been developed to allow easy control of membrane parameters depending on the application areas [6–23]. The interest in AAO nanostructured membranes is confirmed by the number of publications, increasing with each passing year. The statistics of the publications after entering the keyword ‘AAO membranes’ in *ScienceDirect* are presented in Fig. 1.

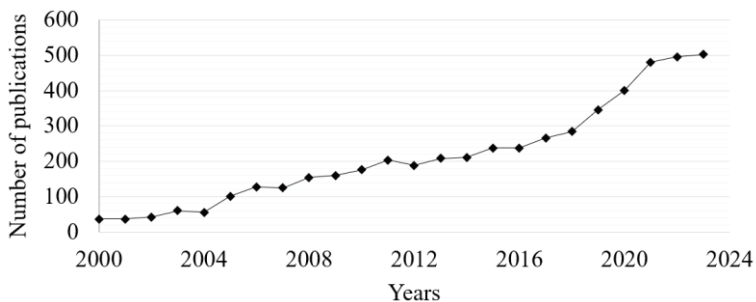


Fig. 1. Number of publications as a function of time obtained for the keyword ‘AAO membranes’

The nanoporous AAO membrane, which is produced by chemical anodization in an electrolyte solution [24], has the potential to be used as a template [25–28]. Aluminum anodization is an electrosynthesis process during which an oxide layer is formed, and the selection of different anodization parameters provides an opportunity to control the geometric parameters, the mechanical strength, and the surface hydrophilicity of AAO membranes [29]. The porous structure is formed when aluminum reacts chemically with an electrolyte, such as phosphoric, oxalic, or sulfuric

acid [30]. The thickness of the porous layer is directly proportional to the anodization time [31, 32]. The geometric feature of the AAO structure mostly depends on the experimental conditions. Usually, the AAO membrane is described by the following parameters: the pore diameter, the distance between the pores, and porosity [33].

Furthermore, research on AAO membranes makes them useful in various applications, such as energy conversion [34], RGB display technology [35], tissue engineering [36], microfluidic devices [37], sensors [38], etc. Research related to the use of aluminum oxide in different fields has also been conducted by Dr. Yatinkumar Patel [39] and Habil. Dr. Sigita Tamulevičius and his team [40, 41] at Kaunas University of Technology (Kaunas, Lithuania). For example, Dr. Yatinkumar Patel performed research and applied AAO membranes for nanoparticle filtration in biomedicine [42].

To apply AAO membranes in different fields, it is important to control the pore diameter of AAO membranes, the distance between the pores, and some other parameters. Therefore, the next sub-section briefly reviews the latest scientific literature related to the main principles of the electrochemical anodization process.

1.2. Electrochemical Anodization Process

In many applications, it is fundamentally important to precisely control the shape and geometry of the nanostructure, and an electrochemical anodization process is one which is used to obtain precise geometric properties of AAO membranes [43]. The parameters of the anodization process, such as the applied voltage, the acid type, the concentration, and temperature, contribute to the formation of the diameter of the pores and the distance between the pores [44–48]. However, it should be noted that the growth rate of porous AAO nanostructures is not constant throughout the anodization process, even when growth occurs at a fixed voltage and electrolyte concentration [49]. For example, the growth rate of AAO is sensitive to the electrolyte temperature. Thus, a higher temperature accelerates growth, whereas a lower temperature slows growth [50]. However, the electrolyte concentration gradually changes during the anodization process, so the change in the electrolyte composition and concentration inevitably affects the anodization rate [51–53]. All these complex factors make it challenging to precisely control the anodization process, especially when strict requirements are imposed on the final thickness of the membrane [54, 55].

Therefore, researchers have been studying the influence of anodization parameters on membrane geometry, and they are looking for solutions to ensure the uniform temperature and concentration during the anodization process [56, 57]. Research related to the anodization process was also conducted by Dr. Yatinkumar Patel [39]. For example, Dr. Yatinkumar Patel performed research at the Faculty of Mechanical Engineering and Design (Kaunas University of Technology, Kaunas, Lithuania), where research was carried out in a glass jar, and the anodization process with a magnetic stirrer and a cooling system was presented [42]. In recent studies, Peltier elements were used to maintain the uniform temperature [58]. However, with such equipment [59], temperature changes were large, and it was necessary to find new solutions to control and ensure the same temperature and electrolyte

concentration throughout the anodization process, so that oxide growth would be uniform throughout the process.

The increasing potential of AAO membranes for template fabrication [60, 61] encourages the study of nanochannels and microchannels of AAO membranes. Since the flow in small fluid volumes is often laminar, fluid heat exchange in microchannels is limited, and the fluid temperature is likely to increase along the microchannel. Thus, to achieve an efficient and fast mixing process of the fluid flow in straight AAO membrane channels, acoustofluidic physics has received great interest in the recent decades [62]. *Surface Acoustic Waves* (SAW) apply the effect of ultrasonic waves, and they have received extensive attention from researchers due to their noninvasive nature and the advantages of efficient fluid control [63]. Researchers have shown that the mixing efficiency of laminar flows of hot and cold fluids can be improved by using acoustic flow [64]. This contributes to changes in the temperature and pH values in the nanopores of AAO membrane during the formation of the oxide layer, thus ensuring the mixing process of the electrolyte liquid and the renewal of the flow throughout the length of the pore [65]. Therefore, after studying the theoretical models of AAO, nanoporous membranes need to be produced in practice by using the improved fabrication methods.

By controlling the anodization parameters, the nanoporous AAO membrane of the required dimensions can be produced. This membrane can be further used as a template to produce biocompatible chitosan membranes. Therefore, the next subsection briefly presents chitosan membranes and their application.

1.3. Chitosan Membranes

Chitosan may be one of the best biopolymers due to its specific properties, including biodegradability, low toxicity, low immunogenicity, antibacterial and antifungal activity, and biocompatibility [66]. Chitin can be soluble in an acid aqueous medium once it has undergone deacetylation to a degree of at least 50%, at which point it becomes chitosan [67].

In terms of its range of applications, chitosan is the most significant chitin derivative because it is abundant, biodegradable, and non-toxic [68]. Insects (cuticles) and crustaceans (skeletons), including crabs, shrimp, and lobsters, are potential sources of chitin, and the exoskeletons of species of cephalopods such as squid, cuttlefish, and octopus are also used to extract chitin [69]. A more affordable alternative method of producing chitosan polymer is by fermentation of fungal cell walls [70]. The primary benefit of this method is the high concentration of chitosan found in the cell walls of zygomycete fungi [71]. By carefully regulating the parameters of the fermentation process, it is possible to produce chitosan with the desired physicochemical properties [72].

The development of biocompatible, bactericidal, and bio-adhesive skin barriers using chitosan has shown promise and is already widely used in commercial wound dressings [73–75]. In addition, various combinations of chitosan with other materials are used in various fields of bioengineering [76–81]. Moreover, the possible use of nanopillars in membranes and films has attracted a lot of attention [82]. Since nanopillars have three effects on the surface biological processes (an increase in the

surface area, an increase in the cell adhesion and growth, and an increase in the ability to penetrate the cell), nanopillar surfaces are more valuable than the conventional planar surfaces [83–85]. Due to the promise of nanopillar membranes and films for the development of protective skin barriers [86, 87], it is important to develop fabrication technologies which would involve the control of the geometry of nanopillars [88, 89]. Therefore, the solvent casting method is presented in the next subsection as one of the suitable methods to produce chitosan membranes with nanopillars.

1.4. Solvent Casting Method

As the emphasis on environmental friendliness increases, nanomaterial templates are gaining a lot of interest because the template enables the structure to be rebuilt with the highest degree of reproducibility. These templates are thought to be one of the most promising strategies [90]. Therefore, the solvent casting method is reliable and widely used among the various polymeric film and membrane design methods [91]. This method is widely used because it is a low-cost alternative to the more expensive methods as 3D printing or spin coating [92, 93]. The solvent casting method involves dissolving the polymer and plasticizer, pouring the solution onto the substrate (template), and evaporating the solvent to form a film or a membrane of the required parameters [94]. Polymer(s) and plasticizer(s) are dissolved in a volatile solvent or a combination of solvents [95].

The solvent casting technique has many advantages, including low-cost processing, the ability to adjust the mechanical and optical properties of the film by changing processing parameters, such as the solvent casting time and temperature. The solvent casting method is a robust process that is easy to scale up on an industrial scale [96]. However, various drawbacks, such as a long drying time and a lack of control over the film thickness, must be considered [97].

1.5. Conclusions of the Chapter

A review of the literature focuses on the advances in nanoporous membrane technologies, with a special focus on AAO membranes, which have received considerable attention for their versatility and controllable properties. The electrochemical anodization process is a key aspect of AAO membrane fabrication, as it allows precise control of the AAO membrane geometry. After reviewing the literature, the following challenges related to the anodization process have been identified:

1. When the anodization process takes place at a set voltage and electrolyte concentration, the growth rate of porous AAO nanostructures is not constant.
2. The rate of the growth of AAO is affected by the temperature and concentration of the electrolyte.
3. During the anodization process, the electrolyte concentration and temperature gradually change; therefore, changes in the electrolyte temperature and concentration necessarily affect the growth rate of AAO.

Additionally, the review examines the potential of chitosan in areas such as wound dressings and bioengineering. The discussion also addresses nanopillar

structures, by highlighting their promise as reproducible structures with improved surface properties. Finally, the solvent-casting method is presented as a reliable and cost-effective way to produce polymeric membranes, especially for wound dressings. In general, this review provides insights into the prevailing membrane research and applications.

The review of scientific publications and the identified challenges made it possible to determine the aim and objectives of the dissertation. Therefore, the aim is to develop and investigate the fabrication technology for nanostructured membranes applied in bioengineering. To achieve the aim, the following objectives have been set:

1. To develop a temperature-controlled vibroelectrochemical reactor for the fabrication of nanoporous AAO membranes using high-frequency excitation during the two-step electrochemical anodization process.
2. To produce nanoporous AAO membranes using high-frequency excitation during the two-step electrochemical anodization process and to evaluate the influence of vibration on the porosity, thickness, hardness, and chemical composition of the membrane.
3. To produce a chitosan membrane with nanopillars as a template using a nanoporous AAO membrane and to determine the flow rates of solutions with different concentrations of chitosan into the nanopores and the influence on the height of the formed nanopillars when vibrations are used during the solvent casting method.
4. To create a patch prototype which simulates an artificial skin barrier characterized by biocompatibility and a larger surface area.

2. REVIEW OF THE PUBLICATIONS

2.1. “Review of nanomembranes: materials, fabrications and applications in tissue engineering (bone and skin) and drug delivery systems” (scientific publication No. [A1])

This subsection is based on the scientific article *Review of nanomembranes: materials, fabrications and applications in tissue engineering (bone and skin) and drug delivery systems* published in *Journal of Materials Science*, Springer, 2021, 56(24), 13479–13498 [IF: 4.682; Q2]. This publication is the result of the collaboration of the following authors: U. Ciganė, A. Palevičius, and G. Janušas. The contribution of U. Ciganė to this publication was the conceptualization, design of the research project, and visualization. Also, the author of this thesis was responsible for the original draft preparation. The co-authors contributed to the revision and editing.

The scientific article reports the problem of biological incompatibility and insufficient mechanical strength of synthetic nanostructured membranes applied in various fields of bioengineering. From the mechanical engineering point of view, the mechanical properties of nanostructured membranes can be influenced by the material of the membrane, the manufacturing method, and the porosity (if the membrane is porous). Therefore, this article provides a classification of synthetic membrane materials by describing each material group in detail with examples. The article also details the various technologies used to produce different nanostructured membranes, thus presenting the essential principles, as well as the advantages, and disadvantages of each technology. The paper also presents the application of synthetic membranes in the fields of skin and bone tissue engineering and drug delivery systems, thereby indicating specific membranes and their application. The article is based on 143 scientific papers, more than 60% of which were published in the last five years.

After a detailed analysis of the literature and considering the prevailing challenges of biocompatibility and the insufficient mechanical strength, materials and production technologies were identified, which were decided to improve and create a nanostructured membrane that would be biocompatible and strong enough to be applied in bioengineering. For that purpose, the anodization technology and the production of the AAO membrane were chosen. The mechanism of the anodization process is presented in Fig. 2. The anodization technology was chosen due to its ability to easily produce AAO membranes, to control the membrane pore diameter on the nanoscale, orderly arrangement of the nanopore structure, as well as simple and inexpensive equipment involved in the process. After the analysis, biocompatible materials were also identified, and one of them was selected to produce the membrane. Chitosan was the alternative of choice – this is a natural biomaterial that has a great advantage compared to other materials due to its low toxicity and a low chronic inflammatory response for application in the field of skin tissue engineering.

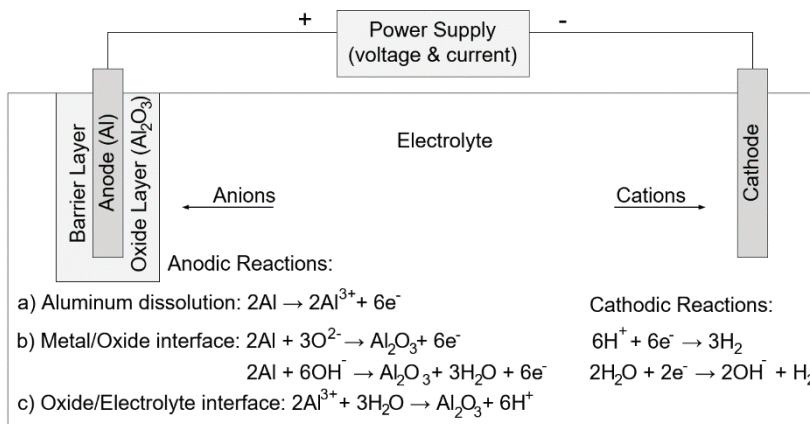


Fig. 2. Visual representation of the anodization process from the first publication *Review of nanomembranes: materials, fabrications and applications in tissue engineering (bone and skin) and drug delivery systems*

The results presented in this article indicate the need to improve the fabrication of nanostructured membranes to obtain biocompatible membranes with a sufficient strength for bioengineering applications. Therefore, the next article presents the developed vibroelectrochemical reactor and the improved technology to produce nanoporous AAO membranes, which will be further used as templates for the fabrication of a biocompatible membrane with sufficient strength.

2.2. “Development and Analysis of Electrochemical Reactor with Vibrating Functional Element for AAO Nanoporous Membranes Fabrication” (scientific publication No. [A2])

This subsection is based on a scientific article *Development and Analysis of Electrochemical Reactor with Vibrating Functional Element for AAO Nanoporous Membranes Fabrication* published in *Sensors*, MDPI, 2022, 22(22), 8856 [IF: 3.900; Q2]. This publication is the result of the collaboration of the following authors: U. Cigane, A. Palevicius, V. Jurenas, K. Pilkauskas, and G. Janusas. U. Cigane contributed to the conceptualization of the research, methodology, and experimental investigation. In addition, the author of this thesis was responsible for the calculation and analysis, visualization, and preparation of the original draft. The co-authors also partially contributed to the methodology, investigation, analysis, validation, review, and editing of the final version of the publication.

The article covers the first and second objectives of the research work related to the development of a controlled temperature vibroelectrochemical reactor and the fabrication of nanoporous AAO membranes. Furthermore, the influence of vibrations on the porosity, hardness, and chemical composition of the AAO membrane was investigated. The aim of this study was to determine the influence of vibrations when using a frequency lower than 10 kHz on the parameters of the AAO membrane.

The scientific article describes the development of an electrochemical reactor with a vibrating element for the fabrication of nanoporous AAO membranes during

the two-step anodization process. The design of the reactor is described in detail by providing a drawing and photographs of the manufactured electrochemical reactor. To evaluate the suitability of the reactor, experiments on temperature variation, the reactor mixing process, and vibration (to monitor the resulting modes) were carried out. Theoretical vibration simulations of the nanoporous AAO membrane were also performed by using *COMSOL Multiphysics 5.4* (COMSOL®, Burlington, United States). The theoretical results obtained from vibration modelling were compared with experimental studies, which were carried out by using the non-contact holographic measurement system (*PRISM*) (Hytec, Los Alamos, United States). After conducting the research, it was determined that the newly designed electrochemical reactor meets the requirements for the anodization process and is suitable for the fabrication of nanoporous AAO membranes, as five vibration mode shapes were obtained at different frequencies: the first mode shape (0, 1) at 3.1 kHz, the second mode shape (1, 1) at 4.1 kHz, the third mode shape (2, 1) at 6.3 kHz, the fourth mode shape (0, 2) at 7.1 kHz, and the fifth mode shape (3, 1) at 9.1 kHz. The novel design of an electrochemical reactor is presented in Fig. 3.

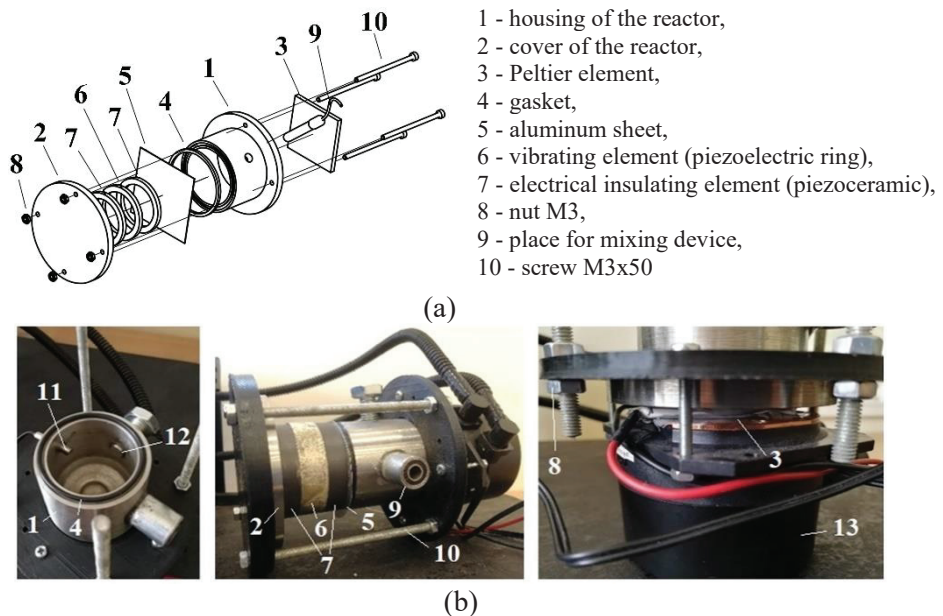


Fig. 3. Electrochemical reactor for fabrication of nanoporous AAO membranes: (a) drawing of the reactor; (b) construction of the novel design electrochemical reactor: 1 – housing of the reactor, 2 – cover of the reactor, 3 – Peltier element, 4 – gasket, 5 – aluminum sheet, 6 – vibrating element (piezoelectric ring), 7 – electrical insulating element (piezoceramic), 8 – nut M3, 9 – place for mixing device, 10 – screw M3x50, 11 – temperature sensor, 12 – hole for electrolyte filling, 13 – cooler

The article also describes the two-step anodization process performed at 5 °C and 40 V voltage when using 0.3 M oxalic acid ($\text{H}_2\text{C}_2\text{O}_4$) as an electrolyte. To produce

fewer brittle membranes that would be suitable for use as templates, an identical anodization process was performed by using vibration. High-frequency vibrations were applied to an aluminum plate which was fixed in the reactor in such a way that the anodization process would take place on one side of the plate, and an oxide layer is formed on the other side. This article presents a comparison of membranes when anodization was being performed without vibration, and when the first and second modes of vibration of the aluminum plate were applied. SEM images of fabricated nanoporous AAO membranes are presented in Fig. 4.

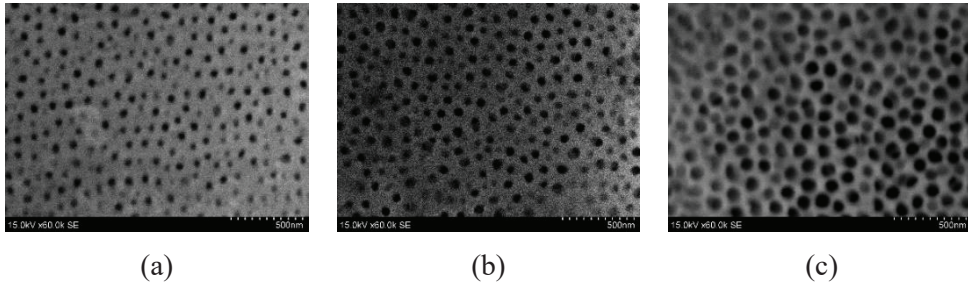


Fig. 4. Nanoporous AAO membranes after the two-step anodization process: (a) without frequency excitation; (b) when using 3.1 kHz frequency excitation; (c) when using 4.1 kHz frequency excitation

Nanoporous AAO membranes with a pore diameter of 55.0 ± 10 nm and a porosity of 19% were fabricated without vibration. When applying a frequency of 3.1 kHz (the first vibration mode) during the anodization process, nanoporous AAO membranes with a pore diameter of 82.6 ± 10 nm were produced, and a porosity of 43% was achieved. When using a frequency of 4.1 kHz (the second vibration mode), AAO membranes with a pore diameter of 86.1 ± 106.1 nm and a porosity of 46% were obtained. The chemical composition of the membranes remained unchanged, but the results showed that the pore diameter increased, which led to a higher porosity. Hardness measurements of the AAO membrane were also performed by using *Vickers* indenters with a diamond tip (*Micro Vickers Hardness Testing Machine: HM-200*, Mitutoyo, Japan). The hardness tests showed that hardness decreases from 4.73 GPa to 1.40 GPa when comparing the nanoporous AAO membrane after the two-step anodization process without high-frequency excitation and the nanoporous AAO membrane after the two-step anodization process with 4.1 kHz frequency excitation. It was established that the hardness value depends on porosity. The hardness of the membrane surface decreases with an increasing porosity.

Considering the theoretical model of the AAO formation mechanism, it was concluded that the resonant frequency promotes a better electrolyte mixing process at the oxide-electrolyte interface, because of which, the electrolyte concentration is constantly renewed at the oxide/electrolyte interface, and, as a result, more efficient chemical processes take place. The paper also concluded that nanoporous AAO membranes are less brittle under high-frequency excitation, but are still strong enough to be used as templates. The results presented in this article show that high-frequency excitation (lower than 10 kHz) affects the properties of the AAO membrane.

Therefore, the following publication focuses on the analysis of the influence of vibrations using a frequency higher than 10 kHz. The influence of vibrations on the most important parameters of the AAO membrane, such as the pore diameter, the interpore distance, the porosity, the membrane thickness, and the surface chemical composition is determined.

2.3. “Vibration-Assisted Synthesis of Nanoporous Anodic Aluminum Oxide (AAO) Membranes” (scientific publication No. [A3])

This subsection is based on the scientific article *Vibration-Assisted Synthesis of Nanoporous Anodic Aluminum Oxide (AAO) Membranes* published in *Micromachines*, MDPI, 2022, 13(12), 2236 [IF: 3.400; Q2]. This publication is the result of the collaboration of the following authors: U. Cigane, A. Palevicius and G. Janusas. U. Cigane’s contribution to this publication was the conceptualization of the research idea, methodology, and experimental investigation. Also, the author of this thesis was responsible for calculation and analysis, visualization, and the preparation of the original draft. The co-authors also partially contributed to the methodology, investigation, analysis, validation, review, and editing.

The paper covers the second objective of the work related to the fabrication of nanoporous AAO membranes and the influence of vibrations on the porosity, thickness, and chemical composition of the membrane. The aim of this study was to determine the influence of vibrations when using a frequency higher than 10 kHz on the parameters of the AAO membrane.

The scientific article describes the two-step anodization process carried out by vibrating an aluminum plate at a frequency of 20 kHz and 40 kHz, when the parameters of the anodization process were: 5 °C temperature, 40 V voltage, 0.3 M concentration of oxalic acid (electrolyte). An illustration of the two-step anodization process is presented in Fig. 5.

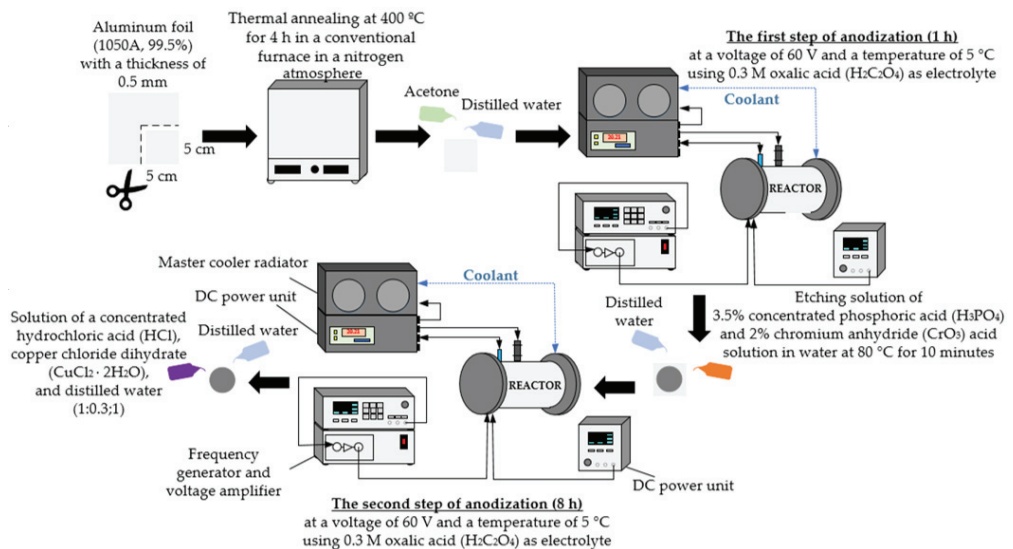


Fig. 5. Illustration of the two-step anodization process

When frequencies of 20 kHz and 40 kHz were applied, it was found that the pore diameter, the interpore distance, and the porosity of AAO membranes do not change. Furthermore, energy-dispersive X-ray analysis concluded that high-frequency excitation does not affect the chemical composition of the AAO membrane. During the anodization process, without applying vibrations, the thickness of the nanoporous AAO membrane was 45 μm . Changes in the membrane thickness were observed at frequencies of 20 kHz and 40 kHz. A 53 μm AAO membrane thickness was obtained at a frequency of 20 kHz, whereas a membrane thickness of 59 μm was obtained at a frequency of 40 kHz. Images of the thickness of the AAO membrane are presented in Fig. 6.

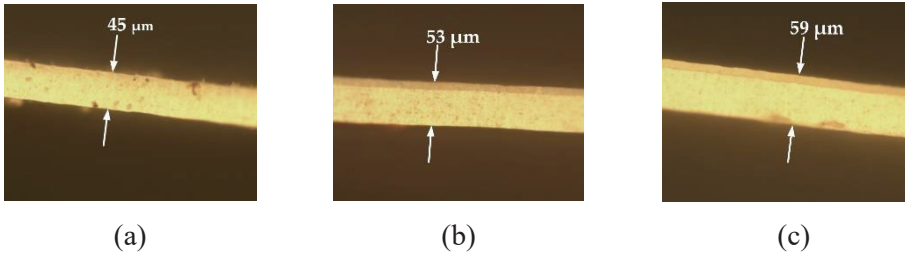


Fig. 6. Images of the thickness of AAO membrane when the membranes were fabricated under different anodization conditions: (a) no frequency excitation; (b) excitation at 20 kHz; (c) excitation at 40 kHz

The obtained experimental results coincided with the theoretical outcomes. At a frequency of 40 kHz, mixing of the liquid flow in the pores is ensured, thus also ensuring a more uniform temperature and pH value of the electrolyte along the entire length of the pore. For this reason, the reaction rate is higher. Therefore, a higher thickness of the AAO membrane was experimentally obtained when the reaction was performed at equal time intervals. Additional experimental results of the current measurement during the anodization process showed that the reaction rate and the oxide formation rate directly depend on the electrolyte concentration in the pores. The results of current measurement are presented in Fig. 7.

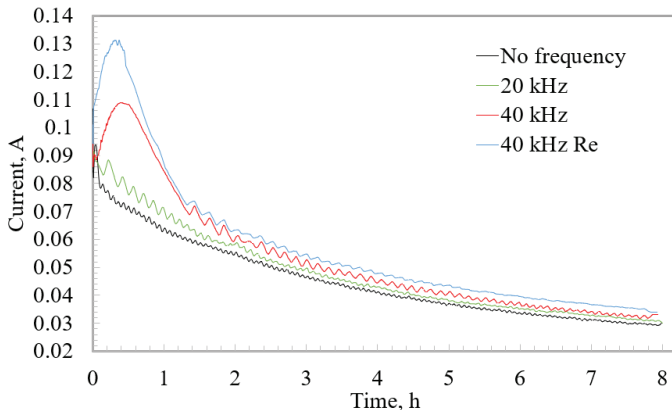


Fig. 7. Current-time curves recorded during the second step of anodization

When using 20 kHz frequency excitation, the experimentally recorded increasing current showed that the anodization reactions were enhanced. This can be explained by the faster ion migration. At a frequency of 40 kHz, the current was higher during the first hour of anodization compared to the frequency of 20 kHz. This was influenced by the increased frequency and the increased amplitude of the oscillations. As the current started to decrease during the anodization process, its value approached the standard current curve (when no excitations were being used), but the current remained slightly higher throughout the process. Although the electrolyte renewal was not as intense as at the beginning of the anodization process, because of the high-frequency excitation, the electrolyte concentration was renewed throughout the process. When the electrolyte is renewed inside the pores, higher oxide growth rates and a deeper structure could be achieved. On the other hand, when high-frequency vibrations are used to obtain a structure of a certain depth, the reaction can be performed in a shorter time.

The results presented in this article show that high-frequency excitation affects the properties of the AAO membrane. Therefore, depending on the need, the characteristics of the AAO membrane can be controlled. Since the AAO membrane is not biocompatible, this membrane is further used as a template to produce biocompatible membranes. Therefore, the following article presents an improved fabrication technology of a biocompatible membrane by using the fabricated AAO membrane as a template.

2.4. “A Free-Standing Chitosan Membrane Prepared by the Vibration-Assisted Solvent Casting Method” (scientific publication No. [A4])

This subsection is based on an overview of the scientific article *A Free-Standing Chitosan Membrane Prepared by the Vibration-Assisted Solvent Casting Method* published in *Micromachines*, MDPI, 2023, 14(7), 1419 [IF: 3.400; Q2]. This publication is the result of the collaboration of the following authors: U. Cigane, A. Palevicius and G. Janusas. U. Cigane’s contribution to this publication was the conceptualization of the research idea, methodology, experimental investigation, calculation and analysis, visualization, and the preparation of the original draft. The co-authors also partially contributed to the methodology, investigation, and analysis. Also, the co-authors were responsible for the validation, revision, and editing.

The article includes the third and fourth objectives related to chitosan membranes. The aim of this study was to fabricate the chitosan membrane with nanopillars as a template using a nanoporous AAO membrane. For this purpose, the improved solvent casting method using high-frequency vibrations was used. Also, the flow rates of solutions of different concentrations of chitosan into the AAO nanopores were determined. In addition, the effect on the height of the formed nanopillars was analyzed when vibrations were used during production. Finally, a patch prototype was developed which would mimic an artificial skin barrier with a larger surface area.

The paper describes a new technology for the solvent casting method using high-frequency vibrations and presents the developed vibration device to produce membranes by the solvent casting method. Nanopillared chitosan membranes were fabricated by using the nanoporous AAO membrane as a template. To improve the

solvent flow into the nanopores, 40 kHz high-frequency excitation was applied for 5 seconds during the solvent casting method. Chitosan membranes with a nanopillar surface were successfully prepared by using 1%, 2% and 3% chitosan solutions in 1% acetic acid. SEM images confirmed the formation of nanopores in the AAO membrane and nanopillars in the chitosan membrane. Three types of chitosan membranes were experimentally obtained, where the height of the nanopillars was 1007 nm, 665 nm and 377 nm when using 1%, 2%, and 3% chitosan solutions, respectively. SEM images of chitosan membranes are presented in Fig. 8.

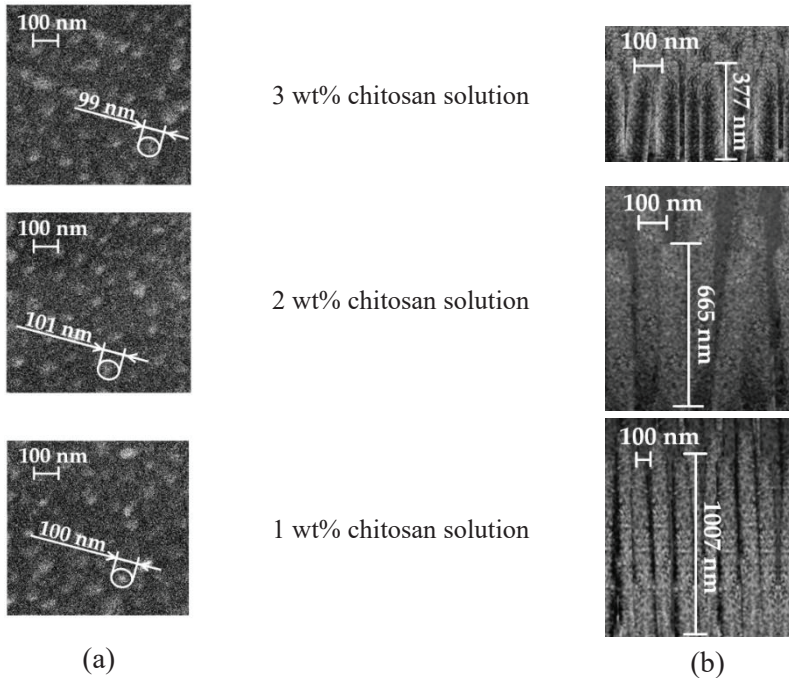


Fig. 8. SEM images of: (a) chitosan membrane; (b) nanopillar of chitosan membrane (cross-section)

The authors also theoretically evaluated the flow speed of chitosan solutions of different concentrations into the nanopores and the influence on the height of the formed nanopillars. With 1% chitosan solution, the theoretical flow speed of the solution into the pores was 250 nm/s, and the theoretical height of the formed nanopillars was 1000 nm. With 2% chitosan solution, the flow rate of the solution into the pores was 169 nm/s, and the height of the nanopillars was 675 nm. With a solution of 3% chitosan, the flow speed of the solution into the pores was 94 nm/s, and the height of the formed nanopillars was 375 nm. The article also presents experimental velocities of 201 nm/s, 133 nm/s, and 75 nm/s of 1%, 2% and 3% concentrations of the chitosan solution flow into pores, respectively.

Based on the surface area formula, the surface areas of chitosan membranes for the development of a prototype patch which would simulate the artificial skin barrier were calculated from the experimentally obtained heights of the nanopillars. The surface areas of chitosan membranes mimicking the artificial skin barrier with a size

of 10×10 mm were obtained as 15.05 cm^2 , 10.28 cm^2 , and 6.26 cm^2 with nanopillar heights of $1007 \pm 10 \text{ nm}$, $665 \pm 10 \text{ nm}$, and $377 \pm 10 \text{ nm}$, respectively. Compared to the flat membrane surface, the surface area with nanopillars increased by 15, 10, and 6 times, respectively. A free-standing chitosan membrane is presented in Fig. 9.

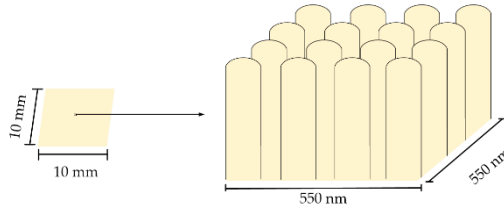


Fig. 9. Free-standing chitosan membrane

This article has experimentally determined how the liquid flow velocities into the nanopores allow the formation of nanopillars of the desired height, which would provide an opportunity to precisely control the surface area of the chitosan membrane. Due to the easily controlled surface area, the research described in this paper contributes to the development and improvement of artificial skin barriers for commercial use.

3. CONCLUSIONS

1. A new design of the temperature-controlled vibroelectrochemical reactor for the fabrication of nanoporous AAO membranes has been introduced. Inside the reactor, a vibrating element in the form of a piezoceramic ring was installed, which created the high-frequency excitation of an aluminum plate. Five vibration mode shapes were obtained at different frequencies: the first mode shape (0, 1) at 3.1 kHz, the second mode shape (1, 1) at 4.1 kHz, the third mode shape (2, 1) at 6.3 kHz, the fourth mode shape (0, 2) at 7.1 kHz, and the fifth mode shape (3, 1) at 9.1 kHz. It was found that the novel design of the electrochemical reactor meets the requirements of the anodization process and is suitable for the fabrication of nanoporous AAO membranes.
2. A novel anodization technology which used high-frequency excitation in the two-step anodization process resulted in AAO membranes with 82.6 ± 10 nm pore diameters and 43% porosity by using frequency excitation at 3.1 kHz and AAO membranes with 86.1 ± 10 nm pore diameters and 46% porosity while using frequency excitation at 4.1 kHz. The thickness and chemical composition of the membranes remained unchanged, but the pore diameter increased, which resulted in a higher porosity and a lower hardness. The nanoporous AAO membranes became less brittle, but were nevertheless tough enough to be used for template synthesis. At 20 kHz and 40 kHz, it was found that the pore diameter, the interpore distance, the porosity, and the surface chemical composition of the AAO membranes did not change when vibrations were being used during anodization. In the case where no vibrations were being applied during the anodization process, the thickness of the nanoporous AAO membrane was 45 μm . Changes in the membrane thickness were observed at 20 kHz and 40 kHz. AAO membrane thicknesses of 53 μm and 59 μm were obtained at 20 kHz and 40 kHz, respectively. It was found that the use of high frequencies up to 10 kHz ensures a better electrolyte mixing process at the electrolyte-oxide interface. When a frequency higher than 10 kHz is applied during anodization, specific electrolyte flows are created inside the pore of the AAO membrane, which leads to a better mixing process along the entire length of the pore.
3. Free-standing nanopillared chitosan membranes have been fabricated by using the improved solvent casting method, where 40 kHz frequency excitation (applied for 5 seconds) was used to improve the fluid flow into the nanopores. Nanopillared chitosan membranes were successfully fabricated by using chitosan solutions of 1 wt%, 2 wt% and 3 wt% concentrations in acetic acid. Thus, three types of biocompatible chitosan membranes with nanopillar heights of 1007 nm, 665 nm, and 377 nm were obtained. By using the 40 kHz frequency, the experimental flow velocities of the chitosan solution into the pores were 201 nm/s, 133 nm/s and 75 nm/s, which were determined at concentrations of 1 wt%, 2 wt% and 3 wt% of the chitosan solution, respectively.
4. To develop a patch prototype which would simulate artificial skin barriers, surface area calculations were performed for a free-standing chitosan membrane with a size of 10×10 mm. The surface areas were 15.05 cm^2 , 10.28 cm^2 , and 6.26 cm^2 with nanopillar heights of 1007 nm, 665 nm, and 377 nm, respectively.

4. SANTRAUKA

IVADAS

Įvairios nanostruktūrizuotos membranos sulaukia didelio mokslininkų dėmesio dėl savo universalumo, stabilumo ir galimybės kontroliuoti struktūros parametrus, nulemiančius unikalių struktūrų kūrimą. Skirtingos membranos yra plačiai naudojamos įvairiose srityse, tokiose kaip vandens valymas, saulės elementai, slėgio, temperatūros ir biojutikliai, lankstūs optoelektroniniai prietaisai ir medicina. Pastaruoju metu didelis proveržis pastebimas ir bioinžinerijos srityse, kur nanostruktūrizuotos membranos praktiškai pritaikomos kaulų ir odos audinių inžinerijose bei vaistų tiekimo sistemose.

Atsižvelgiant į mechaninę inžineriją, vis dar trūksta žinių apie nanostruktūrizuotų membranų mechaninį stiprumą ir biologinį suderinamumą. Kadangi ryšys tarp nanostruktūrizuotų membranų mechaninio stiprumo ir biologinio suderinamumo priklauso nuo medžiagos ir gamybos būdo, aktualu parinkti tinkamą technologiją šiems membranoms gaminti ir jas pritaikyti komerciškai. Kuriant sintetines membranas, svarbu užtikrinti tvarkingą vidinę struktūrą, nes tai nulemia unikalios kiekvienos membranos savybes. Tam tikslui yra naudojami įvairūs gamybos metodai, tokie kaip litografija, 3D spausdinimas, cheminis nusodinimas garais, elektrinis verpimas ir pan. Tačiau šiems gamybos būdams yra reikalinga sudėtinga ir brangi įranga, o patys procesai sudėtingai kontroliuojami ir dažnai nenuspėjami. Todėl kita gerai žinoma ir dažnai taikoma alternatyva – dviejų etapų aliuminio anodavimo procesas, kai elektrocheminiu būdu formuojami metalo oksido sluoksniai. Porėta AAO membrana yra gerai žinoma dėl savo sąlyginai nedidelės gamybos kainos, didelio paviršiaus ploto, tvarkingai išsidėsčiusių nanostruktūrų ir galimybės keisti nanoporų matmenis kontroliuojant anodavimo proceso parametrus, tokius kaip įtampa, srovė, elektrolito koncentracija, pH, elektrolito tipas, temperatūra. Tačiau vis dar išlieka iššūkių siekiant kontroliuoti ir užtikrinti vienodus membranų nanoporų geometrijos parametrus, nes šie priklauso ne tik nuo gamybos technologijos, bet ir nuo parinktų gamybos sąlygų. Kadangi daugumai inžinerinių medžiagų stiprumas ir kietumas yra esminiai reikalavimai, nanoporėtas AAO priskiriamas keramikai ir pasižymi kietumu ir stiprumu. Dėl šių priežasčių, norint pritaikyti nanoporėtą AAO šablonų gamybai, susiduriama su dar vienu iššūkiu – membranų trapumu. Todėl, modeliuojant gamybos parametrų įtaką membranų porų geometrijai, svarbu ne tik kontroliuoti membranų porų dydžius, bet ir pagaminti kuo lankstesnę nanoporėtą membraną iš trapios aliuminio oksido. Siekiant pagaminti mažiau trapų oksidą, reikia analizuoti skirtingus teorinius modelius, kurie paaiškina AAO susidarymą ir suteikia įžvalgų apie oksido struktūros formavimosi priklausomybę nuo skirtingų parametrų.

Vis labiau akcentuojant ekologiškumą, nanomedžiagų šablonai sulaukia daug dėmesio ir yra laikomi vienu perspektyviausių metodų, todėl technologiškai AAO membrana toliau naudojama kaip šablonas. Tačiau susiduriama su dar vienu aktualiu iššūkiu – kaip tiksliai ir su kuo didesniu atkuriamumu perkelti sukurtą AAO membranų geometriją į medžiagą, kuri pasižymėtų biosuderinamumu. Tam tikslui pasirenkama plačiai mokslininkų tiriama medžiaga – chitozanas, kuris perspektyvus kuriant biologiškai suderintus, baktericidiniu poveikiu pasižyminčius odos barjerus.

Be to, šiuo metu chitozano membranos jau yra naudojamos komerciniams žaizdų tvarsčiams ir pleistrams. Norint pagerinti chitozano membranų savybes, gali būti modifikuojamas paviršius arba kuriami įvairūs kompozitai. Norint chitozano membranas naudoti odos tvarsčiams ir pleistrams kurti, svarbu užtikrinti kuo didesnį membranos paviršiaus plotą. Tam tikslui vietoje įprastinių lygių paviršių pranašesni tampa paviršiai su nanostulpeliais, kurie gali padidinti paviršiaus plotą kelis ar net kelias dešimtis kartų. Kadangi chitozano membranos su nanostulpeliais yra perspektyvios kuriant odos apsaugos barjerus, aktualu sukurti ir gamybos technologiją, kuri apimtų nanostulpelių geometrijos valdymą.

Tyrimai, susiję su nanostruktūrizuotomis membranomis, sulaukia didelio mokslininkų ir verslo atstovų dėmesio, todėl svarbu plėtoti technologijas ir gilinti žinias apie gamybos metu vykstančius cheminius ir fizikinius procesus, kad būtų galima išspręsti aktualius iššūkius, susijusius su membranomis. Šioje disertacijoje pristatoma nauja nanoporėtų AAO membranų gamybos technologija, naudojanti virpesius, apimanti gamybos procesus, jų parametrus ir pagamintų membranų savybių aprašymą. Taip pat disertacijoje pristatoma AAO membranų geometrijos atkartojimo biosuderinamoje chitozano membranoje technologija, kai membranos paviršiuje suformuojami nanostulpeliai. Be to, pristatomi tiriami įvairių parametrų ryšiai ir sąveika, pateikiant eksperimentinių rezultatų rinkinius.

Darbo tikslas

Daktaro disertacijos tikslas – sukurti ir ištirti bioinžinerijoje taikomų nanostruktūrinių membranų gamybos technologiją.

Darbo uždaviniai

Daktaro disertacijos tikslui pasiekti iškelti šie uždaviniai:

1. Sukurti kontroliuojamos temperatūros vibroelektrocheminį reaktorių, skirtą nanoporėtų AAO membranų gamybai, kai dviejų etapų elektrocheminio anodavimo metu naudojami virpesiai.

2. Pagaminti nanoporėtas AAO membranas naudojant aukšto dažnio virpesius dviejų etapų elektrocheminio anodavimo metu ir įvertinti virpesių įtaką membranos porėtumui, storiui, kietumui ir cheminei sudėčiai.

3. Pagaminti chitozano membraną su nanostulpeliais kaip šabloną naudojant nanoporėtą AAO membraną ir nustatyti skirtingos chitozano koncentracijos tirpalų tekėjimo greičius į nanoporas ir įtaką susiformavusių nanostulpelių aukščiui, kai tirpalo liejimo (ang. *solvent casting*) metodo gamybos metu naudojami virpesiai.

4. Sukurti dirbtinį odos barjerą imituojantį pleistro prototipą, pasižymintį biologišku suderinamumu ir didesniu paviršiaus plotu.

Tyrimo metodai

Nanoporėtų AAO membranų gamybai, kai dviejų etapų elektrocheminio anodavimo oksalo rūgštyje metu naudojami virpesiai, naudotas sukurtas kontroliuojamos temperatūros vibroelektrocheminis reaktoriaus standas. Eksperimentiniais tyrimais įvertinta temperatūros, maišymo proceso ir virpesių įtaka ir reaktoriaus tinkamumas AAO membranų gamybai. Pagamintų AAO membranų paviršiaus cheminei sudėčiai ir porų geometrijai nustatyti naudotas skenuojamasis

elektroninis mikroskopas „Hitachi S-3400N“ (*Hitachi Ltd.*, Tokijas, Japonija) su integruota „Bruker“ sistema. Gauti vaizdai analizuoti naudojant „ImageJ“ programinę įrangą. AAO membranų paviršiaus mikrokietumo matavimams naudotas Vikerso metodas su deimantiniu antgaliu (Micro Vickers Hardness Testing Machine: HM-200, Japonija). Teorinėms AAO membranų virpesių modoms nustatyti naudota „Ansys 17.0“ (*Ansys®*, Pensilvanija, Jungtinės Valstijos) ir „COMSOL Multiphysics 5.4“ (*COMSOL®*, Berlingtonas, Jungtinės Valstijos) programinės įrangos, o eksperimentinėms membranų virpesių modoms stebėti naudota holografinė interferometrinė „PRISM“ sistema (*Hytec*, Los Alamosas, Jungtinės Valstijos).

Chitozano membranos gamintos tirpalo liejimo ant AAO šablono metodu, naudojant skirtingos koncentracijos chitozano tirpalus. Gamybai naudotas sukurtas vibrostendas. Pagamintų chitozano membranų paviršiaus geometrijai nustatyti naudotas skenuojamasis elektroninis mikroskopas „Hitachi S-3400N“ (*Hitachi Ltd.*, Tokijas, Japonija) ir vaizdų analizavimo „ImageJ“ programinė įrangą. Teoriniams skirtingos koncentracijos chitozano tirpalų tekėjimo į poras greičiams įvertinti naudota „COMSOL Multiphysics 5.4“ (*COMSOL®*, Berlingtonas, Jungtinės Valstijos) programinė įrangą.

Tyrimai atlikti Mechanikos inžinerijos ir dizaino fakultete (Kauno technologijos universitetas, Kaunas, Lietuva), Lietuvos energetikos institute (Kaunas, Lietuva) ir UAB „Hella Lithuania“ Kokybės laboratorijoje (Karmėlava, Lietuva).

Mokslinis darbo naujumas

1. Įvertinta dviejų etapų elektrocheminio anodavimo proceso gamybos metu taikytų virpesių įtaka AAO membranos porėtumui, storiui, kietumui ir cheminei sudėčiai.

2. Nustatyti skirtingos chitozano koncentracijos tirpalų tekėjimo greičiai į nanoporas bei koncentracijos įtaka susiformavusių nanostulpelių aukščiui, kai tirpalo liejimo metodo gamybos metu naudoti virpesiai.

Ginamieji teiginiai

1. Naudojant aukšto dažnio virpesius galima kontroliuoti nanoporėtos AAO membranos porėtumą, storį ir kietumą, nekeičiant membranos paviršiaus cheminės sudėties.

2. Elektrocheminio anodavimo proceso metu naudojant virpesius užtikrinamas elektrolito maišymo procesas išilgai nanoporos, kas lemia skysčio srauto atnaujinimą poros viduje. Taip užtikrinamas efektyvus ir greitas elektrolito srauto maišymasis nanoporoje.

3. Gaminant chitozano membranas su nanostulpeliais, naudojami aukšto dažnio virpesiai didesniai membranos paviršiaus plotui užtikrinti ir nanostulpelių aukščiui kontroliuoti.

Praktinė vertė

1. Sukurtas kontroliuojamos temperatūros vibroelektrocheminis reaktorius, skirtas nanoporėtų AAO membranų gamybai. Taip pat pagamintas reaktorius gali būti naudojamas ir kitiems procesams, kur reikalingas temperatūros, įtampas ir skysčio maišymo proceso valdymas.

2. Sukurta ir aprašyta nanoporėtų AAO membranų technologija, leidžianti užtikrinti reikalingą nanoporų geometriją kontroliuojant temperatūros, įtampos ar virpesių dažnio vertes.

3. Sukurti teoriniai membranos virpesių modų, elektrolito tekėjimo į nanoporas taikant virpesius ir skirtingos koncentracijos chitozano tirpalo tekėjimo į nanoporas naudojant virpesius modeliai, kurie suteikia vertingos informacijos ir žinių tolimesniems technologiniams procesams plėtoti.

4. Sukurtas dirbtinė odos barjerą imituojančio pleistro prototipas, pasižymintis biologiniu suderinamumu ir didesniu paviršiaus plotu.

Tyrimo aprobavimas

Disertacijos rezultatai paskelbti 4 moksliniuose straipsniuose, kurie publikuoti tarptautiniuose žurnaluose, įrašytuose į „ISI Web of Science“ duomenų bazę ir turi citavimo indeksą. Visi keturi straipsniai paskelbti „2 kvartilio“ žurnaluose.

Disertacijos autorės ir bendraautorių keturios publikacijos patvirtintos Mechanikos inžinerijos mokslo krypties Kauno technologijos universiteto ir Vytauto Didžiojo universiteto ŽŪA bendros doktorantūros komiteto kaip tinkamos rašyti disertaciją mokslinių straipsnių rinkinio pagrindu (kaip tai nurodyta Kauno technologijos universiteto Senato 2020 m. lapkričio 30 d. nutarimo Nr. V3-S-37 KTU mokslo doktorantūros reglamento 61 psl.). Komiteto posėdžių protokolų Nr. ST16-T009-12 ir ST16-T009-14 kopijos pateiktos atitinkamai 1 ir 2 prieduose.

Rezultatai taip pat pristatyti 8 tarptautinėse konferencijose, 2 tarptautiniuose moksliniuose seminaruose ir 1 parodoje.

Disertacijos struktūra ir apimtis

Disertaciją sudaro abstraktas, įvadas, literatūros apžvalga, pagrindiniai keturi skyreliai (keturių publikacijų apžvalgos), bendrosios baigiamojo darbo išvados, santrauka lietuvių kalba, literatūros sąrašas, publikacijų kopijos, gyvenimo aprašymas, padėka ir priedai. Iš viso 120 puslapiai, 9 paveikslai, 4 lentelės, 97 literatūros šaltiniai ir 4 mokslinių publikacijų kopijos.

MOKSLINIŲ STRAIPSNŲ APŽVALGA

Moksliniame straipsnyje „**Review of nanomembranes: materials, fabrications and applications in tissue engineering (bone and skin) and drug delivery systems**“ (publikacija nr. [A1]), kuris paskelbtas 2021 m. Springer leidyklos žurnale *Journal of Materials Science*, 56(24), 3479–13498 [IF: 4,682; Q2], pateikiama sintetinių nanostruktūrizuotų membranų, taikomų bioinžinerijos įvairiose srityse, biologinio nesuderinamumo ir nepakankamo mechaninio tvirtumo problema. Mechaninėje inžinerijoje membranų mechaninėms savybėms įtaką gali turėti membranos medžiaga, gamybos būdas ir poringumas (tuo atveju, jeigu membrana yra porėta). Todėl šiame straipsnyje pateikiama sintetinių nanostruktūrizuotų membranų medžiagų klasifikacija išsamiai aprašant kiekvieną medžiagų grupę su pavyzdžiais. Taip pat straipsnyje išsamiai aprašytos įvairios skirtingų nanostruktūrizuotų membranų gamybos technologijos, pateikiant kiekvienos technologijos esminius principus, privalumus ir trūkumus. Taip pat darbe pristatomas sintetinių

nanosuktūrizuotų membranų taikymas odos ir kaulų audinių inžinerijos srityse bei vaistų tiekimo sistemose, nurodant konkrečias membranas ir jų taikymą. Straipsnis parašytas remiantis 143 moksliniais darbais, kurių daugiau nei 60 % publikuoti per pastaruosius penkerius metus. Išsamiai atlikus literatūros analizę ir atsižvelgus į vyraujančius biosuderinamumo ir nepakankamo mechaninio tvirtumo iššūkius, identifikuotos medžiagos ir gamybos technologijos, kurias nuspręsta tobulinti ir sukurti membraną, kuri pasižymėtų biologiniu suderinamumu ir būtų pakankamai tvirta, kad galėtų būti taikoma bioinžinerijoje. Tam tikslui pasirinkta anodacijos technologija ir porėtos AAO membranų gamyba. Ši technologija pasirinkta dėl galimybės nesudėtingai gaminti AAO membranas naudojant nebrangią įrangą ir kontroliuoti membranų nanoporų skersmenį, gaunant tvarkingai išsidėsčiusią nanoporėtą struktūrą. Taip pat atlikus analizę identifikuotos biologiškai suderinamos medžiagos ir viena jų pasirinkta membranų gamybai. Tai chitozanas – natūrali biomedžiaga, kuri turi didelį pranašumą, palyginti su kitomis medžiagomis, dėl mažo toksiškumo ir mažo lėtinio uždegiminio atsako siekiant taikyti odos audinių inžinerijos srityje. Šiame straipsnyje pateiktoje apžvalgoje nustatytas nanosuktūrizuotų membranų gamybos tobulinimo poreikis, kad būtų gautos pakankamai tvirtos biologiškai suderinamos nanosuktūrizuotos membranų bioinžinerijos reikmėms. Todėl kitame straipsnyje pristatomas sukurtas vibroelektrocheminis reaktorius ir patobulinta nanoporėtų AAO membranų gamybos technologija, kur AAO membrana toliau naudojama kaip šablonas gaminant pakankamai tvirtą biologiškai suderinamą membraną.

Straipsnis „**Development and Analysis of Electrochemical Reactor with Vibrating Functional Element for AAO Nanoporous Membranes Fabrication**“ (publikacija nr. [A2]), kuris paskelbtas 2022 m. MDPI leidyklos žurnale *Sensors*, 22(22), 8856 [IF: 3,900; Q2], apima pirmąjį ir antrąjį darbo uždavinius, susijusius su kontroliuojamos temperatūros vibroelektrocheminio reaktoriaus kūrimu ir nanoporėtų AAO membranų gamyba. Taip pat analizuojama virpesių įtaka AAO membranų porėtumui, kietumui ir cheminei sudėčiai. Šio tyrimo tikslas – nustatyti žemesnio nei 10 kHz dažnio virpesių įtaką AAO membranų parametrams. Moksliniame straipsnyje aprašomas sukurtas elektrocheminis reaktorius su vibruojančiu elementu, skirtas nanoporėtų AAO membranų gamybai dviejų etapų anodavimo proceso metu. Išsamiai aprašyta reaktoriaus konstrukcija pateikiant brėžinį ir pagaminto elektrocheminio reaktoriaus nuotraukas. Reaktoriaus tinkamumui įvertinti atlikti temperatūros kitimo, reaktoriaus maišymo proceso tyrimai ir virpesių tyrimai, skirti susidarančioms modoms stebėti. Taip pat atlikti aliuminio oksido nanoporėtos membranų teoriniai virpesių modeliavimai, naudojant „COMSOL Multiphysics 5.4“ (COMSOL®, Berlingtonas, Jungtinės Valstijos) programinę įrangą. Gauti teoriniai virpesių modeliavimo rezultatai palyginti su eksperimentiniais tyrimais, kurie atlikti naudojant bekontaktę holografinę matavimo sistemą „PRISM“ (Hytec, Los Alamosas, Jungtinės Valstijos). Atlikus tyrimus nustatyta, kad naujo dizaino elektrocheminis reaktorius atitinka keliamus anodavimo procesui reikalavimus ir yra tinkamas nanoporėtoms AAO membranoms gaminti. Taip pat straipsnyje aprašomas atliktas dviejų etapų anodavimo procesas 5 °C temperatūroje, esant 40 V įtampai, kaip elektrolitą naudojant 0,3 M koncentracijos oksalo rūgštį (H₂C₂O₄). Siekiant pagaminti

mažiau trapias membranas, kurios būtų tinkamos naudoti šablonams, identiška anodacija atlikta naudojant virpesius. Aukšto dažnio virpesiai taikyti aliuminio plokštelei, kuri įtvirtinta reaktoriuje taip, kad vienoje plokštelės pusėje vyksta anodacijos procesas ir formuojasi oksido sluoksnis, o kitoje pusėje pritvirtintas vibruojantis elementas. Straipsnyje pateikiamas membranų palyginimas, kai anodacija atlikta netaikant virpesių ir taikant pirmąją bei antrąją aliuminio plokštelės virpesių modas. Netaikant virpesių pagamintos nanoporėtos AAO membranos, kurių porų skersmuo $55,0 \pm 10$ nm, o poringumas 19 %. Taikant 3,1 kHz dažnį (pirmoji virpesių moda) anodacijos metu, pagamintos nanoporėtos AAO membranos, kurių porų skersmuo $82,6 \pm 10$ nm, o poringumas 43 %. Naudojant 4,1 kHz dažnį (antroji virpesių moda), gautos AAO membranos, kurių porų skersmuo $86,1 \pm 106,1$ nm, o poringumas 46 %. Membranų cheminė sudėtis išliko nepakitusi, tačiau rezultatai parodė, kad porų skersmuo didėja, o tai lemia didesnį poringumą. Taip pat atlikti AAO membranos kietumo matavimai naudojant Vikerso įdubas su deimantiniu antgaliu (Micro Vickers Hardness Testing Machine: HM-200, Mitutoyo, Japonija). Kietumo testai parodė, kad kietumas sumažėja nuo 4,73 GPa iki 1,40 GPa, lyginant nanoporėtą AAO membraną po dviejų etapų anodavimo proceso be aukšto dažnio virpesių ir nanoporėtą AAO membraną po dviejų etapų anodavimo proceso su 4,1 kHz dažnio virpinimu. Nustatyta, kad kietumo vertė priklauso nuo poringumo. Membranos paviršiaus kietumas mažėja didėjant poringumui. Atsižvelgiant į teorinį aliuminio oksido formavimosi mechanizmo modelį, pateikiama išvada, kad rezonansinis dažnis skatina geresnį elektrolito maišymosi procesą oksido ir elektrolito sąsajoje, todėl oksido ir elektrolito sąsajoje elektrolito koncentracija nuolat atnaujinama ir dėl to efektyviau vyksta cheminiai procesai. Straipsnyje taip pat pateikta išvada, kad nanoporėtos AAO membranos naudojant aukšto dažnio virpesius yra mažiau trapios, bet pakankamai tvirtos, kad būtų toliau naudojamos kaip šablonai. Šiame straipsnyje pateikti rezultatai patvirtina, kad aukšto dažnio virpesiai (iki 10 kHz) turi įtakos AAO membranos savybėms. Todėl kitame straipsnyje pagrindinis dėmesys skiriamas aukšto dažnio virpesių (virš 10 kHz) įtakos svarbiausiems AAO membranos parametrams, tokiems kaip porų skersmuo, atstumas tarp porų, poringumas, membranos storis ir paviršiaus cheminė sudėtis, analizei ir tyrimui.

Straipsnis „**Vibration-Assisted Synthesis of Nanoporous Anodic Aluminum Oxide (AAO) Membranes**“ (publikacija nr. [A3]), kuris paskelbtas 2022 m. MDPI leidyklos žurnale *Micromachines*, 13(12), 2236 [IF: 3,400; Q2], apima antrąjį darbo uždavinį, susijusį su nanoporėtų AAO membranų gamyba ir virpesių įtaka membranos porėtumui, storiui ir cheminei sudėčiai. Šio tyrimo tikslas – nustatyti virpesių, naudojant aukštesnį nei 10 kHz dažnį, įtaką AAO membranos parametrams. Moksliniame straipsnyje aprašomas atliktas dviejų etapų anodavimo procesas aliuminio plokštelę virpinant 20 kHz ir 40 kHz dažniu, kai anodavimo proceso parametrai: 5 °C temperatūra, 40 V įtampa, 0,3 M koncentracijos oksalo rūgštis (elektrolitas). Taikant 20 kHz ir 40 kHz dažnius, nustatyta, kad AAO membranų porų skersmuo, atstumas tarp porų ir poringumas nesikeičia. Be to, atlikus energijos sklaidos rentgeno analizę padaryta išvada, kad aukšto dažnio virpesiai neturi įtakos AAO membranos cheminei sudėčiai. Anodacijos proceso metu netaikant virpesių, nanoporėtos AAO membranos storis gautas 45 μm. Membranos storio pokyčiai

pastebėti taikant 20 kHz ir 40 kHz dažnius. Esant 20 kHz dažniui gautas 53 μm AAO membranų storis, o esant 40 kHz dažniui gautas 59 μm membranų storis. Gauti eksperimentiniai rezultatai sutapo su teoriniais. Esant 40 kHz dažniui, dėl geresnio skysčio srauto porose maišymosi užtikrinama vienodesnė elektrolito temperatūra ir pH vertė per visą poros ilgį. Reakcijos greitis yra didesnis. Todėl AAO membranų storis eksperimentiškai gautas didesnis, kai reakcija vykdoma vienodą laiko intervalą. Papildomi eksperimentiniai srovės matavimo anodacijos proceso metu rezultatai parodė, kad reakcijos greitis ir oksido susidarymo greitis tiesiogiai priklauso nuo elektrolito koncentracijos porose. Naudojant 20 kHz dažnio virpesius eksperimentiškai užfiksuota didėjanti srovė parodė, kad anodavimo reakcijos sustiprėjo. Tai galima paaiškinti greitesne jonų migracija. Esant 40 kHz dažniui, pirmąją anodavimo valandą srovė buvo didesnė, palyginti su 20 kHz dažniu. Tam įtakos turėjo padidėjęs dažnis ir padidėjusi virpesių amplitudė. Anodacijos proceso metu srovei pradėjus mažėti, jos vertė artėjo prie standartinės srovės kreivės (kai virpesiai nenaudojami), tačiau viso proceso metu srovė išliko šiek tiek didesnė. Nors visą procesą elektrolito atnaujinimas nebuvo toks intensyvus kaip anodavimo pradžioje, tačiau dėl aukšto dažnio virpesių elektrolito koncentracija visą procesą atnaujinama. Atnaujinus elektrolitą porų viduje, galima pasiekti didesnę oksido augimo greitį ir gilesnę struktūrą. Kita vertus, kai naudojami aukšto dažnio virpesiai, norint gauti tam tikro gylio struktūrą, reakcija gali būti atlikta per trumpesnę laiką. Šiame straipsnyje pateikti rezultatai rodo, kad aukšto dažnio virpesiai turi įtakos AAO membranų savybėms. Priklausomai nuo poreikio, AAO membranų charakteristikos gali būti kontroliuojamos. Kadangi AAO membranų nepasižymi biologiniu suderinamumu, šios membranų toliau naudojamos kaip šablonai biologiškai suderinamoms membranoms gaminti. Todėl kitame straipsnyje pateikiama patobulinta biologiškai suderinamos membranų gamybos technologija, naudojant pagamintą AAO membraną kaip šabloną.

Straipsnis „**A Free-Standing Chitosan Membrane Prepared by the Vibration-Assisted Solvent Casting Method**“ (publikacija nr. [A4]), kuris paskelbtas 2023 m. MDPI leidyklos žurnale *Micromachines*, 14(7), 1419 [IF: 3,400; Q2], apima trečiąjį ir ketvirtąjį darbo uždavinius, susijusius su chitozano membranomis. Šio tyrimo tikslas – pagaminti chitozano membranų su nanostulpelių struktūra kaip šabloną naudojant porėtą AAO membraną. Šiam tikslui naudota nauja technologija, susijusi su naudojamais aukšto dažnio virpesiais tirpalo liejimo metodu. Tyrimo metu nustatyti skirtingos chitozano koncentracijos tirpalų tekėjimo greičiai į nanoporas. Taip pat buvo analizuojama virpesių įtaka nanostulpelių formavimo aukščiui. Galiausiai sukurtas dirbtinį odos barjerą imituojančio pleistro prototipas. Straipsnyje aprašoma nauja tirpalo liejimo metodo technologija, susijusi su naudojamais aukšto dažnio virpesiais. Taip pat pateikiamas sukurtas vibracinis įrenginys, skirtas membranoms gaminti tirpalo liejimo metodu. Pagamintos chitozano membranų su nanostulpeliais kaip šabloną naudojant nanoporėtą AAO membraną. Siekiant pagerinti tirpalo srauto tekėjimą į nanoporas, 40 kHz aukšto dažnio virpesiai taikyti 5 sekundes tirpalo liejimo metodu. Chitozano membranų su nanostulpelių paviršiumi sėkmingai pagamintos naudojant 1 %, 2 % ir 3 % chitozano tirpalus 1 % acto rūgšties tirpale. SEM vaizdai patvirtino AAO membranų nanoporų

ir chitozono membranos nanostulpelių susiformavimą. Eksperimentiškai gautos trijų tipų chitozono membranos, kur nanostulpelių aukštis 1007 nm, 665 nm ir 377 nm, atitinkamai naudojant 1 %, 2 % ir 3 % chitozono tirpalus. Taip pat straipsnyje teoriškai įvertinti skirtingos koncentracijos chitozono tirpalų tekėjimo į nanoporas greičiai ir įtaka susiformavusių nanostulpelių aukščiui. Turint 1 % chitozono tirpalą, tirpalo tekėjimo į poras teorinis greitis 250 nm/s, o susiformavusių nanostulpelių teorinis aukštis 1000 nm. Su 2 % chitozono tirpalu tirpalo tekėjimo į poras greitis gautas 169 nm/s, susiformavusių nanostulpelių aukštis 675 nm. Turint 3 % chitozono tirpalą, tirpalo tekėjimo į poras greitis siekė 94 nm/s, susiformavusių nanostulpelių aukštis 375 nm. Taip pat straipsnyje pristatyti eksperimentiniai chitozono tirpalo tekėjimo į poras greičiai 201 nm/s, 133 nm/s ir 75 nm/s, atitinkamai esant 1 %, 2 % ir 3 % chitozono tirpalo koncentracijoms. Remiantis paviršiaus ploto formule, iš eksperimentiškai gautų nanostulpelių aukščių buvo apskaičiuoti chitozono membranų, skirtų dirbtinių odos barjerą imituojančiam pleistro prototipui kurti, paviršiaus plotai. Dirbtinių odos barjerą, kurio dydis 10×10 mm, imituojančios chitozono membranos paviršiaus plotai gauti 15,05 cm², 10,28 cm² ir 6,26 cm², kai nanostulpelių aukščiai atitinkamai 1007 ± 10 nm, 665 ± 10 nm ir 377 ± 10 nm. Palyginti su lygiu membranos paviršiumi, paviršiaus su nanostulpeliais plotas padidėjo 15, 10 ir 6 kartus. Straipsnyje eksperimentiškai nustatyti skysčio tekėjimo į nanoporas greičiai leidžia formuoti norimo aukščio nanostulpelius, kurie suteikia galimybę tiksliai valdyti chitozono membranos paviršiaus plotą. Dėl lengvai kontroliuojamo paviršiaus ploto tyrimai, aprašyti šiame darbe, prisideda prie dirbtinių odos barjerų, skirtų komerciniam naudojimui, kūrimo ir tobulinimo.

IŠVADOS

1. Pristatytas naujos konstrukcijos reguliuojamos temperatūros vibroelektrocheminis reaktorius, skirtas nanoporėtų AAO membranų gamybai. Reaktoriaus viduje įmontuotas pjezokeraminis žiedo pavidalo vibruojantis elementas, skirtas aliuminio plokštelę virpinti aukštu dažniu. Gautos penkios virpesių modos esant skirtingiems dažniams: pirmosios modos forma (0, 1) esant 3,1 kHz, antrosios modos forma (1, 1) esant 4,1 kHz, trečiosios modos forma (2, 1) esant 6,3 kHz, ketvirtosios modos forma (0, 2) esant 7,1 kHz, o penktosios modos forma (3, 1) – 9,1 kHz. Nustatyta, kad naujos konstrukcijos elektrocheminis reaktorius atitinka anodavimo proceso reikalavimus ir yra tinkamas nanoporėtų AAO membranų gamybai.
2. Taikant naują anodavimo technologiją, naudojančią aukšto dažnio virpesius dviejų etapų anodavimo procese, gautos AAO membranos, kurių porų skersmuo 82,6 ± 10 nm, o poringumas 43 % esant 3,1 kHz ir AAO membranos su 86,1 ± 10 nm skersmeniu ir 46 % poringumu, naudojant 4,1 kHz. Membranų storis ir cheminė sudėtis nepasikeitė, tačiau padidėjo porų skersmuo, todėl padidėjo poringumas, o kietumas sumažėjo. Nanoporėtos AAO membranos tapo mažiau trapios, bet pakankamai tvirtos, kad būtų taikomos kaip šablonai. Esant 20 kHz ir 40 kHz dažniui, nustatyta, kad dviejų etapų anodavimo proceso metu naudojant aukšto dažnio virpesius, AAO membranų porų skersmuo, atstumas tarp porų, poringumas ir paviršiaus cheminė sudėtis nepasikeitė. Tuo atveju, kai anodavimo proceso metu nebuvo taikomi virpesiai, nanoporėtos AAO membranos storis gautas 45 μm.

Membranos storio pokyčiai buvo matomi esant 20 kHz ir 40 kHz dažniams. AAO membranos storis 53 μm ir 59 μm buvo gautas atitinkamai esant 20 kHz ir 40 kHz. Apibendrinant gautus rezultatus, nustatyta, kad, naudojant aukšto dažnio virpesius iki 10 kHz, užtikrinamas geresnis elektrolito maišymosi procesas elektrolito ir oksido sąsajoje. Kai anodacijos metu taikomas aukštesnis nei 10 kHz dažnis, specifiniai elektrolito srautai sukuriama AAO membranose porose, o tai lemia geresnį maišymosi procesą per visą poros ilgį.

3. Laisvos chitozono membranose su nanostulpeliais pagamintose naudojant patobulintą tirpalo liejimo metodą, kaip šabloną naudojant nanoporėtą AAO membraną. Gamybės metu taikyti 40 kHz aukšto dažnio virpesiai (5 sekundes), kurie naudoti skysčių patekimui į nanoporas pagerinti. Chitozono membranose su nanostulpeliais sėkmingai pagamintose naudojant 1 %, 2 % ir 3 % chitozono tirpalus acto rūgštyje ir gautos trijų tipų biologiškai suderinamos chitozono membranose, kurių nanostulpelių aukštis atitinkamai 1007 nm, 665 nm ir 377 nm. Naudojant aukšto dažnio 40 kHz virpesius, eksperimentiniai chitozono tirpalo srauto į poras greičiai 201, 133 ir 75 nm/s nustatyti, kai chitozono tirpalų koncentracijos atitinkamai 1 %, 2 % ir 3 %.
4. Siekiant kurti ir plėtoti pleistro prototipą, imituojantį dirbtinius odos barjerus, atlikti chitozono membranose, kurios dydis 10×10 mm, paviršiaus ploto skaičiavimai. Kai nanostulpelių aukštis 1007 nm, 665 nm ir 377 nm, chitozono membranose paviršiaus plotas atitinkamai yra 15,05 cm², 10,28 cm² ir 6,26 cm².

REFERENCES

1. TALEBIAN, Sepehr, RODRIGUES, Tiago, NEVES, José, SARMENTO, Bruno, LANGER, Robert and CONDE, João. Facts and Figures on Materials Science and Nanotechnology Progress and Investment. *ACS Nano* [online]. ACS Publications, July 2021, vol. 15, p. 15940–15952. Available from: <https://doi.org/10.1021/acsnano.1c03992>
2. MALIK, Shiza, MUHAMMAD, Khalid and WAHEED, Yasir. Nanotechnology: A Revolution in Modern Industry. *Molecules* [online]. MDPI, January 2023, vol. 28, no. 2, p. 661. Available from: <http://dx.doi.org/10.3390/molecules28020661>
3. NAYANA, D. A., GEORGE, Nithya S., NANDAKUMAR, S., ARAVIND, Arun and MANOJ, P. K. Future of Nanotechnology and Functionalized Nanomaterials. In: *Functionalized Nanomaterials Based Supercapacitor. Materials Horizons: From Nature to Nanomaterials*. Springer, September 2023, p. 655–677. Available from: https://doi.org/10.1007/978-981-99-3021-0_26
4. HAQUE, Syed Rashedul. Preparation, characterization, applications and future challenges of Nanomembrane-A review. *Hybrid Advances* [online]. Elsevier, August 2023, vol. 3, p. 100027. Available from: <https://doi.org/10.1016/j.hybadv.2023.100027>
5. NUNES, Suzana P., CULFAZ–EMECEN, P. Zeynep, RAMON, Guy. Z., VISSER, Tymen, KOOPS, Geert Henk, JIN, Wangin and ULBRICHT, Mathias. Thinking the future of membranes: perspectives for advanced and new membrane materials and manufacturing processes. *Journal of Membrane Science* [online]. Elsevier, March 2020, vol. 598, p. 117761. Available from: <https://doi.org/10.1016/j.memsci.2019.117761>
6. TRIPATHY, Divya Bajpai and GUPTA, Anjali. Nanomembranes-Affiliated Water Remediation: Chronology, Properties, Classification, Challenges and Future Prospects. *Membranes* [online]. MDPI, August 2023, vol. 13, no. 8, p. 713. Available from: <http://dx.doi.org/10.3390/membranes13080713>
7. SURESH, R, RAJENDRAN, Saravanan, GNANASEKARAN, Lalitha, SHOW, Pau Loke, CHEN, Wei–Hsin and SOTO–MOSCOSO, Matias. Modified poly(vinylidene fluoride) nanomembranes for dye removal from water – A review. *Chemosphere* [online]. Elsevier, May 2023, vol. 322, p. 138152. Available from: <https://doi.org/10.1016/j.chemosphere.2023.138152>
8. GÜNAY, M. Gökhan, KEMERLI, Ubade, KARAMAN, Ceren, KARAMAN, Onur, GÜNGÖR, Afşin and KARIMI–MALEH, Hassan. Review of functionalized nano porous membranes for desalination and water purification: MD simulations perspective. *Environmental Research* [online]. Elsevier, January 2023, vol. 217, p. 114785. Available from: <https://doi.org/10.1016/j.envres.2022.114785>
9. CHO, Myeongki, JEON, Gyeong G., SANG, Mingyu, KIM, Tae Soo, SUH, Jungmin, SHIN, So Jeong, CHOI, Min Jun, KIM, Hyun Woo, KIM, Kyubeen, LEE, Ju Young, NOH, Jeong Yeon, KIM, Jong H., KIM, Jincheol, PARK, Nochang and YU, Ki Jun. Ultra-thin thermally grown silicon dioxide nanomembrane for waterproof perovskite solar cells. *Journal of Power Sources* [online]. Elsevier, April 2023, vol. 563, p. 232810. Available from: <https://doi.org/10.1016/j.jpowsour.2023.232810>
10. AOUASSA, Mansour, FRANZÒ, Giorgia, M'GHAIETH, Ridha and CHOUAIB, Hassen. Direct growth and size tuning of InAs/GaAs quantum dots on transferable silicon nanomembranes for solar cells application. *Journal of Materials Science: Materials in*

- Electronics* [online]. Springer, June 2021, vol. 32, p. 18251–18263. Available from: <https://doi.org/10.1007/s10854-021-06368-6>
11. KANG, Kyowon, SANG, Mingyu, XU, Baoxing and YU, Ki Jun. Fabrication of gold-doped crystalline-silicon nanomembrane-based wearable temperature sensor. *STAR Protocols* [online]. Cell Press, March 2023, vol. 4, p. 101925. Available from: <https://doi.org/10.1016/j.xpro.2022.101925>
 12. CHENG, Lixia, HAO, Xiaojian, LIU, Guochang, ZHANG, Wendong, CUI, Jiangong, ZHANG, Guojun, YANG, Yuhua and WANG, Renxin. A Flexible Pressure Sensor Based on Silicon Nanomembrane. *Biosensors* [online]. MDPI, January 2023, vol. 13, no. 1, p. 131. Available from: <http://dx.doi.org/10.3390/bios13010131>
 13. MOHANKUMAR, P., AJAYAN, J., MOHANRAJ, T. and YASODHARAN, R. Recent developments in biosensors for healthcare and biomedical applications: A review. *Measurement* [online]. Elsevier, 2021, vol. 167, p. 108293. Available from: <https://doi.org/10.1016/j.measurement.2020.108293>
 14. AN, Shu, PARK, Hyun Jung and KIM, Munho. Recent advances in single crystal narrow bandgap semiconductor nanomembranes and their flexible optoelectronic device applications: Ge, GeSn, InGaAs, and 2D materials. *Journal of Materials Chemistry C* [online]. Royal Society of Chemistry, January 2023, vol. 11, p. 2430–2448. Available from: <https://doi.org/10.1039/d2tc05041b>
 15. TONEV, Dimitar G. and MOMCHILOVA, Albena B. Therapeutic Plasma Exchange in Certain Immune-Mediated Neurological Disorders: Focus on a Novel Nanomembrane-Based Technology. *Biomedicines* [online]. MDPI, January 2023, vol. 11, no. 2, p. 328. Available from: <http://dx.doi.org/10.3390/biomedicines11020328>
 16. MUNIR, Muhammad Usman, MIKUCIONIENE, Daiva, KHANZADA, Haleema and KHAN, Muhammad Qamar. Development of Eco-Friendly Nanomembranes of Aloe vera/PVA/ZnO for Potential Applications in Medical Devices. *Polymers* [online]. MDPI, March 2022, vol. 14, no. 5, p. 1029. Available from: <http://dx.doi.org/10.3390/polym14051029>
 17. AL-BAADANI, Mohammed A., YIE, Kendrick Hii Ru, AL-BISHARI, Abdullrahman M., ALSHOBI, Bilal A., ZHOU, Zixin, FANG, Kai, DAI, Binwei, SHEN, Yiding, MA, Jianfeng, LIU, Jinsong and SHEN, Xinkun. Co-electrospinning polycaprolactone/gelatin membrane as a tunable drug delivery system for bone tissue regeneration. *Materials & Design* [online]. Elsevier, November 2021, vol. 209, p. 109962. Available from: <https://doi.org/10.1016/j.matdes.2021.109962>
 18. SALERNO, Simona, DE SANTO, Maria Penelope, DRIOLI, Enrico and DE BARTOLO, Loredana. Nano- and Micro-Porous Chitosan Membranes for Human Epidermal Stratification and Differentiation. *Membranes* [online]. MDPI, May 2021, vol. 11, no. 6, p. 394. Available from: <http://dx.doi.org/10.3390/membranes11060394>
 19. VOLOVA, Tatiana G., DEMIDENKO, Aleksey V., MURUEVA, Anastasiya V., DUDAEV, Alexey E., NEMTSEV, Ivan and SHISHATSKAYA, Ekaterina I. Biodegradable Polyhydroxyalkanoates Formed by 3- and 4-Hydroxybutyrate Monomers to Produce Nanomembranes Suitable for Drug Delivery and Cell Culture. *Technologies* [online]. MDPI, August 2023, vol. 11, no. 4, p. 106. Available from: <http://dx.doi.org/10.3390/technologies11040106>
 20. SUN, Meilin, HAN, Kai, GU, Rui, LIU, Dan, FU, Wenzhu and LIU, Wenming. Advances in Micro/Nanoporous Membranes for Biomedical Engineering. *Advanced*

- Healthcare Materials* [online]. Wiley Online Library, January 2021, vol. 10, p. 2001545. Available from: <https://doi.org/10.1002/adhm.202001545>
21. RHEIMA, Ahmed Mahdi, ABBAS, Zainab sabri, KADHIM, Mustafa M., MOHAMMED, Srwa Hashim, ALHAMEEDI, Dheyaa Yahaia, RASEN, Fadhil A., AL-BAYATI, Alaa dhari jawad, RAMADAN, Montather F., ABED, Zainab Talib, JABER, Asala Salam, HACHIM, Safa K., ALI, Farah K., MAHMOUD, Zaid H. and KIANFAR, Ehsan. Aluminum oxide nano porous: Synthesis, properties, and applications. *Case Studies in Chemical and Environmental Engineering* [online]. Elsevier, December 2023, vol. 8, p. 100428. Available from: <https://doi.org/10.1016/j.cscee.2023.100428>
 22. MOHAMMED–SADHAKATHULLAH, Ahammed H. M., PAULO–MIRASOL, Sofia, TORRAS, Juan and ARMELIN, Elaine. Advances in Functionalization of Bioresorbable Nanomembranes and Nanoparticles for Their Use in Biomedicine. *International Journal of Molecular Sciences* [online]. MDPI, June 2023, vol. 24, no. 12, p. 10312. Available from: <http://dx.doi.org/10.3390/ijms241210312>
 23. JAKŠIĆ, Zoran and JAKŠIĆ, Olga. Biomimetic Nanomembranes: An Overview. *Biomimetics* [online]. MDPI, May 2020, vol. 5, no. 2, p. 24. Available from: <http://dx.doi.org/10.3390/biomimetics5020024>
 24. PÉTER, László. Preparation of Nanoporous Oxides from Metals by Electrochemical Anodization. In: *Electrochemical Methods of Nanostructure Preparation. Monographs in Electrochemistry*. Cham: Springer, 2021, p. 477–510. Available from: https://doi.org/10.1007/978-3-030-69117-2_13
 25. ZHANG, Chenghao, LIU, Zhichao, LI, Chun, CAO, Jian and BUIJNSTERS, Josephus G. Templated Synthesis of Diamond Nanopillar Arrays Using Porous Anodic Aluminium Oxide (AAO) Membranes. *Nanomaterials* [online]. MDPI, February 2023, vol. 13, no. 5, p. 888. Available from: <http://dx.doi.org/10.3390/nano13050888>
 26. HAMEED, Riad M., AL–HADDAD, Ahmed and ALBARAZANCHI, Abbas K.H. Facile transformation of graphene oxide nanospheres based on AAO template. *Kuwait Journal of Science* [online]. Elsevier, October 2023, vol. 50, p. 563–568. Available from: <https://doi.org/10.1016/j.kjs.2023.08.002>
 27. RATH, Amrita and THEATO, Patrick. Advanced AAO Templating of Nanostructured Stimuli-Responsive Polymers: Hype or Hope? *Advanced Functional Materials* [online]. Wiley Online Library, January 2020, vol. 30, p. 1902959. Available from: <https://doi.org/10.1002/adfm.201902959>
 28. LI, Dongjing, WU, Aixia, WAN, Qing and LI, Zeping. Controllable fabrication of polymeric nanowires by NIL technique and self-assembled AAO template for SERS application. *Scientific Reports* [online]. Springer, July 2021, vol. 11, p. 14929. Available from: <https://doi.org/10.1038/s41598-021-94513-w>
 29. DOBOSZ, Iwona. Influence of the anodization conditions and chemical treatment on the formation of alumina membranes with defined pore diameters. *Journal of Porous Materials* [online]. Springer, March 2021, vol. 28, p. 1011–1022. Available from: <https://doi.org/10.1007/s10934-021-01052-w>
 30. LIU, Sixiang, TIAN, Junlong and ZHANG, Wang. Fabrication and application of nanoporous anodic aluminum oxide: a review. *Nanotechnology* [online]. IOP Publishing, March 2021, vol. 32, p. 222001. Available from: <https://doi.org/10.1088/1361-6528/abe25f>
 31. LI, Jingui, WEI, Hongyang, ZHAO, Kai, WANG, Meifeng, CHEN, Dongchu and CHEN, Min. Effect of anodizing temperature and organic acid addition on the structure and

- corrosion resistance of anodic aluminum oxide films. *Thin Solid Films* [online]. Elsevier, November 2020, vol. 713, p. 138359. Available from: <https://doi.org/10.1016/j.tsf.2020.138359>
32. BRUERA, Florencia A., KRAMER, Gustavo R., VERA, María L. and ARES, Alicia E. Low-Cost Nanostructured Coating of Anodic Aluminium Oxide Synthesized in Sulphuric Acid as Electrolyte. *Coatings* [online]. MDPI, March 2021, vol. 11, no. 3, p. 309. Available from: <http://dx.doi.org/10.3390/coatings11030309>
 33. JOUAULT, Nicolas and BERNI, Selene. Synthesis of ordered duplex nanoporous alumina with modulated constriction and composition. *Solid State Sciences* [online]. Elsevier, November 2022, vol. 133, p. 107020. Available from: <https://doi.org/10.1016/j.solidstatesciences.2022.107020>
 34. CHEN, Mengyuan, YANG, Kun, WANG, Jin, SUN, Hanjun, XIA, Xing-Hua and WANG, Chen. In Situ Growth of Imine-Bridged Anion-Selective COF/AAOMembrane for Ion Current Rectification and Nanofluidic Osmotic Energy Conversion. *Advanced functional materials* [online]. Wiley Online Library, September 2023, vol. 33, p. 2302427. Available from: <https://doi.org/10.1002/adfm.202302427>
 35. MANZANO, Cristina V., RODRÍGUEZ-ACEVEDO, Julia, CABALLERO-CALERO, Olga and MARTÍN-GONZÁLEZ, Marisol. Interconnected three-dimensional anodized aluminum oxide (3D-AAO) metamaterials using different waveforms and metal layers for RGB display technology applications. *Journal of Materials Chemistry C* [online]. Royal Society of Chemistry, January 2022, vol. 10, p. 1787–1797. Available from: <https://doi.org/10.1039/D1TC05209H>
 36. DAVOODI, Elham, ZHIANMANESH, Masoud, MONTAZERIAN, Hossein, MILANI, Abbas S. and HOORFAR, Mina. Nano-porous anodic alumina: fundamentals and applications in tissue engineering. *Journal of Materials Science: Materials in Medicine* [online]. Springer, July 2020, vol. 31, p. 60. Available from: <https://doi.org/10.1007/s10856-020-06398-2>
 37. O'CONNELL, Killian C. and LANDERSABC, James P. Integrated membranes within centrifugal microfluidic devices: a review. *Lab on a Chip* [online]. Royal Society of Chemistry, June 2023, vol. 23, p. 3130–3159. Available from: <https://doi.org/10.1039/D3LC00175J>
 38. SENNER, Melike, SISMAN, Orhan and KILINC, Necmettin. AAO-Assisted Nanoporous Platinum Films for Hydrogen Sensor Application. *Catalysts* [online]. MDPI, February 2023, vol. 13, no. 3, p. 459. Available from: <http://dx.doi.org/10.3390/catal13030459>
 39. PATEL, Yatinkumar Rajeshbhai. Research and Development of Functional Nanoporous Aluminum Oxide Membranes for Micro/Nano Filtration Devices in Bioengineering. PhD thesis. Online. Kaunas University of Technology, 2022. Available from: <https://www.lvb.lt/permalink/f/16nmo04/ELABAETD149739845>
 40. JURKEVIČIŪTĖ, Aušrinė, DOLMANTAS, Paulius, VASILIAUSKAS, Andrius, TAMULEVIČIENĖ, Asta, MEŠKINIS, Šarūnas, POPLAUSKAS, Raimonds, PRIKULIS, Juris, TAMULEVIČIUS, Sigitas and TAMULEVIČIUS, Tomas. Magnetron sputtering process for deposition of multilayered thin diamond-like carbon films with silver nanoparticles for anti-reflective coatings and refractometric sensing. *Materials Chemistry and Physics* [online]. Elsevier, November 2023, vol. 309, p. 128425. Available from: <https://doi.org/10.1016/j.matchemphys.2023.128425>
 41. PECKUS, Domantas, MEŠKINIS, Šarūnas, VASILIAUSKAS, Andrius, RAJACKAITĖ, Erika, ANDRULEVIČIUS, Mindaugas, KOPUSTINSKAS, Vitoldas

- and TAMULEVIČIUS, Sigitas. Structure and optical properties of diamond like carbon films containing aluminium and alumina. *Applied Surface Science* [online]. Elsevier, November 2020, vol. 529, p. 147040. Available from: <https://doi.org/10.1016/j.apsusc.2020.147040>
42. PATEL, Yatinkumar, JANUSAS, Giedrius, PALEVICIUS, Arvydas and VILKAUSKAS, Andrius. Development of Nanoporous AAO Membrane for Nano Filtration Using the Acoustophoresis Method. *Sensors* [online]. MDPI, July 2020, vol. 20, no. 14, p. 3833. Available from: <http://dx.doi.org/10.3390/s20143833>
 43. BRZÓZKA, Agnieszka, BRUDZISZ, Anna, RAJSKA, Dominika, BOGUSZ, Joanna, PALOWSKA, Renata, WÓJCIKIEWICZ, Dominik and SULKA, Grzegorz D. Chapter two - Recent trends in synthesis of nanoporous anodic aluminum oxides. In *Micro and Nano Technologies, Nanostructured Anodic Metal Oxides*. Elsevier, 2020, p. 35–88. Available from: <https://doi.org/10.1016/B978-0-12-816706-9.00002-9>
 44. ZAJĄCZKOWSKA, Lidia and NOREK, Małgorzata. Peculiarities of Aluminum Anodization in AHAS-Based Electrolytes: Case Study of the Anodization in Glycolic Acid Solution. *Materials* [online]. MDPI, September 2021, vol. 14, no. 18, p. 5362. Available from: <http://dx.doi.org/10.3390/ma14185362>
 45. JEONG, Chanyoung, JUNG, Jeki, SHEPPARD, Keith and CHOI, Chang–Hwan. Control of the Nanopore Architecture of Anodic Alumina via Stepwise Anodization with Voltage Modulation and Pore Widening. *Nanomaterials* [online]. MDPI, January 2023, vol. 13, no. 2, p. 342. Available from: <http://dx.doi.org/10.3390/nano13020342>
 46. ONO, Sachiko. Nanostructure Analysis of Anodic Films Formed on Aluminum-Focusing on the Effects of Electric Field Strength and Electrolyte Anions. *Molecules* [online]. MDPI, November 2021, vol. 26, no. 23, p. 7270. Available from: <http://dx.doi.org/10.3390/molecules26237270>
 47. MOHITFAR, Seyyed Hasan, MAHDAVI, Soheil, ETMINANFAR, Mohamadreza and KHALIL–ALLAFI, Jafar. Characteristics and tribological behavior of the hard anodized 6061-T6 Al alloy. *Journal of Alloys and Compounds* [online]. Elsevier, November 2020, vol. 842, p. 155988. Available from: <https://doi.org/10.1016/j.jallcom.2020.155988>
 48. POZNYAK, Alexander, PLIGOVKA, Andrei, TURAVETS, Ulyana and NOREK, Małgorzata. On-Aluminum and Barrier Anodic Oxide: Meeting the Challenges of Chemical Dissolution Rate in Various Acids and Solutions. *Coatings* [online]. MDPI, September 2020, vol. 10, no. 9, p. 875. Available from: <http://dx.doi.org/10.3390/coatings10090875>
 49. LV, Jiang, CHEN, Zhi–Li, TANG, Jin, CHEN, Li, XIE, Wen–Jing, SUN, Meng–Xi, HUANG, Xiao–Jun and YANG, Yue–Ping. Effect and mechanism of pyrophosphoric acid anodizing technological parameters on the superhydrophilicity coupled corrosion resistance of aluminum alloy distillation desalination tubes. *Surface and Coatings Technology* [online]. Elsevier, July 2023, vol. 465, p. 129581. Available from: <https://doi.org/10.1016/j.surfcoat.2023.129581>
 50. ARAUJO, João Victor de Sousa, MILAGRE, Mariana and COSTA, Isolda. A historical, statistical and electrochemical approach on the effect of microstructure in the anodizing of Al alloys: a review. *Critical Reviews in Solid State And Materials Sciences* [online]. Taylor & Francis Online, July 2023. Available from: <https://doi.org/10.1080/10408436.2023.2230250>
 51. GASCO–OWENS, A., VEYS–RENAUX, D., CARTIGNY, V. and ROCCA, E. Large-pores anodizing of 5657 aluminum alloy in phosphoric acid: an in-situ electrochemical

- study. *Electrochimica Acta* [online]. Elsevier, June 2021, vol. 382, p. 138303. Available from: <https://doi.org/10.1016/j.electacta.2021.138303>
52. TERASHIMA, Ayasa, IWAI, Mana and KIKUCHI, Tatsuya. Nanomorphological changes of anodic aluminum oxide fabricated by anodizing in various phosphate solutions over a wide pH range. *Applied Surface Science* [online]. Elsevier, December 2022, vol. 605, p. 154687. Available from: <https://doi.org/10.1016/j.apsusc.2022.154687>
 53. POZNYAK, Alexander, PLIGOVKA, Andrei, LARYN, Tsimafei and SALERNO, Marco. Porous Alumina Films Fabricated by Reduced Temperature Sulfuric Acid Anodizing: Morphology, Composition and Volumetric Growth. *Materials* [online]. MDPI, February 2021, vol. 14, no. 4, p. 767. Available from: <http://dx.doi.org/10.3390/ma14040767>
 54. WANG, Kaijie, CAO, Yongzhi, CUI, Yaowen, YE, Aiyong, YI, Shaofan and HU, Zhenjiang. Study on Parameter Correlation of Thickness and Performance of Anodizing Film on 6061 Aluminum Alloy Frame in High Energy Laser System. *Coatings* [online]. MDPI, December 2022, vol. 12, no. 12, p. 1978. Available from: <http://dx.doi.org/10.3390/coatings12121978>
 55. BRUERA, Florencia A., KRAMER, Gustavo R., VERA, María L. and ARES, Alicia E. Evaluation of the influence of synthesis conditions on the morphology of nanostructured anodic aluminum oxide coatings on Al 1050. *Surfaces and Interfaces* [online]. Elsevier, 2020, vol. 18, p. 100448. Available from: <https://doi.org/10.1016/j.surfin.2020.100448>
 56. PU, Yuanjing, HU, Jiajun, YAO, Taicang, LI, Linfeng, ZHAO, Jie and GUO, Yu. Influence of anodization parameters on film thickness and volume expansion of thick- and large-sized anodic aluminum oxide film. *Journal of Materials Science: Materials in Electronics* [online]. Springer, May 2021, vol. 32, p. 13708–13718. Available from: <https://doi.org/10.1007/s10854-021-05948-w>
 57. GUO, Feng, CAO, Yongzhi, WANG, Kaijie, ZHANG, Peng, CUI, Yaowen, HU, Zhenjiang and XIE, Zhiwen. Effect of the Anodizing Temperature on Microstructure and Tribological Properties of 6061 Aluminum Alloy Anodic Oxide Films. *Coatings* [online]. MDPI, February 2022, vol. 12, no. 3, p. 314. Available from: <http://dx.doi.org/10.3390/coatings12030314>
 58. PATEL, Yatinkumar, JANUSAS, Giedrius and PALEVICIUS, Arvydas. Fabrication of nanoporous alumina in 0.3 M oxalic acid and study on mechanical properties using micro indentation test. *Materials Today: Proceedings* [online]. Elsevier, February 2023, vol. 57, p. 630–635. Available from: <https://doi.org/10.1016/j.matpr.2022.02.044>
 59. PATEL, Yatinkumar, JANUSAS, Giedrius and PALEVICIUS, Arvydas. Fabrication of nanoporous free standing anodic alumina using two-step anodization for applicability in microhydraulic system as nano filter using surface acoustics. *Materials Today: Proceedings* [online]. Elsevier, February 2021, vol. 45, p. 5059–5064. Available from: <https://doi.org/10.1016/j.matpr.2021.01.571>
 60. SUN, Kexi, DENG, Quan and TANG, Haibin. AAO Template-Assisted Fabrication of Ordered Ag Nanoparticles-Decorated Au Nanotubes Array for Surface-Enhanced Raman Scattering Detection. *Sustainability* [online]. MDPI, January 2022, vol. 14, no. 3, p. 1305. Available from: <http://dx.doi.org/10.3390/su14031305>
 61. ZHANG, Huanming, ZHOU, Min, ZHAO, Huaping and LEI, Yong. Ordered nanostructures arrays fabricated by anodic aluminum oxide (AAO) template-directed methods for energy conversion. *Nanotechnology* [online]. IOP Publishing, October 2021, vol. 32, p. 502006. Available from: <https://doi.org/10.1088/1361-6528/ac268b>

62. LI, Sining, ZHANG, Hongna, CHENG, Jianping, CAI, Weihua, LI, Xiaobin, WU, Jian and LI, Fengchen. A Numerical Study on Heat Transfer Performance in a Straight Microchannel Heat Sink with Standing Surface Acoustic Waves. *Heat Transfer Engineering* [online]. Taylor & Francis Online, February 2021, vol. 43:3–5, p. 371–387. Available from: <https://doi.org/10.1080/01457632.2021.1874670>
63. CHEN, Zhenzhen, SHEN, Liang, ZHAO, Xiong, CHEN, Hongqiang, XIAO, Yaxuan, ZHANG, Yonghai, YANG, Xiaoping, ZHANG, Jinhua, WEI, Jinjia and HAO, Nanjing. Acoustofluidic micromixers: From rational design to lab-on-a-chip applications. *Applied Materials Today* [online]. Elsevier, March 2022, vol. 26, p. 101356. Available from: <https://doi.org/10.1016/j.apmt.2021.101356>
64. HSU, Jin–Chen and CHANG, Chih–Yu. Enhanced acoustofluidic mixing in a semicircular microchannel using plate mode coupling in a surface acoustic wave device. *Sensors and Actuators A: Physical* [online]. Elsevier, April 2022, vol. 336, p. 113401. Available from: <https://doi.org/10.1016/j.sna.2022.113401>
65. MARAMIZONOUZ, Sadaf, JIA, Changfeng, RAHMATI, Mohammad, ZHENG, Tengfei, LIU, Qiang, TORUN, Hamdi, WU, Qiang and FU, YongQing. Acoustofluidic Patterning inside Capillary Tubes Using Standing Surface Acoustic Waves. *International Journal of Mechanical Sciences* [online]. Elsevier, January 2022, vol. 214, p. 106893. Available from: <https://doi.org/10.1016/j.ijmecsci.2021.106893>
66. REZAEI, Farnoush Sadat, SHARIFIANJAZI, Fariborz, ESMAEILKHANIAN, Amirhossein and SALEHI, Ehsan. Chitosan films and scaffolds for regenerative medicine applications: A review. *Carbohydrate Polymers* [online]. Elsevier, December 2021, vol. 273, p. 118631. Available from: <https://doi.org/10.1016/j.carbpol.2021.118631>
67. KHAJAVIAN, Mohammad, VATANPOUR, Vahid, CASTRO–MUÑOZ, Roberto and BOCZKAJ, Grzegorz. Chitin and derivative chitosan-based structures — Preparation strategies aided by deep eutectic solvents: A review. *Carbohydrate Polymers* [online]. Elsevier, January 2022, vol. 275, p. 118702. Available from: <https://doi.org/10.1016/j.carbpol.2021.118702>
68. BUTNARIU, Monica. Biological and Chemical Aspects of Chitosan. In: *Chitosan Nanocomposites. Biological and Medical Physics, Biomedical Engineering*. Singapore: Springer, 2023, p. 27–54. Available from: https://doi.org/10.1007/978-981-19-9646-7_2
69. KHAN, Ajahar, and ALAMRY, Khalid A. Recent advances of emerging green chitosan-based biomaterials with potential biomedical applications: A review. *Carbohydrate Research* [online]. Elsevier, August 2021, vol. 506, p. 108368. Available from: <https://doi.org/10.1016/j.carres.2021.108368>
70. SEBASTIAN, Joseph, ROUISSI, Tarek and BRAR, Satinder Kaur. Chapter 14 - Fungal chitosan: prospects and challenges. In: *Handbook of Chitin and Chitosan*. Elsevier, 2020, vol. 1, p. 419–452. Available from: <https://doi.org/10.1016/B978-0-12-817970-3.00014-6>
71. HUQ, Tanzina, KHAN, Avik, BROWN, David, DHAYAGUDE, Natasha, HE, Zhibin and NI, Yonghao. Sources, production and commercial applications of fungal chitosan: A review. *Journal of Bioresources and Bioproducts* [online]. Chinese Roots Global Impact, May 2022, vol. 7, p. 85–98. Available from: <https://doi.org/10.1016/j.jobab.2022.01.002>
72. ELSOUD, Mostafa M. Abo, ELMANSY, Eman A. and ABDELHAMID, Sayeda A. Economic and Non-Seasonal Source for Production of Chitin and Chitosan. *Journal of*

- Chemical reviews* [online]. June 2022, vol. 4, p. 222–240. Available from: <https://doi.org/10.22034/jcr.2022.342454.1173>
73. JI, Maocheng, LI, Jianyong, WANG, Yi, LI, Fangyi, MAN, Jis, LI, Jianfeng, ZHANG, Chuanwei, PENG, Sixian and WANG, Shiqing. Advances in chitosan-based wound dressings: Modifications, fabrications, applications and prospects. *Carbohydrate Polymers* [online]. Elsevier, December 2022, vol. 297, p. 120058. Available from: <https://doi.org/10.1016/j.carbpol.2022.120058>
 74. HAMED, Hamid, MORADI, Sara, HUDSON, Samuel M., TONELLI, Alan E. and KING, Martin W. Chitosan based bioadhesives for biomedical applications: A review. *Carbohydrate Polymers* [online]. Elsevier, April 2022, vol. 282, p. 119100. Available from: <https://doi.org/10.1016/j.carbpol.2022.119100>
 75. GENESI, Bianca P., BARBOSA, Raquel de Melo, SEVERINO, Patricia, RODAS, Andrea C.D., YOSHIDA, Cristiana M.P., MATHOR, Mônica B., LOPES, Patrícia S., VISERAS, César, SOUTO, Eliana B. and DA SILVA, Classius Ferreira. Aloe vera and copaiba oleoresin-loaded chitosan films for wound dressings: Microbial permeation, cytotoxicity, and in vivo proof of concept. *International Journal of Pharmaceutics* [online]. Elsevier, March 2023, vol. 634, p. 122648. Available from: <https://doi.org/10.1016/j.ijpharm.2023.122648>
 76. AUGUSTINE, Robin, REHMAN, Syed Raza Ur, AHMED, Rashid, ZAHID, Alap Ali, SHARIFI, Majid, FALAHATI, Mojtaba and HASAN, Anwarul. Electrospun chitosan membranes containing bioactive and therapeutic agents for enhanced wound healing. *International Journal of Biological Macromolecules* [online]. Elsevier, August 2020, vol. 156, p. 153–170. Available from: <https://doi.org/10.1016/j.ijbiomac.2020.03.207>
 77. GUO, Shujuan, HE, Linlin, YANG, Ruqian, CHEN, Boyuan, XIE, Xudong, JIANG, Bo, WEIDONG, Tian and DING, Yi. Enhanced effects of electrospun collagen-chitosan nanofiber membranes on guided bone regeneration. *Journal of Biomaterials Science, Polymer Edition* [online]. Taylor & Francis Online, November 2020, vol. 31, p. 155–168. Available from: <https://doi.org/10.1080/09205063.2019.1680927>
 78. WANG, Liangyu, DU, Lin, WANG, Mengmeng, WANG, Xing, TIAN, Saihua, CHEN, Yan, WANG, Xiaoyue, ZHANG, Jie, NIE, Jun and MA, Guiping. Chitosan for constructing stable polymer-inorganic suspensions and multifunctional membranes for wound healing. *Carbohydrate Polymers* [online]. Elsevier, June 2022, vol. 285, p. 119209. Available from: <https://doi.org/10.1016/j.carbpol.2022.119209>
 79. MADNI, Ahmed, KOUSAR, Rozina, NAEEM, Naveera and WAHID, Fazli. Recent advancements in applications of chitosan-based biomaterials for skin tissue engineering. *Journal of Bioresources and Bioproducts* [online]. Chinese Roots Global Impact, February 2021, vol. 6, p. 11–25. Available from: <https://doi.org/10.1016/j.jobab.2021.01.002>
 80. GOVINDASAMY, Kavitha, DAHLAN, Nuraina Anisa, JANARTHANAN, Pushpamalar, GOH, Kheng Lim, CHAI, Siang-Piao and PASBAKSH, Pooria. Electrospun chitosan/polyethylene-oxide (PEO)/halloysites (HAL) membranes for bone regeneration applications. *Applied Clay Science* [online]. Elsevier, June 2020, vol. 190, p. 105601. Available from: <https://doi.org/10.1016/j.clay.2020.105601>
 81. XIA, Jian, ZHANG, Hao, YU, Faquan, PEI, Ying and LUO, Xiaogang. Superclear, Porous Cellulose Membranes with Chitosan-Coated Nanofibers for Visualized Cutaneous Wound Healing Dressing. *ACS Applied Materials & Interfaces* [online]. ACS

- Publications, May 2020, vol. 12, p. 24370–24379. Available from: <https://doi.org/10.1021/acsami.0c05604>
82. VALIEI, Amin, LIN, Nicholas, MCKAY, Geoffrey, NGUYEN, Dao, MORAES, Christopher, HILL, Reghan J. and TUFENKJI, Nathalie. Surface Wettability Is a Key Feature in the Mechano-Bactericidal Activity of Nanopillars. *ACS Applied Materials & Interfaces* [online]. ACS Publications, June 2022, vol. 14, p. 27564–27574. Available from: <https://doi.org/10.1021/acsami.2c03258>
 83. JENKINS, J., MANTELL, J., NEAL, C., GHOLINIA, A., VERKADE, P., NOBBS, A.H. and SU, B. Antibacterial effects of nanopillar surfaces are mediated by cell impedance, penetration and induction of oxidative stress. *Nature Communications* [online]. Springer, April 2020, vol. 11, p. 1626. Available from: <https://doi.org/10.1038/s41467-020-15471-x>
 84. SAM, Samanta, JOSEPH, Blessy and THOMAS, Sabu. Exploring the antimicrobial features of biomaterials for biomedical applications. *Results in Engineering* [online]. Elsevier, March 2023, vol. 17, p. 100979. Available from: <https://doi.org/10.1016/j.rineng.2023.100979>
 85. RAY, Pragyana, CHAKRABORTY, Ruchira, BANIK, Oindrila, BANOTH, Earu and KUMAR, Prasoon. Surface Engineering of a Bioartificial Membrane for Its Application in Bioengineering Devices. *ACS Omega* [online]. ACS Publications, January 2023, vol. 8, p. 3606–3629. Available from: <https://doi.org/10.1021/acsomega.2c05983>
 86. ALTUNTAS, Sevde, DHALIWAL, Harkiranpreet Kaur, RADWAN, Ahmed Eid, AMIJI, Mansoor and BUYUKSERIN, Fatih. Local epidermal growth factor delivery using nanopillared chitosan–gelatin films for melanogenesis and wound healing. *Biomaterials Science* [online]. Royal Society of Chemistry, January 2023, vol. 11, p. 181–194. Available from: <https://doi.org/10.1039/d2bm00836j>
 87. THIRUPATHI, Kokila, RAORANE, Chaitany Jayaprakash, RAMKUMAR, Vanaraj, ULAGESAN, Selvakumari, SANTHAMOORTHY, Madhappan, RAJ, Vinit, KRISHNAKUMAR, Gopal Shankar, PHAN, Thi Tuong Vy and KIM, Seong–Cheol. Update on Chitosan-Based Hydrogels: Preparation, Characterization, and Its Antimicrobial and Antibiofilm Applications. *Gels* [online]. MDPI, December 2022, vol. 9, no. 1, p. 35. Available from: <http://dx.doi.org/10.3390/gels9010035>
 88. HEEDY, Sara, MARSHALL, Michaela E., PINEDA, Juvarelli J., PEARLMAN, Eric and YEE, Albert F. Synergistic Antimicrobial Activity of a Nanopillar Surface on a Chitosan Hydrogel. *ACS Applied Bio Materials* [online]. ACS Publications, October 2020, vol. 3, p. 8040–8048. Available from: <https://doi.org/10.1021/acsabm.0c01110>
 89. TAN, Ruwen, MARZOLINI, Nicolas, JIANG, Peng and JANG, Yeongseon. Bio-Inspired Polymer Thin Films with Non-Close-Packed Nanopillars for Enhanced Bactericidal and Antireflective Properties. *ACS Applied Polymer Materials* [online]. ACS Publications, November 2020, vol. 2, p. 5808–5816. Available from: <https://doi.org/10.1021/acsapm.0c01054>
 90. ZHENG, Xinmin, ZHANG, Pan, FU, Zhenxiang, MENG, Siyu, DAI, Liangliang and YAN, Hui. Applications of nanomaterials in tissue engineering. *RSC Advances* [online]. Royal Society of Chemistry, May 2021, vol. 11, p. 19041. Available from: <https://doi.org/10.1039/D1RA01849C>
 91. BORBOLLA–JIMÉNEZ, Fabiola V., PEÑA–CORONA, Sheila I., FARAH, Sonia J., JIMÉNEZ–VALDÉS, María Teresa, PINEDA–PÉREZ, Emiliano, ROMERO–MONTERO, Alejandra, DEL PRADO–AUDELO, María Luisa, BERNAL–CHÁVEZ,

- Sergio Alberto, MAGAÑA, Jonathan J. and LEYVA-GÓMEZ, Gerardo. Films for Wound Healing Fabricated Using a Solvent Casting Technique. *Pharmaceutics* [online]. MDPI, July 2023, vol. 15, no. 7, p. 1914. Available from: <http://dx.doi.org/10.3390/pharmaceutics15071914>
92. SAVENCU, Ioana, IURIAN, Sonia, PORFIRE, Alina, BOGDAN, Cătălina and TOMUȚĂ, Ioan. Review of advances in polymeric wound dressing films. *Reactive and Functional Polymers* [online]. Elsevier, November 2021, vol. 168, p. 105059. Available from: <https://doi.org/10.1016/j.reactfunctpolym.2021.105059>
 93. KILDEEVA, N. R., ZAKHAROVA, V. A., BARANOV, O. V., METELIN, V. B. and VASILENKO, I. A. On the Surface Properties and Biocompatibility of Films Obtained from Chitosan Solutions by Spin Coating with a Crosslinking Agent. *Nanobiotechnology Reports* [online]. Springer, June 2023, vol. 18, p. 39–46. Available from: <https://doi.org/10.1134/S2635167623010044>
 94. TAYEBI, Tahereh, BARADARAN-RAFII, Alireza, HAJIFATHALI, Abbas, RAHIMPOUR, Azam, ZALI, Hakimeh, SHAABANI, Alireza and NIKNEJAD, Hassan. Biofabrication of chitosan/chitosan nanoparticles/polycaprolactone transparent membrane for corneal endothelial tissue engineering. *Scientific Reports* [online]. Springer, March 2021, vol. 11, p. 7060. Available from: <https://doi.org/10.1038/s41598-021-86340-w>
 95. DONG, Xiaobo, LU, David, HARRIS, Tequila A. L. and ESCOBAR, Isabel C. Polymers and Solvents Used in Membrane Fabrication: A Review Focusing on Sustainable Membrane Development. *Membranes* [online]. MDPI, April 2021, vol. 11, no. 5, p. 309. Available from: <http://dx.doi.org/10.3390/membranes11050309>
 96. CHEERAROT, Onanong and SAIKRASUN, Sunan. Effects of different preparation methods (solvent casting and melt blending) on properties of chitosan-filled polylactic acid biocomposite films. *Journal of Elastomers & Plastics* [online]. Sage Journals, August 2023, vol. 55, p. 1173–1198. Available from: <http://dx.doi.org/10.1177/00952443231198468>
 97. ZENA, Yezihalem, PERIYASAMY, Selvakumar, TESFAYE, Melaku, TUMSA, Zelalem, JAYAKUMAR, Mani, MOHAMED, Badr A., ASAITHAMBI, Perumal and AMINABHAVI, Tejraj M. Essential characteristics improvement of metallic nanoparticles loaded carbohydrate polymeric films - A review. *International Journal of Biological Macromolecules* [online]. Elsevier, July 2023, vol. 242, p. 124803. Available from: <https://doi.org/10.1016/j.ijbiomac.2023.124803>



Review of nanomembranes: materials, fabrications and applications in tissue engineering (bone and skin) and drug delivery systems

Urtė Ciganė^{1,*} , Arvydas Palevičius¹, and Giedrius Janušas¹

¹ Faculty of Mechanical Engineering and Design, Kaunas University of Technology, Studentu str. 56, 51424 Kaunas, Lithuania

Received: 1 March 2021

Accepted: 9 May 2021

© The Author(s), under exclusive licence to Springer Science+Business Media, LLC, part of Springer Nature 2021

ABSTRACT

Nanomembrane is an independent structure with a thickness of 1–100 nm and with much large lateral dimensions. Due to the unique properties of nanomembranes, research on the category of structures is valuable. Furthermore, nanomembranes have received a lot of attention from scientists because those types of structures can be used in various bioengineering branches. However, biocompatibility and toxicity of nanomembranes are not fully understood yet. In terms of mechanical engineering, nanomembranes must have mechanical strength, surface treatment to ensure the required structure. Mechanical properties can be affected through the material, fabrication method, porosity. For the application of nanomembranes in bioengineering, it is important to develop research to improve the biocompatibility and mechanical strength of nanomembranes. In this paper, according to the recent achievements, classification of materials, fabrication methods, and porosity are reviewed and summarized. Applications of nanomaterials in tissue engineering (bone and skin) as well as in drug delivery systems are also presented. The aim of the paper is to highlight the role of synthetic nanomembranes in the context of nanotechnologies and provide applications of functionalized nanomembranes in bioengineering. Before continuing noble and costly research, it is necessary to know the key principles and references for understanding progress of nanomembranes over the past decade.

Handling Editor: Annela M. Seddon.

Address correspondence to E-mail: urte.cigane@ktu.lt

<https://doi.org/10.1007/s10853-021-06164-x>

Published online: 20 May 2021

 Springer

Introduction

Nowadays, nanomembranes are an interesting and growing field of nanoscience that is important economically and ecologically [1]. Nanomembranes are one of the classes of nanomaterials that is a particularly attractive topic in the field of nanotechnology [2]. Ultra-thin-structured nanomembranes have relatively large lateral dimensions (millimeter or even centimeter scales) and are strong enough to stand freely without additional support or base. Versatility, unique structure, high stability, wide range of control parameters distinguish nanomembranes compared to other platforms; in addition, studies have shown that the porous structure of the nanomembrane can be used for a variety of future purposes [3].

From the view of appropriate nanostructure membrane, mechanical properties play a key role [4]. Mechanical properties can be affected through the material, fabrication method or porosity [5]. For instance, as porosity increases, permeability and bioactivity increase, and mechanical properties decrease exponentially [4]. However, there are not many nanomembranes that are biocompatible and have good mechanical strength. For this reason, it is important to analyze, search for and develop nanomembranes that would be applicable for various areas.

Notably, the application of different materials changed over time [6]. The application can be affected through the environmental changes, various research, new technologies, requirements or human needs [7–9]. Therefore, the materials used in the fabrication of nanomembranes are also changing [10, 11]. Over time, a wide range of nanomembranes has been developed. There are ~ 937 publications on 'ScienceDirect' that included the keyword of 'nanomembrane' that they were published 2010–2020. The number of publications on

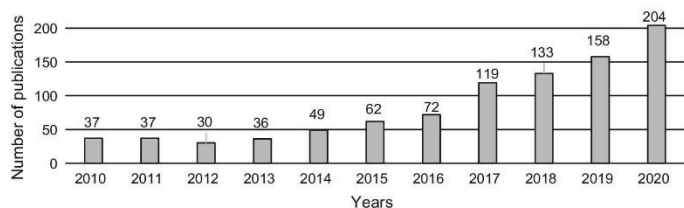
nanomembranes has increased every year since 2012 (Fig. 1), and this confirms that interest in nanomembranes has grown over the past decade.

A wide range of nanomembranes has led to the classification of these structures in several groups [12]. Because mechanical properties of nanomembrane can be affected through the material, fabrication method or porosity, all nanomembranes can be categorized according to their various characteristics, fabrication techniques, etc. [13]. One of the classifications is related to the fabrication methods of nanomembranes [14]. Moreover, considering the porosity, nanomembrane strength, permeability, chemical or thermal stability, the suitable method for fabrication of nanomembranes should be selected [15, 16].

Nanomembrane technology allows the creation of unique properties using nanogeometry [17, 18]. Due to their unique properties, nanomembranes are attracted to utilizing in a variety fields [19–22]. Bioengineering is one of the fields where nanomembranes have made progress [23–25]. Nanomembranes can be used in bioengineering (bones or skin tissues), as well as in the drug delivery systems, and this provides an opportunity to treat patients with various diseases more effectively [26–28]. However, a combination of biocompatibility, porosity and mechanical strength is not fully understood and revealed yet; therefore, it is essential to ensure mechanical strength in biocompatible nanomembranes [29], because it is one of the most important parameters in nanomembranes [30].

The aim of the paper is to highlight the role of synthetic nanomembranes in the context of nanotechnologies and provide applications of functionalized nanomembranes in bioengineering. Before continuing noble and costly research, it is necessary to know the key principles and references for understanding progress of nanomembranes over the past decade. For this reason, we have tried to review

Figure 1 Number of publications as a function of time, obtained by typing the keyword 'nanomembrane'.



and classify as many different synthetic nanomembranes as possible in our capabilities. More than 60% of cited references were published in the last five years. We provide a concise overview to help understand the properties, the main fabrication methods and applications of current nanomembranes in tissue engineering (bone and skin) as well as in drug delivery systems to see the potential for the development of biocompatible and mechanically strong nanomembranes in the future.

Classification of nanomembranes

The rapid development in nanomaterials encourages a focus on nanomembranes. The definition of nanomembrane may vary slightly in the scientific literature. Therefore, there is currently no widely accepted single definition. For instance, Kunitake and co-workers [31, 32] developed the concept of free-standing nanomembranes, reducing confusion in the development of nanomembranes. They described 'large nanomembrane' in three aspects. First, its thickness is in the range of 1–100 nm. Second, the self-supporting (free-standing) property is a necessary feature for nanomembrane. Third, the aspect ratio of size and thickness should be greater than 10^6 , for example, if thickness is 10 nm, its size should be greater than 1 cm. Moreover, researchers highlighted two important structural features that are required for nanomembranes. It is mechanical strength and a uniform, defect-free nature over a large area. In this review paper, the nanomembrane is described as an independent structure with a thickness of 1–100 nm and with much large lateral dimensions [33]. "Large" means at least two orders of magnitude, but a much higher aspect ratio can be achieved. Moreover, nanomembranes can be classified according to their types of material, porosity or fabrication method [19, 34]. Consequently, the classifications of nanomembranes are discussed in the following sections.

Materials

Based on material, nanomembranes can be divided mainly into three categories: inorganic, organic, hybrid (composite) [13, 19].

Inorganic materials

Nanomembranes can be composed of a variety inorganic material, such as metals, composites, alloys, semiconductors. Various metals and oxides are used for the fabrication of metal nanomembranes, for example, gold (Au), palladium (Pd), aluminum oxide (Al_2O_3), titanium dioxide (TiO_2), zinc oxide (ZnO), etc. [20, 22, 35–37]. One of the widely investigated nanomembranes is anodic aluminum oxide (AAO) membranes [18]. Even though AAO nanomembranes have been known for more than six decades, AAO remains very attractive due to highly ordered porous structure, high density and wide range of pore diameter [38]. Further on, metal composites and alloys nanomembranes consist of components composed of several atoms/molecules. For example, it could be nanomembrane where the main material is metallic alloys [39]. One of the most widely known and used semiconductor nanomembranes are made of silicon [40]. Semiconductor nanomembranes can be made of materials, such as germanium sulfide (GeS), molybdenum disulfide (MoS_2) [41, 42]. Various inorganic nanomembranes can be characterized by physical and chemical stability. Furthermore, inorganic nanomembranes with well-ordered pores have better mechanical properties [13].

Organic materials

Because organic compounds are defined as carbon compounds, organic nanomembranes constitute a huge class of nanomembranes. In addition, organic nanomembrane may be composed of one or more organic materials. Examples of organic nanomembranes are polyacrylonitrile (PAN), polyvinylchloride (PVC), polyamide, polysulfone, etc. [2, 43–46]. The advantages of organic nanomembranes are relatively low cost and quite good biocompatibility [13].

Hybrid materials

The structures of these nanomembranes are often made by polymers and inorganic nanofillers. An example is a poly(3,4-ethylenedioxythiophene) (PEDOT) and carbon nanotube sheets (CNS) hybrid nanomembrane with a nanoscopic thickness (≈ 112 nm) [47]. Another example may be the high-aspect-ratio functionalized conductive graphene (FCG) and silver (Ag) nanomembrane [48]. Hybrid

nanomembranes can be made of a variety organic and inorganic component. For this reason, hybrid nanomembranes are often difficult to synthesize. However, hybrid membranes can have a variety required properties [49].

Porosity

Other classification of nanomembranes is based on porosity. The nanometer size of the pores is one of the most important criteria in nanomembranes because many functions of nanomembranes depend on the porosity [14], including mechanical strength. Nanoporous materials are often classified according to pore size, shape and pore distribution [13, 14]. Following this, classifications are presented and discussed below.

Pore size

One of the typical classifications of nanomembranes is based on pore size. Classification is shown in Table 1.

Such classification of pore size is used most often because it is based on the International Union of Pure and Applied Chemistry (IUPAC) [14, 50]. In other literature source [51], all pores with a diameter of less than 100 nm are referred to as nanopores.

All types of nanomembranes (inorganic, organic, hybrid) can be characterized by different pore sizes. It depends on the specific nanomembrane. For example, the pore size of polymeric nanomembranes generally is meso-macrosized (> 20 nm) [13]. Meanwhile, the pores size of oxides is micro-mesozized in most cases.

Pore shape

Depending on the shape of the pores, the pores can be divided into channels, regular shapes (cylinders, spheres, cones), irregular shapes and complementary [13, 14, 51]. Examples of possible pores shapes are given in Fig. 2.

Table 1 Pore size of nanomembranes [13, 14]

Pore size of nanomembranes	
Microporous	< 2 nm
Mesoporous	2–50 nm
Macroporous	> 50 nm

In addition to this, other classification of pores' shapes is also possible, for instance, nanomembranes with straight or curved pores [14].

Inorganic, organic and hybrid nanomembranes may have pores of different shapes. It depends on nanomembrane material. For example, carbon nanomembrane (which is fabricated from terphenylthiol) has channels [52].

Pore distribution

Pore distribution can be classified into two types: ordered and disordered. To apply nanomembranes in various fields, orderly distribution of pores is very important, because with an orderly structure it is easier to control required processes. An example of highly ordered nanopores may be aluminum oxide (Al_2O_3) [53], titanium dioxide (TiO_2) [54] or silicon dioxide (SiO_2) [55].

Summarizing the nanomembranes classification by pore geometry, it can be confirmed that different nanomembranes have different pore size, porosity, surface properties. These properties of inorganic, organic and hybrid nanomembranes are summarized and presented in Table 2.

Thermal and chemical stability, costs of fabrication and lifetime are also important for nanomembranes. For example, metal oxides nanomembranes have the best thermal, chemical and mechanical stability [61]. However, polymeric nanomembranes are characterized by low fabrication cost [62].

Fabrication methods

Another classification of nanomembranes is according to fabrication method. There are many techniques to fabricate various nanomembranes. In this paper, the main methods, including anodization, lithography, micromachining, chemical vapor deposition, layer-by-layer deposition, sol-gel processing, 3D printing and other methods, were carefully reviewed. Following, the main principles, advantages, disadvantages and nanomembranes produced by each method are presented and discussed below.

Anodization

Based on previous research reports of AAO studies, it appears that the anodizing process of AAO can be classified [53]. The main research on the method of

Figure 2 Examples of possible pore shapes.

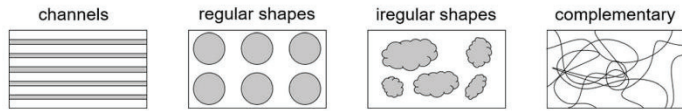


Table 2 Properties of inorganic, organic and hybrid nanomembranes [11, 36, 53–60]

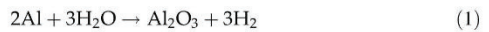
	Inorganic nanomembranes		Organic nanomembranes		Hybrid nanomembranes
	Metal	Oxides	Carbon	Polymeric	
Pore size	Meso–macro	Micro–meso	Micro–meso	Meso–macro	Micro–meso Meso–macro
Porosity	Low	Medium	High	Low	Medium
Strength	Strong	Medium	Low	Medium	Medium–strong
Biocompatibility	Low–medium	Low–medium	High	High	Medium–high
Permeability	High	Low–medium	Low–medium	Low–medium	Low–Medium
Chemical stability	High	Very high	High	Low–medium	Medium–high
Thermal stability	High	Medium–high	High	Low	Medium
Fabrication costs	Medium	Medium	Medium	Low	Medium–high
Lifetime	Long	Long	Long	Short	Medium–long

preparation of porous alumina film is classified into two methods: steady state and non-steady state [63]. Steady-state anodization is consisted of two methods: mild (soft) and hard anodization [53]. Comparing these two methods, the hard anodizing reaction process is fiercer, and the growth rate of the porous AAO film is faster. For these reasons, a lot of heat is released, which means that more requirements for cooling equipment are needed [63]. Non-steady-state anodization is generally consisted of two methods: periodic and pulsed anodization [63]. Comparing these two methods, the periodic anodizing method can more precisely regulate AAO film porous internal structure. Due to appearance, AAO nanomembranes with a special structure can be applied in many areas [63].

It is known that a protective layer is formed on the aluminum surface during the anodizing process. The parameters (such as the thickness of the barrier layer, pore diameter) of the anodic layer depend on the voltage which is used to form the layer [64]. Also, the surface of aluminum depends on voltage and current. At low voltages and high currents, electric polishing effects occur. As the voltage is increased, the current decreases, and a porous layer is formed. When the value of current is low and voltage is high, a thick layer of aluminum oxide is formed.

AAO patterns are gradually grown in acid solutions that anodize aluminum under the electric field between two electrodes. The mechanism of the anodization technique is presented in Fig. 3.

Anodization can be described by chemical reactions occurring on the electrodes [56, 65]. Chemical reactions are given in Fig. 2. Overall anodization Eq. (1) is given below:



It is known that different electrolytes can result different pore diameters and mutual resistances in AAO [66]. Different electrolytes are shown in Table 3. Research has shown that other acids, such as boric and chromium, can also be used for AAO fabrication. However, AAO pores are much inferior to these electrolytes [67].

The pore diameters and the interpore distances often increase as the anodizing voltage increases [56, 65, 66]. As the electrolyte concentration increases, the pore diameter increases as well [19, 68]. Pore size also depends on the temperature and pH of the solution. Recently, it has been reported that the pore diameter decreases with decreasing temperature and pH of the solution [68]. The main advantages and disadvantages of anodization are presented in Table 4.

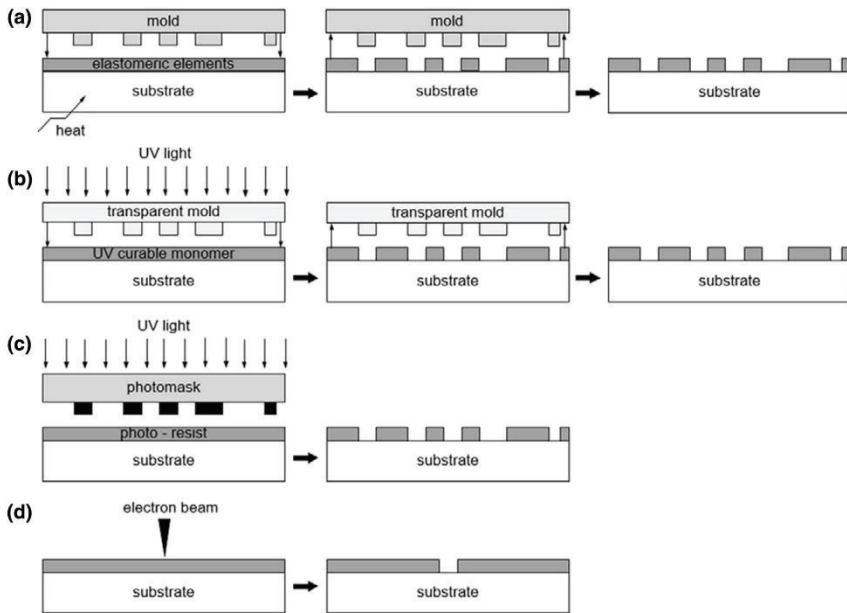


Figure 4 Schematic illustrations of the main steps of: **a** nanohot-embossing imprint lithography; **b** nano-UV-imprint lithography; **c** photolithography; **d** E-beam lithography.

nanoimprint lithography and electron beam lithography are presented in Fig. 4.

Applying nanohot-embossing imprint lithography (Fig. 4a), the structure is formed when the mold is pressed on the heated elastomeric element [74]. Although significant progress was made in a short time in nanoimprint lithography [75], during nano-UV-imprint lithography (Fig. 4b), the transparent mold contacts ultraviolet (UV) curable monomer, then the monomer is exposed to UV light and the desired structure on the surface is obtained [76]. One of the important challenges is the useful lifetime of the mold because mold requires replacement after about fifty imprints. Another challenge is the high

viscosity of polymeric films because it limits pattern size and feature density [75]. More advantages and disadvantages of nanoimprint lithography are presented in Table 5.

During photolithography (Fig. 4c), UV light passes through a photomask and effects certain areas of the photo-resist surface [72]. Photo-resist is organic material that is sensitive to UV light. Photolithography has advantages, such as very high efficiency, the possibility to use any base shape and size, easy monitoring of substrate shape and size [71]. However, photolithography has disadvantages as well. The main disadvantages are that a clean environment with dim lights is required, expensive machines are

Table 5 Advantages and disadvantages of nanoimprint lithography [73]

Nanoimprint lithography	
Advantages	Disadvantages
Easy production of nanoscale features	Difficult production of mold Stamp deformation
Possibility of using stamps many times	
Extremely small resolutions features (lower than 10 nm)	
Relatively inexpensive method compared to UV lithography	

Table 6 Advantages and disadvantages of photolithography [71, 73]

Photolithography	
Advantages	Disadvantages
Versatility of the process	Very expensive equipment
Process efficiency	A clean environment and a room with dim lights is a must
Easy monitoring of substrate shape and size	

required, and the surface chemical properties cannot be controlled and have a rigid structure [71]. The main advantages and disadvantages of photolithography are summarized in Table 6.

During e-beam lithography process (Fig. 4d), a small spot of the electron beam moves over the electron-sensitive resist surface [77]. In this way, the desired surface pattern is formed. The main advantages and disadvantages of electron beam lithography are presented in Table 7.

As well, other lithographic methods have their advantages and disadvantages, which are already presented in the scientific literature [70–73, 75, 78]. Additionally, lithography is used to fabricate different nanomembranes, such as carbon nanomembranes, various types of hybrid nanomembranes [58–60].

The main advantages of lithography are process efficiency and versatility. However, lithography is an expensive method due to the equipment.

Micromachining

Many different nanostructures can be fabricated on various metals, alloys, semiconductors and polymers by micromachining [57, 79]. Micromachining involves specific methods that can be used for micro- and nanoscale membranes. Noteworthy that nanoimprint lithography can be classified as one of the micromachining techniques, but in this review,

micromachining includes one of the latest technologies which has received great attention in nanomembranes fabrication [79, 80]. It is a laser micromachining. Laser micromachining is the process when a laser beam moves in a defined path and creates the required pattern [81]. Various nanostructures can be fabricated on metals (Au, Ag, nickel (Ni)), semiconductors (gallium nitride (GaN), silicon (Si), MoS₂), organics and polymers (protein, polyimide foil) using laser process [82]. This type of micromachining aims to produce membranes with high-precision and very restrictive dimensional tolerances.

Laser micromachining has some advantages over other methods. The main pluses are simple equipment, one-step process, efficient process, contactless machining, the possibility of various structures [57]. Although the equipment is simple, it is expensive. More advantages and disadvantages of laser micromachining are presented in Table 8.

In summary, micromachining is a relatively simple method and has many alternatives for the nanomembranes fabrication. One of the main disadvantages is the expensive equipment.

Chemical vapor deposition

Among the various nanomembrane manufacturing technologies, chemical vapor deposition (CVD) is receiving a lot of attention [86]. The deposition of a

Table 7 Advantages and disadvantages of electron beam lithography [71, 73]

Electron beam lithography	
Advantages	Disadvantages
Easy production of nanoscale features	Very expensive equipment
Pattern writing directly to the wafer	System is more complex than other methods systems
Fast turn-around time	Inefficient industrial processing
Flexibility of the technique	Large scatter of minimum features
	Long time of patterning entire wafer

Table 8 Advantages and disadvantages of laser micromachining [57, 82–85]

Laser micromachining	
Advantages	Disadvantages
Simple equipment	Expensive equipment
One-step process	Significant number of process parameters
Efficient process	Thermal stresses of material
Contactless machining	
Application of the process to the surfaces of any 3D object	
The possibility of various structures	
Possibility to machine using many different environments (gases, liquids, vacuum)	

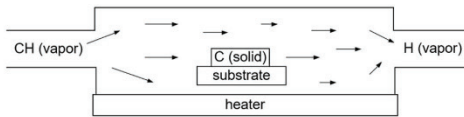


Figure 5 Schematic illustration of chemical vapor deposition (CVD).

solid heater surface due to a chemical reaction in the vapor phase can be called CVD. Schematic illustration of CVD is presented in Fig. 5.

During the CVD process, the precursor decomposes at high temperature. Then the gaseous atoms adsorb and deposit on the substrate. During the surface chemical reaction, a continuous film is formed [87]. Consequently, various oxides (iron, tin, titanium, etc.), polymers (polypyrrole, poly(3,4-dimethoxythiophene) (PDMT), polythiophene, polyaniline, etc.) semiconductors (molybdenum disulfide), metal alloys (platinum-cobalt) and other nanoporous materials can be produced by CVD [86, 88–92]. The advantages and disadvantages of chemical vapor deposition are presented in Table 9.

Chemical vapor deposition method can be easily applied to mass production, and it gives an advantage over other methods.

Layer-by-layer deposition

Another method of nanomembrane fabrication is layer-by-layer deposition which involves the adsorption of different charged molecules. For example, the substrate is immersed in a dilute solution of a cationic polyelectrolyte [93]. The polyelectrolyte is adsorbed as a single monomolecular sheet with a thickness of about 1 nm [14]. Then the wafer is washed and dried. Further, the polish-coated substrate is placed in a dilute dispersion of polyanions [93]. A new monolayer is formed over the previously deposited layer. Then the wafer is washed and dried again. The process can be repeated with the same or new materials, and thus, the desired number of layers can be obtained [14]. Layer-by-layer deposition method gives multilayers with a thickness 5 nm to over 500 nm [19]. Schematic illustration of layer-by-layer deposition is presented in Fig. 6.

Table 9 Advantages and disadvantages of chemical vapor deposition (CVD) [88, 90, 91]

Chemical vapor deposition	
Advantages	Disadvantages
Very fast synthesis of monodisperse nanoparticles	High temperature required (the most versatile at temperatures of 600 °C and higher)
Easy control of binary compositions	Instability of substrates at high temperatures
Easily adaptable to large volume	Relatively complex equipment
Membrane uniformity	
Material composition and phase control	
Good density of microstructures	

Figure 6 Schematic illustration of layer-by-layer deposition.

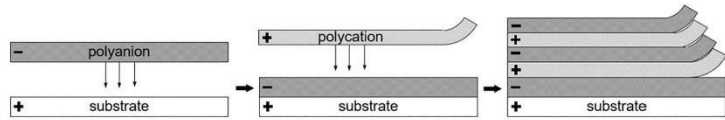


Table 10 Advantages and disadvantages of layer-by-layer deposition [62, 94].

Layer-by-layer deposition	
Advantages	Disadvantages
Simple equipment	Free standing nanocomposite membrane
Cost-effective time-efficient fabrication	Extreme robustness of nanomembranes
A wide variety of different composite nanomembranes	Multistep process

The main advantages and disadvantages of layer-by-layer deposition are presented in Table 10.

Various metals (gold), carbon materials (graphene) and other materials (polyamide, poly(sodium 4-styrene sulfonate), poly(alkylamine hydrochloride)) can be used to fabricate multilayered nanomembranes which are made by using layer-by-layer deposition [62, 95–97].

Because layer-by-layer deposition can be adapted to produce a wide variety nanomembranes, it is a relatively inexpensive and simple method.

Sol-gel processing

Sol-gel formation technique can be used to fabricate various nanomembranes. This method is a wet chemical forming technique that usually consists of four main forming steps [98]. During first step, a homogeneous solution with salt or metal must be prepared. Second, the concentration of the homogeneous solution needs to be increased. The third step is to form the gel by condensation. The last step is to dry the gel. Sol-gel method makes it possible to obtain various structures which can have excellent electrical, optical, thermal, magnetic or mechanical properties. This method is relatively economical process. Moreover, the advantages of this method are reproducibility, low-temperature chemistry, high surface to volume ratio [99]. The main advantages and disadvantages of sol-gel method are presented in Table 11.

By using sol-gel method, various ceramics, metals, oxides and polymers can be used to fabricate nanomembranes [2, 98, 100–103]. Furthermore, modified sol-gel method can be also used, such as ultrasonic-assisted sol-gel method, precipitation,

Table 11 Advantages and disadvantages of sol-gel processing [99]

Sol-gel processing	
Advantages	Disadvantages
Simple equipment	Need of costly organic solvents
Cost-effective	Multistep process
Highly controllable synthesis	
Low-temperature chemistry	

aerogel method [104]. By using modified sol-gel methods, it is possible to improve mechanical properties and porosity of the nanomembranes, as well as to introduce the desired functionalities. In addition, sol-gel process has opened several new branches in bioengineering, including drug delivery or organ implantation. The quality of the process has led researchers to investigate this method over the past few decades [99].

3D printing

3-Dimensional (3D) printing, commonly referred to as additive manufacturing (AM), allows to create complex and diverse geometric shapes in different materials [105]. 3D printing is a process of joining materials when production takes place layer upon layer [106]. According to International Standard ISO/ASTM 529,000:2015, AM processes can be classified into seven categories: binder jetting, directed energy deposition, material extrusion, material jetting, powder bed fusion, sheet lamination, vat photopolymerization. Seven AM processes are reviewed and summarized in [106]. The main advantages and

Table 12 Advantages and disadvantages of 3D printing [105–107]

Process	Configuration of 3D-printed membrane	Advantages	Disadvantages
Binder jetting	Any geometry	The possibility of using a wide range of materials Cost-effective	Poor strength Moisture-removal required (after processing) Limited mechanical properties
Directed energy deposition	Any geometry	High material deposition rate High material utilization	Poor surface resolution Poor-dimensional accuracy Limited materials for production
Material extrusion	Any geometry	The possibility of using a wide range of materials (including biocompatible and medical-grade materials) Simple equipment Versatile and easy to customize	Relatively long fabrication time Requires support structures Reduced strength in the vertical direction
Material jetting	Any geometry	High resolution and accuracy The possibility of multi-materials The possibility of multi-colors	Non-recyclable support materials Limited mechanical properties
Powder bed fusion	Any geometry	The possibility of using a wide range of materials No support structures High resolution for metals	Relatively long fabrication time Expensive equipment
Sheet lamination	Flat sheet	Time-efficient fabrication No support structures The possibility of multi-material The possibility of multi-colors	Noxious fumes during thermal cutting Poor strength
Vat photopolymerization	Any geometry	The possibility of using a wide range of materials Time-efficient fabrication Nanometer resolution	Require support structures Support-removal required (after processing)

disadvantages of seven AM processes are presented in Table 12.

3D-printed nanomembranes are an interesting and emerging field of membrane research [108]. The highest resolution membranes are obtained using two-photon polymerization (vat photopolymerization) [109]. Resolution is about 100 nm. Method is based on the absorption of two photons in a transparent resin. Unfortunately, other AM processes are not suitable to produce nanomembranes due to their limited resolution [105]. All processes are constantly improving to make nanomembrane fabrication applicable.

There are many materials that can be used in 3D printing. Due to simple processing, low cost, biocompatibility, mechanical properties, polymers are widely used in 3D printing. To improve properties such as processability, mechanical strength and

bioactivity, ceramic and hybrid materials (composites) can also be used for 3D printing, but 3D printing of such materials has limitations [110]. A variety of materials have already been used for tissue engineering, including polycaprolactone (PCL), bioactive glasses, polylactic acid (PLA)/polyethylene glycol (PEG), zirconia, tricalcium phosphate, poly(3-hydroxybutyrate), hydroxyapatite (HA), etc. [111, 112]. Moreover, mechanical strength is an important characteristic because materials can be exposed to relatively high pressures in a variety of environments during 3D printing. Unfortunately, due to low resolution, 3D printing technology is not yet sufficiently advanced for nanomembranes fabrication [108].

Other methods

There are also many other methods that can be used to fabricate and develop various organic, inorganic or

hybrid nanomembranes. For polymeric membrane fabrication, the key factors of track etching and sintering, electrospinning, non-solvent-induced phase separation, vapor-induced phase separation methods are critically reviewed in [113]. Other methods, including thermally induced phase separation, melt-spinning and cold-stretching, phase separation micromolding, soft molding and manual punching, are well introduced and discussed in [114]. Moreover, block copolymer, dip coating, drop coating and other methods have been widely used in the fabrication of various types of nanomembranes. Each method is described in detail in [19]. Also, novel methods for nanomembranes fabrication are introduced in [1, 115]. Various novel methods to produce nanomembranes are constantly being developed. The evolution of nanotechnology has opened new possibilities, leading to the development and improvement of different nanomembrane fabrication methods that enable the production of better quality and mechanically stronger nanomembranes [1].

Application in bioengineering

Bioengineering is a multifunctional science that includes a lot of different fields, such as mechanical and chemical engineering, chemistry and biochemistry, materials science. Bioengineering can also be defined as a combination of natural and engineering science [116]. Accordingly, nanomembranes have played an important role in bioengineering [117], and due to various properties, nanomembranes can be applied in this field [118]. To achieve specific results, such as wound closure, control of fluid loss by strengthening the treated tissue, it is necessary to know the properties of nanomaterials because they change tremendously at the nanometer scale [119]. Even if a small number of nanoparticles is embedded in any other polymeric matrix, the performance can be improved to unprecedented levels [120]. Special attention is paid to tissue engineering or drug delivery systems, due to their unlimited potential to improve the quality of human health. Every year, a lot of people suffer from bone defects resulting from trauma, tumor or bone disease, which means that nanomembranes can open a huge number of possibilities in medicine [121]. Sterilizability, storability, processability are essential for clinical applications [122]. In the following, various (organic, inorganic or

hybrid) nanomembranes which can be used in bioengineering are presented.

The skin is the largest organ of the human body that acts as a protection against pathogens in the external environment. Also, the skin helps regulate heat and retain moisture throughout the body. For the skin to perform its function well, skin must be healthy, and in case of damages (burns, acute wounds, etc.)—it must be treated and renewed. Nanomaterials can be used to restore the lost skin anatomy and physiology [119]. Natural biomaterials, such as chitosan, have a great advantage because of low toxicity and low chronic inflammatory response [119]. However, synthetic nanomaterials have advantages, such as low cost, and can be described over natural materials. For example, carbon nanostructures have low toxicity, good mechanical properties and can mimic the natural mechanical strength of bone [123]. Among inorganic nanomaterials used to treat wounds, for example, metals and oxides (silver, gold, etc.), play an important role. Silver has been used as a therapeutic agent to treat wounds. In other studies, titanium dioxide (TiO_2) was embedded in several scaffolds to improve mechanical strength, which is required for skin tissue engineering [119]. Among organic nanomaterials, graphene oxide acts as a soft nanomembrane with high stiffness and biocompatibility, so this oxide can be one of the alternatives in the development of stem cell culture [123]. Other studies have reported that Rana chensinensis skin collagen/poly(L-lactide) (PLLA) hybrid nanomembrane, produced by electrospinning, was characterized by higher mechanical strength compared to natural collagen nanofiber [124]. Studies have shown that new hydrogen bonds have been formed between the collagen amide groups and PLLA carboxyl groups. Such membranes provide a promising approach to the production of skin wound dressings. Furthermore, nanoporous PLA nanomembranes have been successfully fabricated by using phase segregation technique and it is argued that significant advances can be made in the use of nanoporous PLA nanomembranes for tissue regeneration processes [125]. Silicon carbide nanomembranes have features such as chemical stability, specific ion permeability, flexibility and durability. Polyvinylpyrrolidone blended nanofibrous membrane was prepared by an electrospinning technique [126]. Studies have shown the efficacy of this membrane and its potential to be used in

biomedical wound dressings that would accelerate the healing of acute skin wounds. Moreover, silicon carbide nanomembranes have been found to be suitable for flexible implantable devices because biocompatibility and required mechanical strengths show the prospects for these nanomembranes [127].

Bone is one of the most durable tissues that supports and protects vital organs in the body [128]. Thus, bone tissue engineering is receiving increasing attention due to significant advances in cell and organ transplantation, as well as advances in engineering [129]. Accordingly, bone is mainly composed of organic and inorganic components, so a variety of different nanomaterials and combinations can be used in bone tissue engineering. Some of the most popular materials used in bone tissue engineering are ceramics (hydroxyapatite or tricalcium phosphate), chitosan, collagen, polystyrene, acrylates, polyglycolic acid, etc. [19]. Moreover, a lot of carbon-based nanomaterials, such as graphene, carbon nanotubes, carbon nanofiber, can be used in bone tissue engineering. For example, graphene oxide has good biocompatibility and high minimal cytotoxicity to living cells, so graphene oxide can be used as a nanomembrane for bone tissue engineering [130, 131]. The advantages of carbon nanomaterials are very good mechanical stability and commercial availability [132]. As well, organic material, such as ultra-high molecular weight polyethylene, is often used in bone structures, too [133]. Another example is the inorganic materials. Inorganic nanomaterials, such as pure titanium, titanium alloys, ceramics, are generally used in bone structures [133]. The advantages of silica nanomaterials and composites are good biocompatibility, low toxicity, a large active surface area, ability to act as carriers for drugs or essential minerals [132].

Effective drug delivery remains a challenging task and gets more attention nowadays. Nanomembranes have great potential for drug delivery systems. For example, porous anodic alumina is one of the oldest and most attractive nanomembrane that could be applied in bioengineering [134]. However, AAO biocompatibility is one of the most challenging issues. There is concern about the use of AAO when it comes in direct and constant contact with the human body. It has been shown that AAO pores diameter can affect the diffusion of molecules across the membrane. So, AAO scaffolds can be mechanobiologically implants to which cells respond

positively [135]. Therefore, AAO can be used for drug delivery. On the other hand, the application of titanium dioxide nanotubes is also a viable alternative for the development of various localized drug delivery systems. TiO_2 has useful drug delivery properties, such as nanotube dimensions, geometry, surface chemistry, large surface area, universal drug loading capability for multiple drugs. Studies have shown that TiO_2 implants have significant clinical therapy potential that can be realized commercially [28]. Importantly, long-term toxicity studies and tolerability studies in animals should be evaluated before initiating human clinical trials to evaluate the safety of empty TiO_2 and drug-filled TiO_2 . More *in vivo* studies are urgently needed. Another example is organic nanomaterials that can be used for drug delivery [136]. Such examples may be polymeric nanostructures: polyglycidyl methacrylate nanotubes, PEG, PEDOT nanotubes, etc. [137]. Due to the proper pore geometry and large surface area, these and other nanomaterials have great potential for being used in drug delivery systems. Moreover, polylactic-co-glycolic acid (PLGA) nanomembrane made by electrospinning technique is popular in drug delivery systems [138]. Studies have shown that PLGA nanomembrane is effective in reducing pain. Using CVD method, nanostructures of poly(*n*-isopropylacrylamide), poly(methacrylic acid) and poly(hydroxyethyl methacrylate) were synthesized [139]. Due to the response to temperature and pH, the structures can be externally activated. Other examples could be nanofiber membranes. Poly(*N*-isopropylacrylamide) (PNIPAM)/gelatin nanofibers produced by electrospinning showed the release of anti-cancer drug from the membrane at a specific temperature [140]. Besides, PLA/graphene oxide nanofiber membranes with different structures were prepared by electrospinning and demonstrated the promising potential for scaffolds in drug delivery systems [141]. Core-sheath nanofibers for drug delivery application still have many challenges, which are highlighted in review article [142]. Furthermore, PCL/shellac/PCL nanofiber sandwich-structured membrane possessed good mechanical and other properties and met the requirements for membrane to be used in overnight skin care applications on the face as drug release process takes 8 h [143]. All the results can be the basis for further research in development of nanomembranes.

Conclusions

Mechanical strength plays a crucial role in nanomembranes. However, many nanomembranes cannot already be used in bioengineering because a lot of membranes are characterized by insufficient mechanical strength, biological incompatibility or toxicity to the human body. Because mechanical properties of nanomembrane can be affected through the material, fabrication method or porosity, we summarized various classifications of nanomembranes in this review. According to the material, nanomembranes are divided into three groups: inorganic, organic and hybrid. Noteworthy, inorganic nanomembranes have better properties and adaptability when their pores are ordered; meanwhile, the advantages of organic nanomembranes are relatively low cost and good biocompatibility. Even though hybrid nanomembranes are often difficult to fabricate, it can have a wide range of desirable properties. According to nanomembranes porosity, it was determined that when porosity increases, mechanical strength decreases exponentially. Moreover, the main nanomembranes fabrication methods, including anodization, lithography, micromachining, chemical vapor deposition, layer-by-layer deposition, sol-gel processing, 3D printing and other methods, were presented. The main advantages of anodization are well-ordered porous structures, the ability to control pore diameter and low fabrication cost. However, the main advantages of lithography are process efficiency and versatility. On the other hand, lithography is an expensive method due to the required equipment. For the same reason, micromachining is expensive method, too. Chemical vapor deposition method can be easily applied to mass production and give the advantage over other methods. In terms of layer-by-layer deposition, this method is simple and relatively inexpensive. 3D printing is a relatively new method of manufacturing nanomembranes; unfortunately, AM processes are still not suitable for producing nanomembranes due to their limited resolution. 3D printing technologies are constantly improving to make nanomembrane fabrication applicable. To produce better quality and mechanically stronger nanomembranes, various new fabrication methods are constantly being developed. Therefore, there are still many challenges and opportunities for nanomembrane technologies in bioengineering branches, such as tissue (skin and bone) engineering

or drug delivery systems. Connection between mechanical strength and biocompatibility of nanomembranes will depend on innovation, new material combinations, scalability and sustainability of new methods. In rapidly expanding bioengineering branches, this review article contributes to further research on nanomembranes.

Acknowledgements

This research was funded by a Grant No. S-MIP-19-43 from the Research Council of Lithuania.

Declaration

Conflict of interest The authors declare that they have no conflict of interest.

References

- [1] Figovsky O (2020) Producing nanomembranes by novel methods. In: Kharisova O, Martinez L, Kharisov B (eds) Handbook of nanomaterials and nanocomposites for energy and environmental applications. Springer, Cham. https://doi.org/10.1007/978-3-030-11155-7_82-1
- [2] Agboola O, Sadiku ER, Mokrani T (2016) Nanomembrane materials based on polymer blends. In: Thomas S, Shanks R, Chandrasekharakurup S (eds) Design and applications of nanostructured polymer blend and nanocomposite systems. William Andrew Publishing, New York. <https://doi.org/10.1016/B978-0-323-39408-6.00006-6>
- [3] Nunes SP, Culfaz-Emecen PZ, Ramon GZ, Visser T, Koops GH, Jin W, Ulbricht M (2020) Thinking the future of membranes: perspectives for advanced and new membrane materials and manufacturing processes. *J Membr Sci*. <http://doi.org/10.1016/j.memsci.2019.117761>
- [4] Christy PN, Basha SK, Kumari VS, Bashir AKH, Maaza M, Kaviyarasu K, Arasu MV, Al-Dhabi NA, Ignacimuthu S (2020) Biopolymeric nanocomposite scaffolds for bone tissue engineering applications: a review. *J Drug Deliv Sci Technol*. <https://doi.org/10.1016/j.jddst.2019.101452>
- [5] Yang Y, He C, Yang W, Qi F, Xie D, Shen L, Peng S, Shuai C (2020) Mg bone implant: Features, developments and perspectives. *Mater Des* 185:108259. <https://doi.org/10.1016/j.matdes.2019.108259>
- [6] Cha GD, Kang D, Lee J, Kim DH (2019) Bioresorbable electronic implants: history, materials, fabrication, devices, and clinical applications. *Adv Healthcare Mater* 8:1801660. <https://doi.org/10.1002/adhm.201801660>

- [7] Andrew JJ, Srinivasan SM, Arokiarajan A, Dhakal HN (2019) Parameters influencing the impact response of fiber-reinforced polymer matrix composite materials: a critical review. *Compos Struct*. <https://doi.org/10.1016/j.compstruct.2019.111007>
- [8] Gibson R (2010) A review of recent research on mechanics of multifunctional composite materials and structures. *Compos Struct* 92:2793–2810. <https://doi.org/10.1016/j.compstruct.2010.05.003>
- [9] Xiang Y, Xu Z, Wei Y, Zhou Y, Xiao Y, Yang Y, Yang J, Luo L, Zhou Z (2019) Carbon-based materials as adsorbent for antibiotics removal: Mechanisms and influencing factors. *J Environ Manage* 237:128–138. <https://doi.org/10.1016/j.jenvman.2019.02.068>
- [10] Bhat A, Elleuch O, Cui X, Guan Y, Scott SA, Kuech TF, Lagally MG (2020) High-Ge-content SiGe alloy single crystals using the nanomembrane platform. *ACS Appl Mater Interfaces* 12:20859–20866. <https://doi.org/10.1021/acsmi.0c02747>
- [11] Li G, Ma Z, You C, Huang G, Song E, Pan R, Zhu H, Xin J, Xu B, Lee T, An Z, Di Z, Mei Y (2020) Silicon nanomembrane phototransistor flipped with multifunctional sensors toward smart digital dust. *Sci Adv* 6:eaaz6511. <https://doi.org/10.1126/sciadv.aaz6511>
- [12] Palit S, Hussain CM (2019) Nanomembranes for Environment. In: Hussain C (ed) *Handbook of environmental materials management*. Springer, pp 1033–1056. https://doi.org/10.1007/978-3-319-73645-7_31
- [13] Adiga S, Jin C, Curtiss L, Monteiro-Riviere N, Narayan RJ (2009) Nanoporous membranes for medical and biological applications. *WIREs Nanomed Nanobiotechnol* 1:568–581. <https://doi.org/10.1002/wnan.050>
- [14] Jakšić Z, Matovic J (2010) Functionalization of artificial freestanding composite nanomembranes. *Mater* 3:165–200. <https://doi.org/10.3390/ma3010165>
- [15] Fan F, Yu Y, Amiri SHE, Quandt D, Bimberg D, Ning CZ (2017) Fabrication and room temperature operation of semiconductor nano-ring lasers using a general applicable membrane transfer method. *Appl Phys Lett*. <https://doi.org/10.1063/1.4982621>
- [16] Zahid M, Rashid A, Akram S, Rehan Z, Razzaq W (2018) A comprehensive review on polymeric nano-composite membranes for water treatment. *J Membr Sci Technol* 8:1000179. <https://doi.org/10.4172/2155-9589.1000179>
- [17] Guo Q, Di Z, Lagally MG, Mei Y (2018) Strain engineering and mechanical assembly of silicon/germanium nanomembranes. *Mater Sci Eng R Rep* 128:1–31. <https://doi.org/10.1016/j.mser.2018.02.002>
- [18] Ma F, Xu B, Wu S, Wang L, Zhang B, Huang G, Du A, Zhou B, Mei Y (2019) Thermal-controlled releasing and assembling of functional nanomembranes through polymer pyrolysis. *Nanotechnol*. <https://doi.org/10.1088/1361-6528/ab1dce>
- [19] Jakšić Z, Jakšić O (2020) Biomimetic nanomembranes: an overview. *Biomimetics* 5:24. <https://doi.org/10.3390/biomimetics5020024>
- [20] Jia P, Zuber K, Guo Q, Gibson BC, Yang J, Ebendoff-Heidepriem H (2019) Large-area freestanding gold nanomembranes with nanoholes. *Mater Horiz* 6:1005–1012. <https://doi.org/10.1039/c8mh01302k>
- [21] Wang X, Chen Y, Schmidt OG, Yan C (2016) Engineered nanomembranes for smart energy storage devices. *Chem Soc Rev* 45:1308. <https://doi.org/10.1039/c5cs00708a>
- [22] Zanghelini F, Frias IAM, Rêgo MJB, Pitta MGR, Saciloti M, Oliveira MDL, Andrade CAS (2017) Biosensing breast cancer cells based on a three-dimensional TiO₂ nanomembrane transducer. *Biosens Bioelectron* 92:313–320. <https://doi.org/10.1016/j.bios.2016.11.006>
- [23] Hong YJ, Jeong H, Cho KW, Lu N, Kim DH (2019) Wearable and implantable devices for cardiovascular healthcare: from monitoring to therapy based on flexible and stretchable electronics. *Adv Funct Mater* 29:1808247. <https://doi.org/10.1002/adfm.201808247>
- [24] Hussain MM, Ma ZJ, Shaikh SF (2018) Flexible and stretchable electronics-progress, challenges, and prospects. *Electrochem Soc Interface* 27:65–69. <https://doi.org/10.1149/2.F08184if>
- [25] Mossu A, Rosito M, Khire T, Chung H, Nishihaar H, Gruber I, Luke E, Dehouck L, Sallusto F, Gosselet F, Mcgrath J, Engelhardt B (2019) A silicon nanomembrane platform for the visualization of immune cell trafficking across the human blood-brain barrier under flow. *J Cereb Blood Flow Metab* 39:395–410. <https://doi.org/10.1177/0271678X18820584>
- [26] Aktürk Ö, Keskin D (2016) Collagen/PEO/gold nanofibrous matrices for skin tissue engineering. *Turk J Biol* 40:380–398. <https://doi.org/10.3906/biy-1502-49>
- [27] Beck GR, Ha SH, Camalier CE, Yamaguchi M, Li Y, Lee JK, Weitzmann MN (2011) Bioactive silica-based nanoparticles stimulate bone forming osteoblasts, suppress bone resorbing osteoclasts, and enhance bone mineral density in vivo. *Nanomed: Nanotechnol Biol Med* 8:793–803. <https://doi.org/10.1016/j.nano.2011.11.003>
- [28] Wang Q, Huang J, Li HQ, Zhao AZJ, Wang Y, Zhang KQ, Sun HT, Lai YK (2017) Recent advances on smart TiO₂ nanotube platforms for sustainable drug delivery applications. *Int J Nanomed* 12:151–165. <https://doi.org/10.2147/IJN.S117498>
- [29] Prasadh S, Wong RCW (2018) Unraveling the mechanical strength of biomaterials used as a bone scaffold in oral and

- maxillofacial defects. *Oral Sci Int* 15:48–55. [https://doi.org/10.1016/S1348-8643\(18\)30005-3](https://doi.org/10.1016/S1348-8643(18)30005-3)
- [30] Sharma BB, Parashar A (2020) Mechanical strength of a nanoporous bicrystalline h-BN nanomembrane in a water submerged state. *Phys Chem Chem Phys* 22:20453. <https://doi.org/10.1039/d0cp03235b>
- [31] Kunitake T (2008) Supramolecular assembly and hybridization in giant nanomembranes. *Macromol Symp* 270:8–13. <https://doi.org/10.1002/masy.200851002>
- [32] Watanabe H, Vendamme R, Kunitake T (2007) Development of fabrication of giant nanomembranes. *Bull Chem Soc Jpn* 80:433–440. <https://doi.org/10.1246/bcsj.80.433>
- [33] Huang G, Mei Y (2018) Assembly and self-assembly of nanomembrane materials—from 2D to 3D. *Small* 14:1–23. <https://doi.org/10.1002/sml.201703665>
- [34] Matovic J, Jakšić Z (2009) Nanomembrane: a new MEMS/NEMS Building block. In: Takahata K (ed) *Micro electronic and mechanical systems*. INTECH, New York, pp 61–84. <https://doi.org/10.5772/004>
- [35] Koklu A, Li J, Sengor S, Beskok A (2017) Pressure driven water flow through hydrophilic alumina nanomembranes. *Microfluid Nanofluid* 21:124. <https://doi.org/10.1007/s10404-017-1960-1>
- [36] Naeem F, Naeem S, Zhao Z, Shu G, Zhang J, Mei Y, Huang G (2020) Atomic layer deposition synthesized ZnO nanomembranes: a facile route towards stable supercapacitor electrode for high capacitance. *J Power Sour*. <https://doi.org/10.1016/j.jpowsour.2020.227740>
- [37] Tian Z, Wang Y, Chen Y, Xu B, Di Z, Mei Y (2020) Inorganic stimuli-responsive nanomembranes for small-scale actuators and robots. *Adv Intell Syst* 2:1900092. <https://doi.org/10.1002/aisy.201900092>
- [38] Malinovskis U, Poplauskas R, Apsite I, Meija R, Prikulis J, Lombardi F, Ertz D (2014) Ultrathin anodic aluminum oxide membranes for production of dense sub-20 nm nanoparticle arrays. *J Phys Chem C* 118:8685–8690. <https://doi.org/10.1021/jp412689y>
- [39] Mönch I, Schumann J, Stockmann M, Arndt KF, Schmidt OG (2011) Multifunctional nanomembranes self-assembled into compact rolled-up sensor-actuator devices. *Smart Mater Struct*. <https://doi.org/10.1088/0964-1726/20/8/085016>
- [40] Yan Z, Nan K, Rogers JA (2016) Synthesis, assembly, and applications of semiconductor nanomembranes. In: Rogers JA, Ahn JH (eds) *Silicon nanomembranes: fundamental science and applications*. John Wiley & Sons, Weinheim, pp 3–35
- [41] Radisavljevic B, Radenovic A, Brivio J, Giacometti V, Kis A (2011) Single-layer MoS₂ transistors. *Nat Nanotechnol* 6:147–150. <https://doi.org/10.1038/nnano.2010.279>
- [42] Rogers J, Lagally M, Nuzzo R (2011) Synthesis, assembly and applications of semiconductor nanomembranes. *Nature* 477:45–53. <https://doi.org/10.1038/nature10381>
- [43] Asmatulu R (2016) Highly Hydrophilic Electrospun polyacrylonitrile/ polyvinylpyrrolidone nanofibers incorporated with gentamicin as filter medium for dam water and wastewater treatment. *J Membr Separation Technol* 5:38–56. <https://doi.org/10.6000/1929-6037.2016.05.02.1>
- [44] Chan EP, Lee SC (2017) Thickness-dependent swelling of molecular layer-by-layer polyamide nanomembranes. *J Polym Sci Part B Polym Phys* 55:412–417. <https://doi.org/10.1002/polb.24285>
- [45] Kadam VV, Wang L, Padhye R (2018) Electrospun nanofibre materials to filter air pollutants-A review. *J Ind Text* 47:2253–2280. <https://doi.org/10.1177/1528083716676812>
- [46] Lou LH, Qin XH, Zhang H (2017) Preparation and study of low-resistance polyacrylonitrile nano membranes for gas filtration. *Text Res J* 87:208–215. <https://doi.org/10.1177/0040517515627171>
- [47] Kim KJ, Lee JA, Lima M, Baughman R, Kim SJ (2016) Highly stretchable hybrid nanomembrane supercapacitors. *RSC Adv* 6:24756–24759. <https://doi.org/10.1039/C6RA02757A>
- [48] Kwon YT, Kim YS, Kwon S, Mahmood M, Lim HR, Park SW, Kang SO, Choi JJ, Herbert R, Jang YC, Choa YH, Yeo WH (2020) All-printed nanomembrane wireless bioelectronics using a biocompatible solderable graphene for multimodal human-machine interfaces. *Nat Commun* 11:3450. <https://doi.org/10.1038/s41467-020-17288-0>
- [49] Li R, Jiang J, Liu Q, Xie Z, Zhai J (2018) Hybrid nanochannel membrane based on polymer/MOF for high-performance salinity gradient power generation. *Nano Energy* 53:643–649. <https://doi.org/10.1016/j.nanoen.2018.09.015>
- [50] Polarz S, Smarsly B (2002) Nanoporous materials. *J Nanosci Nanotechnol* 2:581–612
- [51] Aksimentiev A, Brunner RK, Cruz-Chú E, Comer J, Schulten K (2009) Modeling transport through synthetic nanopores. *IEEE Nanotechnol Mag* 3:20–28. <https://doi.org/10.1109/MNANO.2008.931112>
- [52] Yang Y, Dementyev P, Biere N, Emmrich D, Stohmann P, Korzetz R, Zhang X, Beyer A, Koch S, Anselmetti D, Götzhäuser A (2018) Rapid water permeation through carbon nanomembranes with sub-nanometer channels. *ACS Nano* 12:4695–4701. <https://doi.org/10.1021/acsnano.8b01266>
- [53] Sulka GD (2008) Highly ordered anodic porous alumina formation by Self-organized anodizing. In: Eftekhari A (ed)

- Nanostructured materials in electrochemistry. <https://doi.org/10.1002/9783527621507.ch1>
- [54] Grimes C (2017) synthesis and application of highly ordered arrays of TiO₂ nanotubes. *J Mater Chem* 17:1451–1457. <https://doi.org/10.1039/B701168G>
- [55] Cavallo F, Lagally M (2010) Semiconductors turn soft: inorganic nanomembranes. *Soft Matter* 6:439–455. <https://doi.org/10.1039/b916582g>
- [56] Absalan G, Barzegar S, Moradi M, Behaein S (2017) Fabricating Al₂O₃-nanopores array by an ultrahigh voltage two-step anodization technique: Investigating the effect of voltage rate and Al foil thickness on geometry and ordering of the array. *Mater Chem Phys* 199:265–271. <https://doi.org/10.1016/j.matchemphys.2017.07.015>
- [57] Ahmmed KMT, Grambow C, Kietzig AM (2014) Fabrication of micro/nano structures on metals by femtosecond laser micromachining. *Micromachines* 5:1219–1253. <http://doi.org/10.3390/mi5041219>
- [58] Oh CM, Park KH, Choi JH, Hwang S, Noh H, Yu YM, Jang JW (2017) Polycrystalline Au nanomembrane as a tool for two-tone micro/nanolithography. *Chem Mater* 29:3863–3872. <https://doi.org/10.1021/acs.chemmater.6b04268>
- [59] Winter A, Ekinci Y, Gölzhäuser A, Turchanin A (2019) Freestanding carbon nanomembranes and graphene monolayers nanopatterned via EUV interference lithography. *2D Mater* 6:021002. <https://doi.org/10.1088/2053-1583/ab0014>
- [60] Zhang X, Vieker H, Beyer A, Gölzhäuser A (2014) Fabrication of carbon nanomembranes by helium ion beam lithography. *Nanotechnol* 5:188–194. <https://doi.org/10.3762/bjnano.5.20>
- [61] Prasanna SRVS, Balaji K, Pandey S, Rana S (2019) Metal oxide based nanomaterials and their polymer nanocomposites. In: Karak N (ed) *Nanomaterials and polymer nanocomposites: raw materials to applications*. Matthew Deans, India, pp 123–144
- [62] Markutsya S, Jiang C, Pikus Y, Tsukruk VV (2005) Freely suspended layer-by-layer nanomembranes: testing micromechanical properties. *Adv Funct Mater* 15:771–780. <https://doi.org/10.1002/adfm.200400149>
- [63] Li H, Lin Y, Chen Z (2020) Study on the realization of high specific surface area Al₂O₃ through internal Anodization of honeycomb aluminum. *Archit Eng Sci* 1:1
- [64] Poinern E, Ali N, Fawcett D (2011) Progress in nano-engineered anodic aluminum oxide membrane development. *Mater* 4:487–526. <https://doi.org/10.3390/ma4030487>
- [65] Michalska-Domańska M, Norek M, Stępniewski WJ, Budner B (2013) Fabrication of high quality anodic aluminum oxide (AAO) on low purity aluminum—a comparative study with the AAO produced on high purity aluminum. *Electrochim Acta* 105:424–432. <https://doi.org/10.1016/j.electacta.2013.04.160>
- [66] Mankotia D, Singh PS, Kaur M (2015) Review of anodic porous alumina membrane development. *SSRG Int J Hum Soc Sci* 1:48–53
- [67] Jani AMM, Losic D, Voelcker NH (2013) Nanoporous anodic aluminum oxide: advances in surface engineering and emerging applications. *Prog Mater Sci* 58:636–704. <https://doi.org/10.1016/j.pmatsci.2013.01.002>
- [68] Buhr CR, Wiesmann N, Tanner RC, Brieger J, Eckrich J (2020) The chorioallantoic membrane assay in nanotoxicological research—an alternative for In vivo experimentation. *Nanomater* 10:2328. <https://doi.org/10.3390/na10122328>
- [69] Patel Y, Janusas G, Palevicius A, Vilkauskas A (2020) Development of nanoporous AAO membrane for nano filtration using the acoustophoresis method. *Sensors* 20:3833. <https://doi.org/10.3390/s20143833>
- [70] Panzarasa G, Soliveri G (2019) Photocatalytic lithography. *Appl Sci* 9:1266. <https://doi.org/10.3390/app9071266>
- [71] Sebastian EM, Jai SK, Purohit R, Dhakad SK, Rana RS (2020) Nanolithography and its current advancements. *Mater Today Proc* 26:2351–2356. <https://doi.org/10.1016/j.matpr.2020.02.505>
- [72] Pimpin A, Srituravanich W (2012) Review on micro- and nanolithography techniques and their applications. *Eng J* 16:37–56. <https://doi.org/10.4186/ej.2012.16.1.37>
- [73] Venugopal G, Kim SS (2013) Nanolithography. In: Takahata K (ed) *Advances in micro/nano electromechanical systems and fabrication technologies*. INTECH, New York, pp 187–206. <https://doi.org/10.5772/55527>
- [74] Chen Y (2015) Applications of nanoimprint lithography/hot embossing: a review. *Appl Phys A* 121:451–465. <https://doi.org/10.1007/s00339-015-9071-x>
- [75] Gates BD, Xu Q, Stewart M, Ryan D, Willson CG, Whitesides GM (2005) New approaches to nanofabrication: molding, printing, and other techniques. *Chem Rev* 105:1171–1196. <https://doi.org/10.1021/cr030076o>
- [76] Truskett VN, Watts MPC (2006) Trends in imprint lithography for biological applications. *Trends Biotechnol* 24:312–317. <https://doi.org/10.1016/j.tibtech.2006.05.005>
- [77] Grigorescu AE, Hagen CW (2009) Resists for sub-20-nm electron beam lithography with a focus on HSQ: state of the art. *Nanotechnol*. <https://doi.org/10.1088/0957-4484/20/29/292001>
- [78] Traub MC, Longsine W, Truskett VN (2016) Advances in nanoimprint lithography. *Annu Rev Chem Biomol Eng*

- 7:583–604. <https://doi.org/10.1146/annurev-chembioeng-080615-034635>
- [79] Gentili E, Tabaglio L, Aggogeri F (2005) Review on micromachining techniques. In: Kuljanic E (ed) AMST'05 advanced manufacturing systems and technology. CISM international centre for mechanical sciences (courses and lectures). Springer: Vienna, pp 387–396. https://doi.org/10.1007/3-211-38053-1_37
- [80] Enderlein T, Nestler J, Stiehl C, Morschhauser A, Otto T (2019) Electrically controlled actuation of strained nanomembranes. *Phys Status Solidi A* 216:1800840. <http://dx.doi.org/10.1002/pssa.201800840>
- [81] Gao S, Huang H (2017) Recent advances in micro- and nano-machining technologies. *Front Mech Eng* 12:18–32. <https://doi.org/10.1007/s11465-017-0410-9>
- [82] Yang L, Wei J, Ma Z, Song P, Ma J, Zhao Y, Huang Z, Zhang M, Yang F, Wang X (2019) The fabrication of micro/nano structures by laser machining. *Nanomaterials* 9:1789. <https://doi.org/10.3390/nano9121789>
- [83] Bordatchev E, Nikumb S (2008) Fabrication of moulds and dies using precision laser micromachining and micromilling technologies. *J Laser Micro / Nanoeng* 3:175–181. <https://doi.org/10.2961/jlmm.2008.03.0009>
- [84] Cheng J, Liu C, Shang S, Liu D, Perrie W, Dearden G, Watkins K (2013) A review of ultrafast laser materials micromachining. *Opt Laser Technol* 46:88–102. <https://doi.org/10.1016/j.optlastec.2012.06.037>
- [85] Gattass RR, Mazur E (2008) Femtosecond laser micromachining in transparent materials. *Nat Photonics* 2:219–225. <https://doi.org/10.1038/nphoton.2008.47>
- [86] Mathur S, Sivakov V, Shen H, Barth S, Cavalius C, Nilsson A, Kuhn P (2006) Nanostructured films of iron, tin and titanium oxides by chemical vapor deposition. *Thin Solid Films* 502:88–93. <https://doi.org/10.1016/j.tsf.2005.07.249>
- [87] Wang J, Ren Z, Hou Y, Yan X, Liu P, Zhang H, Zhang HX, Guo J (2020) A review of graphene synthesis at low temperatures by CVD methods. *New Carbon Mater* 35:193–208. [https://doi.org/10.1016/S1872-5805\(20\)60484-X](https://doi.org/10.1016/S1872-5805(20)60484-X)
- [88] Choi DS, Robertson AW, Warner JH, Ki SO, Kim H (2016) Low-temperature chemical vapor deposition synthesis of Pt-Co alloyed nanoparticles with enhanced oxygen reduction reaction catalysis. *Adv Mater* 28:7115–7122. <https://doi.org/10.1002/adma.201600469>
- [89] Li X, Rafie A, Smolin YY, Simotwo S, Kalra V, Lau KKS (2019) Engineering conformal nanoporous polyaniline via oxidative chemical vapor deposition and its potential application in supercapacitors. *Chem Eng Sci* 194:156–164. <https://doi.org/10.1016/j.ces.2018.06.053>
- [90] Li X, Rafie A, Kalra V, Lau KKS (2020) Deposition behavior of polyaniline on carbon nanofibers by oxidative chemical vapor deposition. *Langmuir* 36:13079–13086. <https://doi.org/10.1021/acs.langmuir.0c02539>
- [91] Manawi YM, Ihsanullah SA, Al-Ansari T, Atieh MA (2018) A review of carbon nanomaterials' synthesis via the chemical vapor deposition (CVD) method. *Mater* 11:822. <https://doi.org/10.3390/ma11050822>
- [92] Shanmugam M, Durcan CA, Yu B (2012) Layered semiconductor molybdenum disulfide nanomembrane based schottky-barrier solar cells. *Nanoscale* 4:7399. <https://doi.org/10.1039/c2nr32394j>
- [93] Villiers MM, Otto DP, Strydom SJ, Lvov YM (2011) Introduction to nanocoatings produced by layer-by-layer (LbL) self-assembly. *Adv Drug Deliv Rev* 63:701–715. <https://doi.org/10.1016/j.addr.2011.05.011>
- [94] Kulkarni DD, Choi I, Singamaneni SS, Tsukruk V (2010) Graphene oxide-polyelectrolyte nanomembranes. *ACS Nano* 4:4667–4676. <https://doi.org/10.1021/nn101204d>
- [95] Chan EP, Lee SC (2016) Thickness-dependent swelling of molecular layer-by-layer polyamide nanomembranes. *J Polym Sci Part B Polym Phys* 55:412–417. <https://doi.org/10.1002/polb.24285>
- [96] Jiang C, Markutsya S, Tsukruk VV (2004) Compliant, robust, and truly nanoscale free-standing multilayer films fabricated using Spin-assisted layer-by-layer Assembly. *Adv Mater* 16:157–161. <https://doi.org/10.1002/adma.200306010>
- [97] Xiong R, Hu K, Zhang S, Lu C, Tsukruk VV (2016) Ultrastrong freestanding graphene oxide nanomembranes with surface enhanced raman scattering functionality by solvent-assisted single-Component layer by layer assembly. *ACS Nano* 10:6702–6715. <https://doi.org/10.1021/acsnano.6b02012>
- [98] Pierre AC (2020) Introduction to sol-gel processing (second edition). Springer, Cham. <https://doi.org/10.1007/978-3-030-38144-8>
- [99] Thiagarajan S, Sanmugam A, Vikraman D (2017) Chapter 1: Facile methodology of sol-gel synthesis for metal oxide nanostructures. In: Chandra U (ed) recent applications in sol-gel synthesis. IntechOpen, London, pp 1–16. <https://doi.org/10.5772/intechopen.68708>
- [100] Armelin E, Gomes AL, Pérez-Madrígal MM, Puiggali J, Franco L, Valle L, Rodríguez-Galán A, Campos JS, Ferrer-Anglada N, Alemán C (2012) Biodegradable free-standing nanomembranes of conducting polymer:polyester blends as bioactive platforms for tissue engineering. *J Mater Chem* 22:585–594. <https://doi.org/10.1039/C1JM14168F>
- [101] Chen X, Zhang W, Lin Y, Cai Y, Qiu M, Fan Y (2015) Preparation of high-flux γ -alumina nanofiltration


- membranes by using a modified sol-gel method. *Microporous Mesoporous Mater* 214:195–203. <https://doi.org/10.1016/j.micromeso.2015.04.027>
- [102] Shayesteh M, Samimi A, Afarani MS, Khorram M (2016) Synthesis of titania- γ -alumina multilayer nanomembranes on performance-improved alumina supports for wastewater treatment. *Desalin Water Treat* 57:9115–9122. <https://doi.org/10.1080/19443994.2015.1030703>
- [103] Sim K, Rao Z, Zou Z, Ershad F, Lei J, Thukral A, Chen J, Huang Q, Xiao J, Yu C (2019) Metal oxide semiconductor nanomembrane-based soft unnoticeable multifunctional electronics for wearable human-machine interfaces. *Sci Adv* 5:aav9653
- [104] Macwan DP, Dave PN, Chaturvedi S (2011) A review on nano-TiO₂ sol-gel type syntheses and its applications. *J Mater Sci* 46:3669–3686. <https://doi.org/10.1007/s10853-011-5378-y>
- [105] Low Z-X, Chua YT, Ray BM, Mattia D, Metcalfe IS, Patterson DA (2017) Perspective on 3D printing of separation membranes and comparison to related unconventional fabrication techniques. *J Membr Sci* 523:596–613. <https://doi.org/10.1016/j.memsci.2016.10.006>
- [106] Lee J-Y, An J, Chua CK (2017) Fundamentals and applications of 3D printing for novel materials. *Appl Mater Today* 7:120–133. <https://doi.org/10.1016/j.apmt.2017.02.004>
- [107] Balogun HA, Sulaiman R, Marzouk SS, Giwa A, Hasan SW (2019) 3D printing and surface imprinting technologies for water treatment: a review. *J Water Process Eng*. <https://doi.org/10.1016/j.jwpe.2019.100786>
- [108] Lee J-Y, Tan WS, An J, Chua CK, Tang CY, Fane AG, Chong TH (2016) The potential to enhance membrane module design with 3D printing technology. *J Membr Sci* 499:480–490. <https://doi.org/10.1016/j.memsci.2015.11.008>
- [109] Tijjng LD, Dizon JRC, Ibrahim I, Nisay ARN, Shon HK, Advincula RC (2020) 3D printing for membrane separation, desalination and water treatment. *Appl Mater Today*. <https://doi.org/10.1016/j.apmt.2019.100486>
- [110] Guvendiren M, Molde J, Soares RMD, Kohn J (2016) Designing biomaterials for 3D printing. *ACS Biomater Sci Eng* 2:1679–1693. <https://doi.org/10.1021/acsbomaterials.6b00121>
- [111] Bandyopadhyay A, Bose S, Das S (2015) 3D printing of biomaterials. *MRS Bull* 40:108–115. <https://doi.org/10.1557/mrs.2015.3>
- [112] Chia HN, Wu BM (2015) Recent advances in 3D printing of biomaterials. *J Biol Eng* 9:4. <https://doi.org/10.1186/s13036-015-0001-4>
- [113] Tan X, Rodrigue D (2019) A review on porous polymeric membrane preparation: part I: production techniques with polysulfone and poly vinylidene fluoride. *Polymers* 11:1160. <https://doi.org/10.3390/polym11071160>
- [114] Tan X, Rodrigue D (2019) A review on porous polymeric membrane preparation: part II: production techniques with polyethylene, polydimethylsiloxane, polypropylene, polyimide, and polytetrafluoroethylene. *Polymers* 11:1310. <https://doi.org/10.3390/polym11081310>
- [115] Tan EYS, Agarwala S, Yap YL, Tan CSH, Laude A, Yeong WY (2017) Novel method for fabrication ultrathin, free-standing and porous polymer membranes for retinal tissue engineering. *J Mater Chem B* 5:5616. <https://doi.org/10.1039/C7TB00376E>
- [116] Dias RR, Zepka LQ, Jacob-Lopes E (2019) Introductory chapter: biotechnology and bioengineering. In: Jacob-Lopes E, Zepka LQ (eds) *Biotechnology and bioengineering*. IntechOpen, London, pp 1–3. <https://doi.org/10.5772/intechopen.86380>
- [117] Bhat S, Kumar A (2013) Biomaterials and bioengineering tomorrow's healthcare. *Biomater*. <https://doi.org/10.4161/biom.24717>
- [118] Deng D, Nothorn D, Liaw D, Liu T, Peterson P, Gilchrist B, Millunchick J (2011) Modeling, design and fabrication of a freestanding nanoporous membrane. *Microelectron Eng* 88:3219–3223. <https://doi.org/10.1016/j.mee.2011.08.002>
- [119] Singla R, Abidi S, Dar A, Acharya A (2019) Nanomaterials as potential and versatile platform for next generation tissue engineering applications: nanobiomaterials for tissue engineering applications. *J Biomed Mater Res B Appl Biomater* 107:2433–2449. <https://doi.org/10.1002/jbm.b.34327>
- [120] Mohamed A, Xing M (2012) Nanomaterials and nanotechnology for skin tissue engineering. *Int J Burn Trauma* 2:29–41. ISSN: 2160-2026/IJBT1201002
- [121] Li X, Liu W, Sun L, Fan Y, Feng Q (2014) The application of inorganic nanomaterials in bone tissue engineering. *J Biomater Tissue Eng* 4:1–10. <https://doi.org/10.1166/jbt.2014.1253>
- [122] Sridhar R, Sundarajan S, Venugopal JR, Ravichandran R, Ramakrishna S (2013) Electrospun inorganic and polymer composite nanofibers for biomedical applications. *J Biomater Sci Polym Ed* 24:365–385. <https://doi.org/10.1080/09205063.2012.690711>
- [123] Venkatesan J, Pallela R, Kim S (2014) Applications of carbon nanomaterials in bone tissue engineering. *J Biomed Nanotechnol* 10:3105–3123. <https://doi.org/10.1166/jbm.2014.1969>
- [124] Zhang M, Wang J, Xu W, Luan J, Li X, Zhang Y, Dong H (2015) The mechanical property of Rana chensinensis skin

- collagen/poly (L-lactide) fibrous membrane. *Mater Lett* 139:647–470. <https://doi.org/10.1016/j.matlet.2014.10.085>
- [125] Puiggali-Jou A, Medina J, Valle LJ, Alemán C (2016) Nanoperforations in poly(lactic acid) free-standing nanomembranes to promote interactions with cell filopodia. *Eur Polym J* 75:552–564. <https://doi.org/10.1016/j.eurpolymj.2016.01.019>
- [126] Dai XY, Nie W, Wang YC, Shen Y, Li Y, Gan SJ (2012) Electrospun emodin polyvinylpyrrolidone blended nanofibrous membrane: a novel medicated biomaterial for drug delivery and accelerated wound healing. *J Mater Sci Mater Med* 23:2709–2716. <https://doi.org/10.1007/s10856-012-4728-x>
- [127] Phan HP, Zhong Y, Nguyen K, Park Y, Dinh T, Song E, Vadivelu R, Masud M, Li J, Shiddiky M, Dao YY, Rogers J, Nguyen N (2019) Long-lived, transferred crystalline silicon carbide nanomembranes for implantable flexible Electronics. *ACS Nano* 13:11572–11581. <https://doi.org/10.1021/acsnano.9b05168>
- [128] Rashid R, Sofi HS, Macossay J, Sheikh FA (2020) Polycaprolactone-based nanofibers and their in-vitro and in-vivo applications in bone tissue engineering. In: Sheikh F (ed) *Application of nanotechnology in biomedical sciences*. Springer, Singapore. https://doi.org/10.1007/978-981-15-5622-7_2
- [129] Shadjo N, Hasanzadeh M (2016) Graphene and its nanostructure derivatives for use in bone tissue engineering: recent advances. *J Biomed Mater Res, Part A* 104:1250–1275. <https://doi.org/10.1002/jbm.a.35645>
- [130] Foong LK, Foroughi MM, Mirhosseini AF, Safaei M, Jahani S, Mostafavi M, Ebrahimpoor N, Sharifi M, Varma RS, Khatami M (2020) Applications of nano-materials in diverse dentistry regimes. *RSC Adv* 10:15430–15460. <https://doi.org/10.1039/D0RA00762E>
- [131] Zhang J, Chen H, Zhao M, Liu G, Wu J (2020) 2D nanomaterials for tissue engineering application. *Nano Res* 13:2019–2034. <https://doi.org/10.1007/s12274-020-2835-4>
- [132] Eivazzadeh-Keihan R, Chenab K, Taheri-Ledari R, Mosafer J, Hashemi S, Mokhtarzadeh A, Maleki A, Hamblin M (2020) Recent advances in the application of mesoporous silica-based nanomaterials for bone tissue engineering. *Mater Sci Eng C* 107:110267. <https://doi.org/10.1016/j.msec.2019.110267>
- [133] Hill M, Qi B, Bayaniahangar R, Araban V, Bakhtiary Z, Doschak M, Goh B, Shokouhimehr M, Vali H, Presley J, Zadpoor A, Harris M, Abadi P, Mahmoudi M (2019) Nanomaterials for bone tissue regeneration: updates and future perspectives. *Nanomedicine*. <https://doi.org/10.2217/nmm-2018-0445>
- [134] Kwak D, Yoo J, Kim D (2010) Drug release behavior from nanoporous anodic aluminum oxide. *J Nanosci Nanotechnol* 10:345–348. <https://doi.org/10.1166/jnn.2010.1531>
- [135] Davoodi E, Zhiannanesh M, Montazerian H, Milani AS, Hoorfar M (2020) Nano-porous anodic alumina: fundamentals and applications in tissue engineering. *J Mater Sci Mater Med* 31:60. <https://doi.org/10.1007/s10856-020-06398-2>
- [136] Zhang Y, Fang F, Li L, Zhang J (2020) Self-assembled organic nanomaterials for drug delivery, bioimaging and cancer therapy. *ACS Biomater Sci Eng* 6:4816–4833. <https://doi.org/10.1021/acsbomaterials.0c00883>
- [137] Zhou X, Wang Y, Gong C, Liu B, Wei G (2020) Production, structural design, functional control, and broad applications of carbon nanofiber-based nanomaterials: a comprehensive review. *Chem Eng J*. <https://doi.org/10.1016/j.cej.2020.126189>
- [138] He Y, Qin L, Fang Y, Dan Z, Shen Y, Tan G, Huang Y, Ma C (2020) Electrospun PLGA nanomembrane: a novel formulation of extended-release bupivacaine delivery reducing postoperative pain. *Mater Des*. <https://doi.org/10.1016/j.matsdes.2020.108768>
- [139] Armagan E, Ince GO (2015) Coaxial nanotubes of stimuli responsive polymers with tunable release kinetics. *Soft Matter* 11:8070–8075. <https://doi.org/10.1039/c5sm01074h>
- [140] Slemming-Adamsen P, Song J, Dong M, Besenbacher F, Chen M (2015) In situ cross-linked PNIPAM/gelatin nanofibers for thermo-responsive drug release. *Macromol Mater Eng* 12:1226–1231. <https://doi.org/10.1002/mame.201500160>
- [141] Mao Z, Li J, Huang W, Jiang H, Zimba BL, Chen L, Wan J, Wu Q (2018) Preparation of poly(lactic acid)/graphene oxide nanofiber membranes with different structures by electrospinning for drug delivery. *RSC Adv* 8:16619–16625. <https://doi.org/10.1039/C8RA01565A>
- [142] Pant B, Park M, Park SJ (2019) Drug delivery applications of core-sheath nanofibers prepared by coaxial electrospinning: a review. *Pharmaceutics* 11(7):305. <https://doi.org/10.3390/pharmaceutics1107030>
- [143] Ma K, Qiu Y, Fu Y, Ni QQ (2018) Electrospun sandwich configuration nanofibers as transparent membranes for skin care drug delivery systems. *J Mater Sci* 53:10617–10626. <https://doi.org/10.1007/s10853-018-2241-4>

Publisher's Note Springer Nature remains neutral with regard to jurisdictional claims in published maps and institutional affiliations.

Article

Development and Analysis of Electrochemical Reactor with Vibrating Functional Element for AAO Nanoporous Membranes Fabrication

Urte Cigane ¹, Arvydas Palevicius ¹ , Vytautas Jurenas ², Kestutis Pilkauskas ¹ and Giedrius Janusas ^{1,*} 

¹ Faculty of Mechanical Engineering and Design, Kaunas University of Technology, Studentu Str. 56, 51424 Kaunas, Lithuania

² Institute of Mechatronics, Kaunas University of Technology, Studentu Str. 56, 51424 Kaunas, Lithuania

* Correspondence: giedrius.janusas@ktu.lt

Abstract: Nanoporous anodic aluminum oxide (AAO) is needed for a variety of purposes due to its unique properties, including high hardness, thermal stability, large surface area, and light weight. Nevertheless, the use of AAO in different applications is limited because of its brittleness. A new design of an electrochemical reactor with a vibrating element for AAO nanoporous membranes fabrication is proposed. The vibrating element in the form of a piezoceramic ring was installed inside the developed reactor, which allows to create a high-frequency excitation. Furthermore, mixing and vibration simulations in the novel reactor were carried out using ANSYS 17 and COMSOL Multiphysics 5.4 software, respectively. By theoretical calculations, the possibility to excite the vibrations of five resonant modes at different frequencies in the AAO membrane was shown. The theoretical results were experimentally confirmed. Five vibration modes at close to the theoretical frequencies were obtained in the novel reactor. Moreover, nanoporous AAO membranes were synthesized. The novel aluminum anodization technology results in AAO membranes with 82.6 ± 10 nm pore diameters and 43% porosity at 3.1 kHz frequency excitation and AAO membranes with 86.1 ± 10 nm pore diameters and 46% porosity at 4.1 kHz frequency excitation. Furthermore, the chemical composition of the membrane remained unchanged, and the hardness decreased. Nanoporous AAO has become less brittle but hard enough to be used for template synthesis.

Keywords: electrochemical reactor; two-step anodization method; high-frequency excitation method; AAO nanoporous membrane



Citation: Cigane, U.; Palevicius, A.; Jurenas, V.; Pilkauskas, K.; Janusas, G. Development and Analysis of Electrochemical Reactor with Vibrating Functional Element for AAO Nanoporous Membranes Fabrication. *Sensors* **2022**, *22*, 8856. <https://doi.org/10.3390/s22228856>

Academic Editor: Rosa Garriga

Received: 21 October 2022

Accepted: 14 November 2022

Published: 16 November 2022

Publisher's Note: MDPI stays neutral with regard to jurisdictional claims in published maps and institutional affiliations.



Copyright: © 2022 by the authors. Licensee MDPI, Basel, Switzerland. This article is an open access article distributed under the terms and conditions of the Creative Commons Attribution (CC BY) license (<https://creativecommons.org/licenses/by/4.0/>).

1. Introduction

The growth rate of the global nanotechnology market is so rapid that it far exceeds the market growth forecasts and is even more impressive because most nanomaterials are still in the early stages of the product life cycle [1]. As well, rapid progress has been made in the field of nanomembrane research, from basic research to the development of next-generation technologies [2]. Ultrathin 2D nanomaterials have many unique physical, electronic, chemical, and optical properties that provide many advantages and distinguish nanomembranes from other nanomaterials [3]. Nanomembranes are a new type of nanomaterial that has great potential and can be applied in a variety of fields, such as biosensors [4,5], chemical sensors [6–8], various biomedical applications [9,10], the food industry [11], nano- and microelectromechanical systems [12,13], etc. Nanomembranes can be classified according to the material used in their fabrication [14]. According to the membrane material, synthetic nanomembranes can be organic, inorganic, hybrid, or biological [15]. While developing synthetic nanomembranes, it is important to control their internal structure, because physical and mechanical properties affect the unique properties of the nanomembranes [16]. Different fabrication methods, such as lithography [17],

laser machining [18], layer-by-layer deposition [19], sol-gel processing [20], and 3D printing [21,22], are used to create nanoporous structures. These methods require expensive and high-tech equipment; therefore, another well-known alternative method to develop nano-membranes is the electrochemical anodization process [23].

In many applications, control of the geometry of membrane nanopores is a significant criterion [24,25]. Anodic aluminum oxide (AAO) is well known for its large surface area, relatively low cost, well-ordered structure, and ability to control the diameter of nanopores [26]. AAO can be obtained by controlling the parameters of the electrochemical anodization process [27,28]. AAO gradually grows in acidic solutions that anodize aluminum under an electric field between the anode and the cathode. The diameter of AAO pores depends on the anodization potential (voltage), temperature, electrolyte, and concentration [29,30]. The pore diameter and the distance between the pores often increase as the anodization voltage or the electrolyte concentration increases [14,31,32]. Moreover, it has recently been reported that the pore diameter decreases with decreasing electrolyte temperature [27]. According to previous AAO research, the electrochemical anodization process consists of two stages: mild (soft) and hard anodization [26]. In comparison to these two stages, the hard anodization process is more intense, the growth rate of the porous AAO film is higher, and a high amount of heat is released. To obtain nanoscale pores of uniform size, a constant temperature must be ensured throughout the anodization process. Therefore, more requirements for cooling equipment are set.

There are many scientific publications related to the vibrations of nanoporous AAO membrane and their effects in various fields such as microfiltration/nanofiltration [33] or the mitigation of fouling [34]. However, the effect of high-frequency excitation during the anodization process on the geometry of the nanopores in the AAO membrane has not yet been investigated. Vibrations during the electrochemical anodization process can be generated by using a piezoelectric ceramic material, which vibrates during excitation. It is widely used in various applications, such as microfluidic devices [35,36], particle manipulation [37], sensors [38], etc. Lead zirconate titanate (PZT) is an attractive piezoelectric ceramic material with good electromechanical properties; e.g., PZT rings are widely used in the development of various devices [39]. Accordingly, the piezoelectric ceramic ring can be used to control the geometry of nanopores in the membrane during the two-step anodization process. An analysis of the scientific literature [40,41] allows concluding that it is necessary to improve technologies for the development of novel nanoporous AAO membranes.

For most engineering materials, strength and toughness are essential requirements [42]. Ceramics have high hardness and strength due to strong atomic bonds, but strong bonds and the lack of plastic deformation result in ceramic brittleness [43]. To adapt nanoporous AAO to the production of templates [41] or use for ultrasonic nanoimprinting [44], it is important for the oxide to be characterized by nonbrittle nanopore deformation [45]. To create a super thin and more flexible nanoporous membrane from brittle aluminum oxide and to improve the quality of AAO membranes, it is necessary to create a novel electrochemical reactor for the fabrication of AAO membranes by applying high-frequency excitation during the two-step anodization process.

The aim of this work is to design an electrochemical reactor with a vibrating functional element and to produce nanoporous AAO membranes using the high-frequency excitation method.

2. Materials and Methods

2.1. Design of Electrochemical Reactor

To design an electrochemical reactor with a vibrating functional element for the fabrication of AAO nanoporous membranes, the effect of high-frequency excitation on the geometry of the nanopores during the anodization process will be investigated. An electrochemical reactor of the novel design is being developed, and its structure is shown in Figure 1.

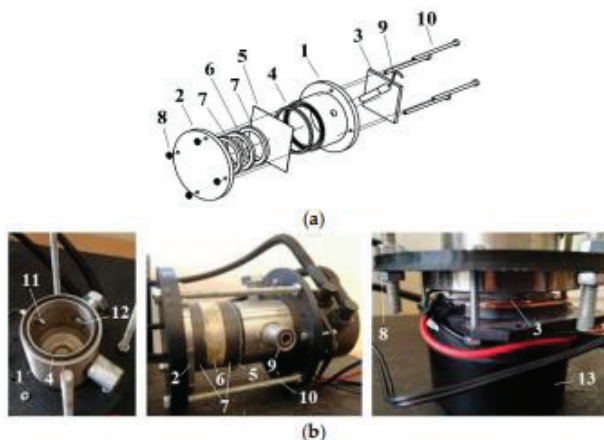


Figure 1. Electrochemical reactor for manufacturing AAO nanoporous membrane. (a) Drawing of the electrochemical reactor: 1: corps of the reactor, 2: cover of the reactor, 3: Peltier element, 4: gasket, 5: aluminum sheet, 6: vibrating element (piezoelectric ring), 7: electrical insulating element (piezoceramic), 8: nut M3, 9: mixing device, 10: screw M3x50; (b) Construction of the electrochemical reactor: 1: corps of the reactor, 2: cover of the reactor, 3: Peltier element, 4: gasket, 5: aluminum sheet, 6: vibrating element (piezoelectric ring), 7: electrical insulating element (piezoceramic), 8: nut M3, 9: place for mixing device, 10: screw M3x50, 11: temperature sensor, 12: hole for electrolyte filling, 13: cooler.

In terms of reactor structure, all reactor components are assembled through fittings. The reactor corps (Figure 1(1)) and the cover (Figure 1(2)) are composed of AISI 304 stainless steel (this steel does not react with acids during the anodization process). Moreover, as the diameter decreases with decreasing acid temperature, it is important to ensure low temperature during anodization to produce nanoscale pores [46]. For this purpose, the Peltier element (Figure 1(3)) model ‘TEC1 12715’ (12 V; 15 A) is selected. The cooler is connected to the Peltier element and the reactor corps. The Peltier element is lubricated on both sides with a thermal paste, which improves heat exchange and increases the contact area between the cooler, the Peltier element, and the reactor corps. Steel screws (Figure 1(10)) M3 × 50 and steel nuts (Figure 1(8)) are used to reinforce the reactor structure. An aluminum sheet (Figure 1(5)) with a thickness of 0.5 mm is the main material used to manufacture the AAO nanoporous membrane. The aluminum sheet is mounted to the stainless-steel reactor cylinder using an acid-resistant rubber gasket (Figure 1(4)) to prevent liquid leakage. The piezo ring (diameter 50 mm) is clamped on the other side of the aluminum plate. The piezoceramic material PZT 8 is chosen because it is considered to be a good choice for resonant devices [47]. To isolate different anodization and high-frequency excitation currents, the piezoceramic ring (actuator) (Figure 1(6)) is covered on both sides with piezoceramic rings (Figure 1(7)) because the ceramic has impermeability and good transmission of acoustic waves. Finally, the cover and screws are used to assemble all components. It guarantees good contact and vibration transmission during the electrochemical process that will be performed by the two-stage anodization method, which is described in detail in [33]. In addition, a temperature sensor (Figure 1(11)) is installed in the assembled reactor. Because low temperature is a crucial parameter of the anodization process, it is important to ensure an equivalent distribution of electrolytes throughout the reactor volume. Therefore, the mixing impeller is a necessary structural element. The impeller material of the mixing device (Figure 1(9)) is also stainless steel, which is resistant to the electrolyte.

2.2. Experimental Setup

The experimental setup for manufacturing the AAO nanoporous membrane is presented in Figure 2. Its closed-loop control system consists of the following elements: temperature control device (Figure 2a(2)), temperature sensor (Figure 2a(8)), and Peltier element (Figure 2a(11)). This closed-loop control system is automatic and can be called an automatic control system.

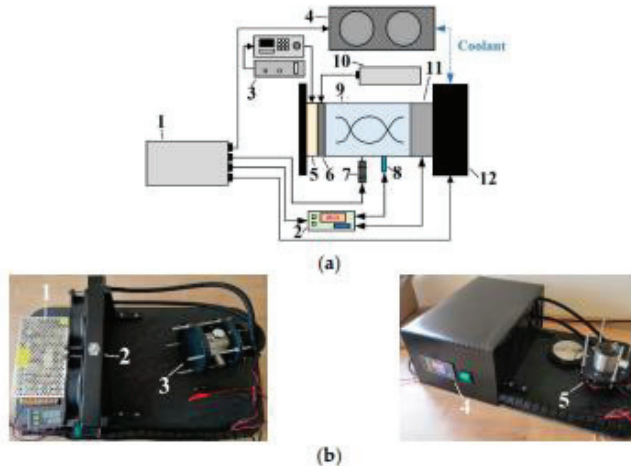


Figure 2. Experimental setup for manufacturing the AAO nanoporous membrane. (a) A schematic representation of the experimental setup: 1: DC 1 power unit, 2: temperature control device, 3: voltage amplifier and frequency generator, 4: master cooler radiator, 5: piezoelectric actuator, 6: membrane, 7: mixing device, 8: temperature sensor, 9: electrochemical reactor, 10: DC 2 power unit, 11: Peltier element, 12: master cooler pump; (b) Experimental equipment: 1: DC 1 power unit, 2: master cooler, 3: closed electrochemical reactor, 4: temperature control device, 5: open electrochemical reactor.

The experimental platform is composed of a 12 V 15 A direct current power supply unit (Figure 2(1)), a temperature control device with a temperature sensor (Digital Thermostat W3001, Juanjuan, China) (Figure 2b(4)), a cooler (Masterliquid lite 240, Cooler Master, Taiwan) (Figure 2b(2)), a 60 V 5 A direct current power supply unit (AN-11808, WEP, Guangdong, China) (Figure 2a(10)), a 12 V mixing device of 108 RPM (JGA25-370 DC Gearmotor, Cnmaway, China) (Figure 2a(7)), a novel electrochemical reactor (Figure 2b(3)), and a 12 V 15 A thermoelectric cooler Peltier element (TEC1 12715, Hebei, China) (Figure 2a(11)).

2.3. Experimental Setup for Vibration Measurements

The method of holography can be used to visualize dynamic processes [33], so the precise real-time instrument for surface measurement—(PRISM) holography system has been used to measure the frequency. The PRISM system (Hytec, Los Alamos, NM, USA) with the piezoelectric actuator is shown in Figure 3. The system consists of deformation equipment (frequency generator and voltage generator), a vibration measurement (holography) unit, and a computer system with software.

A schematic diagram of the experimental setup of the non-contact holographic measurement system is shown in Figure 3a.

Basically, a two-beam speckle pattern interferometer with a green laser has the beam directed at the acting membrane. The object beam is directed at the membrane, and the reference beam is directly captured in the camera. The laser green light (wavelength 532 nm,

power 20 mV) is scattered from the object and collected by the camera lens, imaging the object on the camera's sensors. The image of the object (membrane) is transferred from the camera to the computer. The data on the computer are analyzed by the program PRISM DAQ (Hytec, Los Alamos, NM, USA).

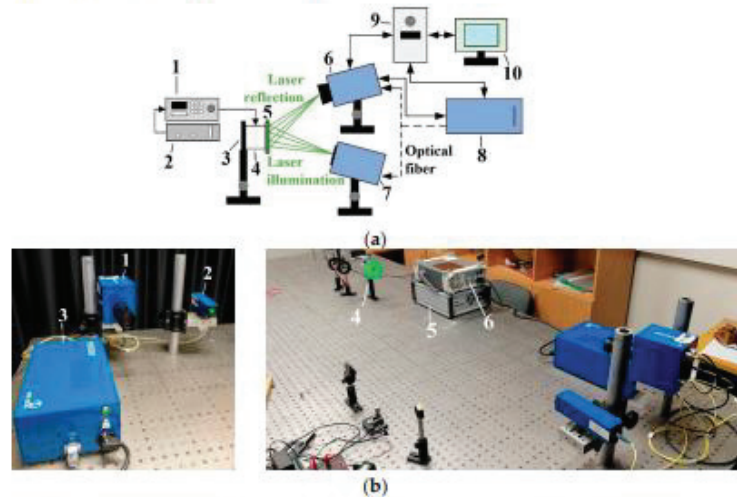


Figure 3. Non-contact holographic measurement system, known as PRISM system. (a) Schematic diagram of the PRISM system experimental setup: 1: frequency generator, 2: voltage amplifier, 3: isolated surface for fixing object, 4: piezoelectric actuator, 5: membrane attached to the piezoelectric actuator, 6: camera, 7: illumination head with a green laser, 8: control block, 9: computer, 10: computer screen (image illusion); (b) Experimental setup: 1: camera, 2: illumination head with a green laser, 3: control block, 4: membrane attached to a piezoelectric actuator, 5: voltage amplifier, 6: frequency generator.

2.4. Simulation Method and Conditions of Vibration Process

Vibration simulations of aluminum membrane sheets were performed using COMSOL Multiphysics 5.4 software. The simulation model consisted of the aluminum membrane with a 40 mm diameter and 0.5 mm thickness. The models' parameters are listed in Table 1.

Table 1. Models' parameters of vibration process.

Parameter	Unit	Values
Membrane radius	mm	20
Membrane thickness	mm	0.5
Material Young's modulus	MPa	68,000
Material mass density	kg/m ³	2712
Material Poisson's ratio	-	0.33
Radial direction pretension load	MPa	38
Common factor in natural frequency	Hz	1256
1st natural frequency mode, mode shape (0, 1)	Hz	3020
2nd natural frequency mode, mode shape (1, 1)	Hz	4812
3rd natural frequency mode, mode shape (2, 1)	Hz	6450
4th natural frequency mode, mode shape (0, 2)	Hz	6933
5th natural frequency mode, mode shape (3, 1)	Hz	8835

Moreover, the model was divided into finite tetrahedron elements with fixed support constraint boundary conditions.

2.5. Simulation Method and Conditions of Mixing Process

The mixing process simulations were performed using ANSYS 17 software. The model was divided into two zones between which a contact region was created to ensure data integrity. The first zone represented the internal volume of the reactor, and the second zone was for the impeller. The model was meshed by finite tetrahedron elements. The simulation conditions were close to the real ones (water density 998.2 kg/m^3 , viscosity $0.001003 \text{ kg/m}\cdot\text{s}$, temperature $20 \text{ }^\circ\text{C}$). A four-blade impeller (diameter 20 mm ; height 10 mm ; blade angle 0 deg ; rotational speed 108 rpm) was used. The k- ϵ realizable turbulence model was applied to simulate the mixing process. Additionally, gravity was included.

3. Results and Discussion

3.1. Vibration Analysis

Vibration simulations of aluminum membrane plates were performed using COM-SOL Multiphysics 5.4 software. The vibration modes of the membrane at different frequencies are shown in Table 2.

Table 2. Surface displacement field of the membrane at different frequencies (at 200 V , with radius 0.020 m).

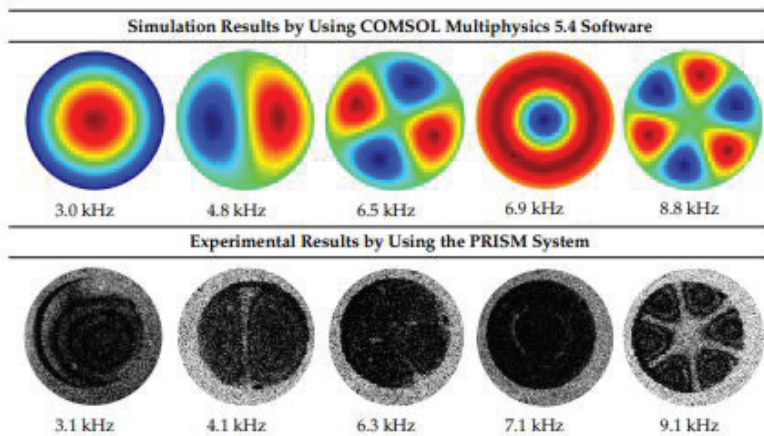


Table 2 shows that vibrations affect the surface of the membrane sheet because different mode shapes were obtained at different frequencies. In the following descriptions of circular membrane mode shapes, the notation (d, c) means d : the number of nodal diameters, and c : the number of nodal circles. Based on theoretical calculations (Table 2), the first natural frequency mode $(0, 1)$, with a membrane radius of 20 mm (voltage of 200 V), was obtained at the frequency of 3.0 kHz . Displacements on the surface of the membrane sheet were concentrated in the center. As the frequency increased, the second natural frequency mode could be seen. For example, the mode shape $(1, 1)$ was obtained at the frequency of 4.8 kHz . Displacements were visible on both sides of the membrane surface. A membrane surface with four displacement regions was obtained at the frequency of 6.5 kHz .

To confirm the results of the vibration simulation, the described above non-contact holographic measurement system was used (Figure 3). The experimental mode shapes of the membrane at different frequencies are presented in Table 2. The simulation results of the membrane vibrations were verified using the experimental ones. Five similar modes of

shapes were obtained by simulation and experiments at the following frequencies: the first natural mode (0, 1) at 3.0 kHz and 3.1 kHz, the second mode (1, 1) at 4.8 kHz and 4.1 kHz, the third mode (2, 1) at 6.5 kHz and 6.3 kHz, the fourth mode (0, 2) at 6.9 kHz and 7.1 kHz, and the fifth mode (3, 1) at 8.8 kHz and 9.1 kHz (Table 2). Comparing the simulation and the experimental results, the errors are estimated due to non-ideal structural stability and material properties and the inaccuracy of the measuring equipment.

3.2. Mixing Analysis

Because low temperature is an important parameter of the anodization process, it is relevant to select a suitable mixing impeller to ensure uniform electrolyte temperature throughout the reactor volume. A mechanical rotary stirrer is often used to create forced flow in the reactor [48]. The mixing process simulations were performed using ANSYS 17 software. The simulation model of the mixing process (with a coordinate system) is presented in Figure 4a. Theoretical velocity vectors in different planes are shown in Figure 4b. The whole volume is mixed. A mixing experiment was performed to confirm the theoretical results. The experimental results of the mixing process are shown in Figure 4c.

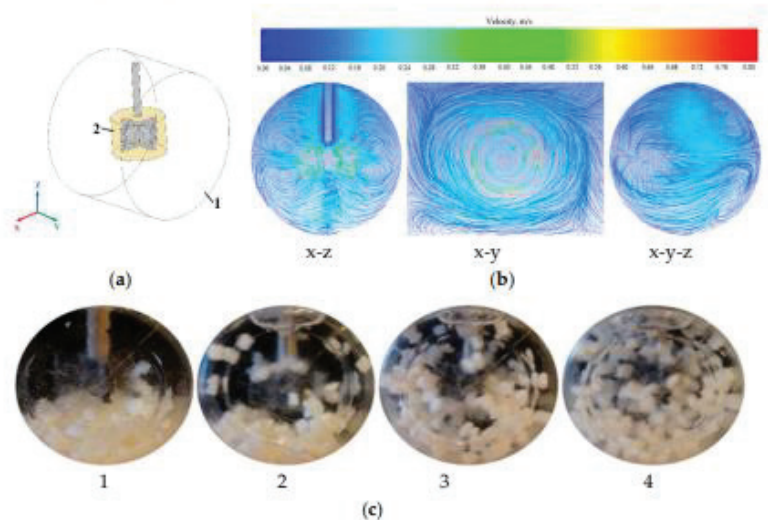


Figure 4. Mixing analysis. (a) Simulation model of mixing process (with a coordinate system): 1: internal volume of the reactor (the first zone of the model), 2: impeller zone (the second zone of the model); (b) Velocity vectors in different planes; (c) Experimental results of mixing process: 1—the mixing process is not running, 2: 0.5 s after the start of mixing, 3: 1 s after the start of mixing, 4: 1.5 s after the start of mixing.

Whereas the electrochemical reactor is composed of stainless steel, its corps is not transparent; as a result, the mixing process is not visible. Therefore, it was necessary to create a transparent experimental reactor with a stirred process inside. An experimental model has been developed that corresponds to the dimensions of the real reactor. Water and acrylonitrile butadiene styrene (ABS) thermoplastic polymer pellets that allowed the visualization of particle movement were used in the mixing experiment. ABS polymer was chosen because its density of 1032–1380 kg/m³ [49] is similar to that of water.

For visual analysis, to monitor the distribution of plastic particles throughout the mixing volume, it was decided to use ABS pellets (the size was approximately 2 mm) to occupy approximately one-third of the total reactor volume. Originally, the plastic particles

sink into the water. When the mixing process begins, ABS polymer particles begin to move and mix throughout the reactor volume (Figure 4c). The specific motions of the particles were not clearly visible during the experiment, but it is assumed that the mixing experiment is consistent with the theoretical mixing results obtained by the ANSYS 17 software simulation because, in the case of mixing, the particles were distributed and moved throughout the reactor volume.

3.3. Temperature Analysis

To create nanoscale pores in the membrane, a low temperature is required inside the electrochemical reactor [46]. For this purpose, an automatic temperature control system was used. During the anodization process, it is crucial to maintain the temperature around 5–8 °C [33]. During the experiment, the temperature of 5 °C in the temperature control device was set. Temperature analysis was performed using two methods: when the liquid inside the reactor was not stirred and when it was stirred. The results of the temperature measurements are shown in Figure 5.

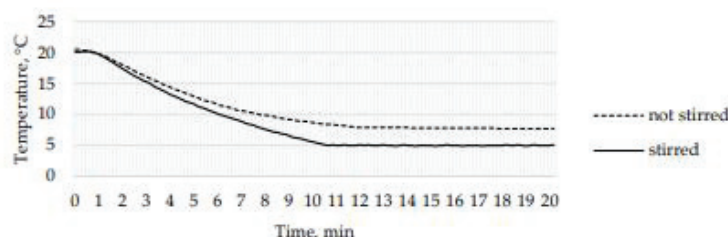


Figure 5. Temperature changes over time inside the reactor.

In the case when the liquid in the reactor was not stirred, the uniform temperature of 5 °C was not reached during the experiment. The temperature sensor near the aluminum plate recorded the lowest temperature at 7.7 °C, but as it was set at 5 °C, the automatic control system was constantly working trying to reach the intended temperature, but due to the unmixed liquid, the areas of different temperatures were formed. Additionally, in some places, the temperature in the reactor was significantly lower, and ice formed in the refrigeration zone. Whereas the temperature near the anodization zone was important, the automatic temperature control system could not reach the target temperature of 5 °C when the liquid was not stirred because the temperature distribution in the reactor's volume was insufficient for the electrochemical process. When the liquid in the reactor was stirred, the temperature inside the reactor ranged from 4.5 °C to 6.0 °C with a functioning automatic temperature control system. Such temperature changes are permissible during the anodization process. Therefore, the temperature control system is suitable for the design of the reactor as it provides the ability to maintain the required temperature during electrochemical processes. The results of the temperature analysis confirm that the mixing process is important in maintaining a constant liquid temperature throughout the reactor volume.

3.4. Fabrication of AAO Nanoporous Membrane

A high-purity aluminum alloy (1050A, 99.5%) sheet of 0.5 mm thickness was the main material used for the fabrication of the AAO nanoporous membrane (radius 20 mm). For fabrication, the experimental setup for the two-step anodization process (Figure 2) was used.

For the experiment, the aluminum sheet was cut into square specimens (5 cm × 5 cm). The specimens were annealed at 400 °C for 4 h in a conventional furnace in a nitrogen atmosphere. After that, the specimens were degreased in acetone. In the novel electrochemical reactor with a vibrating functional element, the aluminum sheet was used as the anodic electrode, whereas the corps of the reactor was used as the cathodic electrode. In the

first-step anodization, the aluminum sheet was anodized at 60 V and 5 °C temperature for 1 h in 0.3 M oxalic acid ($H_2C_2O_4$) electrolyte. After the first-step anodization, the obtained oxide layer was removed by chemical etching in a mixture of 3.5% concentrated phosphoric acid (H_3PO_4) and 2% chromium anhydride (CrO_3) acid solution (by volume) in water at 20 °C for 1 h. After etching, the specimen was rinsed with distilled water. Then, the second anodization was carried out on the same aluminum sheet at 60 V and 5 °C temperature for 8 h in 0.3 M oxalic acid. Then, the specimen was removed from the reactor, rinsed with distilled water, and dried in air.

The same procedure was performed in the two-step anodization process using high-frequency excitation. The first and second mode shape methods were chosen to monitor for significant changes in the AAO nanoporous membranes. The frequency was set at 3.1 kHz and 4.1 kHz, respectively.

AAO morphology and surface chemical composition were determined by scanning electron microscopy (SEM) and energy dispersive spectroscopy (EDS), respectively. The Hitachi S-3400N scanning electron microscope with an integrated Bruker energy dispersive X-ray spectroscopy (EDS) system was used. SEM images of AAO nanoporous membranes are shown in Figure 6.

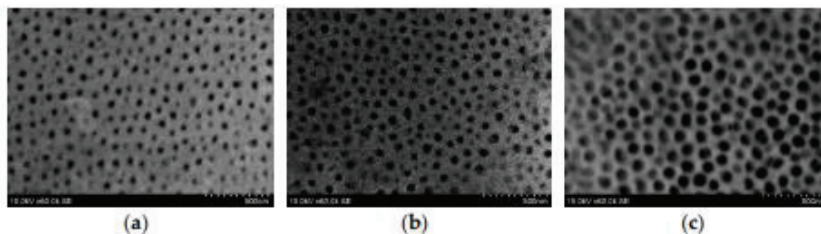


Figure 6. SEM images of AAO nanoporous membrane. (a) AAO nanoporous membrane after the two-step anodization process; (b) AAO nanoporous membrane after the two-step anodization process using 3.1 kHz frequency excitation; (c) AAO nanoporous membrane after the two-step anodization process using 4.1 kHz frequency excitation.

Using the image processing program “ImageJ”, the pore diameter (D_p) and the distance between the pores (D_c) were determined. To characterize the AAO structure of nanopores, the parameter of porosity was used. Porosity (P) can be defined as the ratio of the surface area occupied by pores and the whole surface area. The P value can be calculated as follows [50]:

$$P = 0.907 \cdot (D_p/D_c)^2\%, \quad (1)$$

where D_p : pore diameter, D_c : interpore distance.

The morphological parameters (D_p , D_c , and P) of the nanoporous membranes are shown in Table 3.

Table 3. Morphological parameters (D_p , D_c , and P) of the AAO nanoporous membrane obtained during the two-step anodization process.

Parameter	No Frequency Excitation	Frequency Excitation at 3.1 kHz	Frequency Excitation at 4.1 kHz
Pore diameter (nm)	55.0 ± 10	82.6 ± 10	86.1 ± 10
Interpore distance (nm)	121.4 ± 20	120.0 ± 20	120.5 ± 20
Porosity (%)	19	43	46

The obtained AAO membrane had a pore diameter of 55.0 ± 10 nm, the interpore distance of 121.4 ± 20 nm, and 19% porosity. Using the frequency excitation of 3.1 kHz,

the obtained AAO membrane had a pore diameter of 82.6 ± 10 nm, an interpore distance of 120.0 ± 20 nm, and 43% porosity. Likewise, using frequency excitation of 4.1 kHz, the obtained AAO membrane had a pore diameter of 86.1 ± 10 nm, an interpore distance of 120.5 ± 20 nm, and 46% porosity. Overall, these results reveal that, when frequency excitation is used, the pore diameter increases, leading to an increase in porosity. However, the interpore distance has been found to be independent of the frequency.

Analysis of energy dispersive X-ray spectroscopy (EDS) allowed the qualitative and quantitative determination of chemical composition. The chemical compositions of nanoporous AAO are shown in Table 4. The analysis showed that Al_2O_3 predominates. Other peaks showed a lower carbon and sulfur content (carbon and sulfur are impurities due to amorphous anodic aluminum oxide). There are no significant changes in the chemical composition of AAO membranes. Thus, the elemental composition of porous membranes has been found to be independent of the frequency. Moreover, the detailed chemical composition indicates the successful fabrication of AAO using frequency excitation.

Table 4. Chemical composition of AAO nanoporous membrane.

Element	No Frequency		Frequency Excitation at 3.1 kHz		Frequency Excitation at 4.1 kHz	
	Atomic Concentration, at%	Error, %	Atomic Concentration, at%	Error, %	Atomic Concentration, at%	Error, %
Carbon	1.37	0.2	2.02	0.5	1.36	0.3
Oxygen	62.77	6.1	65.18	7.8	62.69	6.6
Aluminum	35.57	2.4	32.51	2.4	35.67	2.3
Sulfur	0.30	0.0	0.29	0.1	0.29	0.1

Since the porosity of the oxide was increased by frequency excitation, it is important to perform hardness measurements to confirm that the porosity affects the mechanical properties of aluminum oxide.

The hardness measurements were taken with Vickers indentations with a diamond tip (Micro Vickers Hardness Testing Machine: HM-200, Mitutoyo, Japan). Each specimen was measured at least five times, and the average was taken. The hardness measurements were recorded in software and represented in Vickers hardness units.

The hardness tests showed a decrease in hardness from 4.73 GPa to 1.40 GPa comparing the AAO nanoporous membrane after the two-step anodization process without frequency excitation and AAO nanoporous membrane after the two-step anodization process with frequency excitation at 4.1 kHz. Studies performed by other researchers have shown similar results in which the hardness value depends on porosity. The hardness shows a decreasing trend with increasing porosity [51]. In another study, hardness measurements revealed no significant cracks around the indentation [52]. Furthermore, only minor cracks between the pores could be observed inside the indentation [53].

Thus, the obtained results reveal that under the same anodization conditions and using high-frequency excitation, the hardness of the AAO membrane decreases, and the porosity increases. Analyzing the brittleness of the AAO membrane, no additional studies were performed, but based on the researchers' insights that as porosity increases and hardness decreases, brittleness also decreases, we assumed that the AAO membrane produced using high-frequency excitation was less brittle, but hard enough to be used for template synthesis or other applications.

Furthermore, considering the theoretical model of the porous aluminum growth mechanism, it can be assumed that the resonant frequency excitation to the AAO nanoporous membrane promotes better mixing of the electrolyte on the oxide and electrolyte interface. At the oxide/electrolyte interface, the electrolyte concentration is constantly renewed. As a result, high-efficiency oxide growth is obtained. In the future, theoretical calculations should be performed to confirm the theory of high-frequency excitation during the an-

odization process and the effect of high frequency on the growth mechanism of porous aluminum oxide.

4. Conclusions

The development and analysis of an innovative electrochemical reactor with a vibrating element are presented. The reactor to produce nanoporous AAO membranes by the two-step anodization method was proposed. To produce less brittle oxide, the high-frequency excitation method was used; therefore, a vibrating element (piezoceramic ring) was integrated into the reactor's structure. It generates vibrations in the aluminum sheet during anodization. Whereas it is necessary to ensure a temperature of 5–8 °C during the electrochemical process, a Peltier element and a temperature control system were installed in the reactor to ensure the uniform temperature of the liquid throughout the reactor's volume. The reactor also includes a mixing system with a four-blade impeller. In addition, the reactor's corps was composed of stainless steel to ensure its resistance to electrolytes.

Vibration, mixing, and temperature analyses were performed. Mathematical models were simulated using COMSOL Multiphysics 5.4 and ANSYS 17 software. Theoretical calculations were experimentally verified. The following results of the reactor design analysis were obtained:

- The high-frequency excitation method was used during the vibration experiment. Five vibration mode shapes were obtained at different frequencies: the first mode shape (0, 1) at 3.0 kHz and 3.1 kHz, the second mode shape (1, 1) at 4.8 kHz and 4.1 kHz, the third mode shape (2, 1) at 6.5 kHz and 6.3 kHz, the fourth mode shape (0, 2) at 6.9 kHz and 7.1 kHz, and the fifth mode shape (3, 1) at 8.8 kHz and 9.1 kHz. The simulation and the experimental results of membrane surface displacements were close, but not identical, because of nonideal structural stability and material properties and the inaccuracy of the measuring equipment;
- It was found that the designed impeller was sufficient for the mixing process. The whole volume in the reactor was mixed. However, specific particle motions were not clearly captured during the experiment. When the mixing device was turned off, the particles did not move throughout the reactor volume, but in the case of the mixing process, the particles were distributed throughout the reactor volume. It was assumed that the mixing experiment was related to the simulation results;
- In the case where the liquid in the reactor was not stirred, the uniform temperature of 5 °C was not reached during the experiment. In addition, in some places, the temperature in the reactor was significantly lower, and cold zones with ice were formed. The temperature sensor recorded the lowest temperature of 7.7 °C. In the case where the liquid was stirred inside the reactor, the temperature ranged from 4.5 °C to 6.0 °C using an automatic temperature control system. Such temperature changes were acceptable.

The results of the vibration, mixing, and temperature analysis confirmed that the design of the novel electrochemical reactor met the requirements. Analyses have shown that the use of the high-frequency excitation method offers a real opportunity to develop functional nanoporous AAO membranes. A novel aluminum anodization technology, which uses high-frequency excitation in the two-step anodization process, results in AAO membranes with 82.6 ± 10 nm pore diameters and 43% porosity using frequency excitation at 3.1 kHz and AAO membranes with 86.1 ± 10 nm pore diameters and 46% porosity using frequency excitation at 4.1 kHz. The chemical composition of the membranes remained unchanged, but the pore diameter increased, resulting in higher porosity and lower hardness. It can be assumed that the nanoporous AAO has become less brittle but hard enough to be used for template synthesis.

The results obtained under the controlled and well-described two-step anodization process with high-frequency excitation conditions will be useful in synthesizing and improving the structure and quality of AAO nanoporous membranes.

Author Contributions: Conceptualization, U.C.; methodology, U.C. and A.P.; investigation, U.C., V.J. and G.J.; calculation and analysis, U.C. and G.J.; formal analysis, V.J. and K.P.; writing—original draft preparation, U.C. and K.P.; writing—review and editing, A.P., V.J. and K.P.; visualization, U.C.; validation, A.P. and G.J.; funding acquisition G.J. All authors have read and agreed to the published version of the manuscript.

Funding: This research was funded by grant No. 0.1.2.2-CPVA-K-703-03-0015 “Development of new technology for the formation of microstructures in functional materials” from the European Regional Development Fund.

Institutional Review Board Statement: Not applicable.

Informed Consent Statement: Not applicable.

Data Availability Statement: Not applicable.

Conflicts of Interest: The authors declare no conflict of interest.

References

- Domagalski, J.T.; Xifre-Perez, E.; Marsal, L.F. Recent Advances in Nanoporous Anodic Alumina: Principles, Engineering, and Applications. *Nanomaterials* **2021**, *11*, 430. [\[CrossRef\]](#) [\[PubMed\]](#)
- Tan, C.; Cao, X.; Wu, X.; He, Q.; Yang, J.; Zhang, X.; Chen, J.; Zhao, W.; Han, S.; Nam, G.; et al. Recent Advances in Ultrathin Two-Dimensional Nanomaterials. *Chem. Rev.* **2017**, *117*, 6225–6331. [\[CrossRef\]](#) [\[PubMed\]](#)
- Zhang, H. Ultrathin Two-Dimensional Nanomaterials. *ACS Nano* **2015**, *9*, 9451–9469. [\[CrossRef\]](#) [\[PubMed\]](#)
- Hwang, S.; Lee, C.; Cheng, H.; Jeong, J.; Kang, S.; Kim, J.; Shin, J.; Yang, J.; Liu, Z.; Ameer, G.; et al. Biodegradable Elastomers and Silicon Nanomembranes/Nanoribbons for Stretchable, Transient Electronics, and Biosensors. *Nano Lett.* **2015**, *15*, 2801–2808. [\[CrossRef\]](#)
- Zanghelini, F.; Frias, I.; Régo, M.; Pitta, M.; Sacilotti, M.; Oliveira, M.; Andrade, C. Biosensing breast cancer cells based on a three-dimensional TiO₂ nanomembrane transducer. *Biosens. Bioelectron.* **2017**, *92*, 313–320. [\[CrossRef\]](#)
- Vervacke, C.; Bufon, C.; Thurmer, D.; Schmidt, O. Three-dimensional chemical sensors based on rolled-up hybrid nanomembranes. *RSC Adv.* **2014**, *4*, 9723. [\[CrossRef\]](#)
- Liu, X.; Ma, T.; Xu, Y.; Sun, L.; Zheng, L.; Schmidt, O.; Zhang, J. Rolled-up SnO₂ nanomembranes: A new platform for efficient gas sensors. *Sens. Actuators B Chem.* **2018**, *264*, 92–99. [\[CrossRef\]](#)
- Tian, F.; Lyu, J.; Shi, J.; Tan, F.; Yang, M. A polymeric microfluidic device integrated with nanoporous alumina membranes for simultaneous detection of multiple foodborne pathogens. *Sens. Actuators B Chem.* **2016**, *225*, 312–318. [\[CrossRef\]](#)
- Pérez-Madrugal, M.; Armelin, E.; Puiggali, J.; Alemán, C. Insulating and semiconducting polymeric free-standing nanomembranes with biomedical applications. *J. Mater. Chem. B* **2015**, *3*, 5904–5932. [\[CrossRef\]](#)
- Madrugal, M.; Giannotti, M.; Valle, L.; Franco, L.; Armelin, E.; Puiggali, J.; Sanz, F.; Alemán, C. Thermoplastic Polyurethane: Polythiophene Nanomembranes for Biomedical and Biotechnological Applications. *ACS Appl. Mater. Interfaces* **2014**, *6*, 9719–9732. [\[CrossRef\]](#)
- Kumar, L. Role and adverse effects of nanomaterials in food technology. *J. Toxicol. Health* **2015**, *2*, 2. [\[CrossRef\]](#)
- Wang, X.; Chen, Y.; Schmid, O.; Yan, C. Engineered nanomembranes for smart energy storage devices. *Chem. Soc. Rev.* **2016**, *45*, 1308–1330. [\[CrossRef\]](#) [\[PubMed\]](#)
- Thibert, S.; Delaunay, M.; Ghis, A. Carbon-metal vibrating nanomembranes for high frequency microresonators. *Diam. Relat. Mater.* **2018**, *81*, 138–145. [\[CrossRef\]](#)
- Jakšić, Z.; Jakšić, O. Biomimetic Nanomembranes: An Overview. *Biomimetics* **2020**, *5*, 24. [\[CrossRef\]](#) [\[PubMed\]](#)
- Jakšić, Z.; Matovic, J. Functionalization of Artificial Freestanding Composite Nanomembranes. *Materials* **2010**, *3*, 165–200. [\[CrossRef\]](#)
- Huang, G.; Mei, Y. Assembly and Self-Assembly of Nanomembrane Materials-From 2D to 3D. *Small* **2018**, *14*, 1703665. [\[CrossRef\]](#) [\[PubMed\]](#)
- Winter, A.; Ekinci, Y.; Götzhäuser, A.; Turchanin, A. Freestanding carbon nanomembranes and graphene monolayers nanopatterned via EUV interference lithography. *2D Mater.* **2019**, *6*, 021002. [\[CrossRef\]](#)
- Yang, L.; Wei, J.; Ma, Z.; Song, P.; Ma, J.; Zhao, Y.; Huang, Z.; Zhang, M.; Yang, F.; Wang, X. The Fabrication of Micro/Nano Structures by Laser Machining. *Nanomaterials* **2019**, *9*, 1789. [\[CrossRef\]](#)
- Chan, E.; Lee, S. Thickness-dependent swelling of molecular layer-by-layer polyamide nanomembranes. *J. Polym. Sci. Part B Polym. Phys.* **2016**, *55*, 412–417. [\[CrossRef\]](#)
- Chen, X.; Zhang, W.; Lin, Y.; Cai, Y.; Qiu, M.; Fan, Y. Preparation of high-flux γ -alumina nanofiltration membranes by using a modified sol-gel method. *Microporous Mesoporous Mater.* **2015**, *214*, 195–203. [\[CrossRef\]](#)
- Tijing, L.; Dizon, J.; Ibrahim, I.; Nisay, A.; Shon, H.; Advincula, R. 3D printing for membrane separation, desalination and water treatment. *Appl. Mater. Today* **2020**, *18*, 100486. [\[CrossRef\]](#)

22. Lee, J.; Tan, W.; An, J.; Chua, C.; Tang, C.; Fane, A.; Chong, T. The potential to enhance membrane module design with 3D printing technology. *J. Membr. Sci.* **2016**, *499*, 480–490. [[CrossRef](#)]
23. Lee, W.; Park, S. Porous Anodic Aluminum Oxide: Anodization and Templated Synthesis of Functional Nanostructures. *Chem. Rev.* **2014**, *114*, 7487–7556. [[CrossRef](#)] [[PubMed](#)]
24. Velleman, L.; Triani, G.; Evans, P.; Shapter, J.; Losic, D. Structural and chemical modification of porous alumina membranes. *Microporous Mesoporous Mater.* **2009**, *126*, 87–94. [[CrossRef](#)]
25. Jani, A.; Anglin, E.; McInnes, S.; Losic, D.; Shapter, J.; Voelcker, N. Nanoporous anodic aluminium oxide membranes with layered surface chemistry. *Chem. Commun.* **2009**, *2009*, 3062–3064. [[CrossRef](#)]
26. Ateş, S.; Baran, E.; Yazıcı, B. The nanoporous anodic alumina oxide formed by two-step anodization. *Thin Solid Film.* **2018**, *648*, 94–102. [[CrossRef](#)]
27. Sulka, G. Highly Ordered Anodic Porous Alumina Formation by Self-Organized Anodizing. In *Nanostructured Materials in Electrochemistry*; Eftekhari, A., Ed.; Wiley-VCH Verlag GmbH & Co.: Hoboken, NJ, USA, 2008; pp. 1–116. [[CrossRef](#)]
28. Stepniowski, W.; Forbot, D.; Norek, M.; Michalska-Domańska, M.; Król, A. The impact of viscosity of the electrolyte on the formation of nanoporous anodic aluminum oxide. *Electrochim. Acta* **2014**, *133*, 57–64. [[CrossRef](#)]
29. Azami, H.; Omidkhab, M. Modeling and optimization of characterization of nanostructure anodized aluminium oxide membranes. *J. Iran. Chem. Soc.* **2019**, *16*, 985–997. [[CrossRef](#)]
30. Stepniowski, W.; Moneta, M.; Norek, M.; Michalska-Domańska, M.; Scarpellini, A.; Salerno, M. The influence of electrolyte composition on the growth of nanoporous anodic alumina. *Electrochim. Acta* **2016**, *211*, 453–460. [[CrossRef](#)]
31. Absalan, G.; Barzegar, S.; Moradi, M.; Behaein, S. Fabricating Al₂O₃-nanopores array by an ultrahigh voltage two-step anodization technique: Investigating the effect of voltage rate and Al foil thickness on geometry and ordering of the array. *Mater. Chem. Phys.* **2017**, *199*, 265–271. [[CrossRef](#)]
32. Michalska-Domańska, M.; Norek, M.; Stepniowski, W.; Budner, B. Fabrication of high quality anodic aluminum oxide (AAO) on low purity aluminum-A comparative study with the AAO produced on high purity aluminum. *Electrochim. Acta* **2013**, *105*, 424–432. [[CrossRef](#)]
33. Patel, Y.; Janusas, G.; Palevicius, A.; Vilkauskas, A. Development of Nanoporous AAO Membrane for Nano Filtration Using the Acoustophoresis Method. *Sensors* **2020**, *20*, 3833. [[CrossRef](#)] [[PubMed](#)]
34. Kuscer, D.; Rojac, T.; Belavič, D.; Zarnik, M.; Bradeško, A.; Kos, T.; Malič, B.; Boerrigter, M.; Martin, D.; Faccini, M. Integrated piezoelectric vibration system for fouling mitigation in ceramic filtration membranes. *J. Membr. Sci.* **2017**, *540*, 277–284. [[CrossRef](#)]
35. Ogawa, J.; Kanno, I.; Kotera, H.; Wasa, K.; Suzuki, T. Development of liquid pumping devices using vibrating microchannel walls. *Sens. Actuators A Phys.* **2009**, *152*, 211–218. [[CrossRef](#)]
36. Cazorla, P.; Fuchs, O.; Cochet, M.; Maubert, S.; Rhun, G.; Fouillet, Y.; Defay, E. Integration of PZT thin films on a microfluidic complex system. In Proceedings of the 2014 IEEE International Ultrasonics Symposium, Chicago, IL, USA, 3–6 September 2014. [[CrossRef](#)]
37. Janusas, T.; Pilkauskas, K.; Janusas, G.; Palevicius, A. Active PZT Composite Microfluidic Channel for Bioparticle Manipulation. *Sensors* **2019**, *19*, 2020. [[CrossRef](#)]
38. Sathyanarayana, C.; Raja, S.; Ragavendra, H. Procedure to Use PZT Sensors in Vibration and Load Measurements. *Smart Mater. Res.* **2013**, *2013*, 173605. [[CrossRef](#)]
39. Wang, G.; Zhao, Z.; Tan, J.; Cui, S.; Wu, H. A novel multifunctional piezoelectric composite device for mechatronics systems by using one single PZT ring. *Smart Mater. Struct.* **2020**, *29*, 055027. [[CrossRef](#)]
40. Shen, L.; Li, Y.; Zhong, W.; Wu, J.; Cheng, J.; Jin, L.; Hu, X.; Ling, Z. Fabrication of micro/nanoporous templates with a novel hierarchical structure by anodization of a patterned aluminum surface. *Electrochim. Commun.* **2021**, *126*, 107014. [[CrossRef](#)]
41. Mijangos, C.; Hernández, R.; Martín, J. A review on the progress of polymer nanostructures with modulated morphologies and properties, using nanoporous AAO templates. *Prog. Polym. Sci.* **2016**, *54–55*, 148–182. [[CrossRef](#)]
42. Wei, Q.; Fu, Y.; Zhang, G.; Yang, D.; Meng, G.; Sun, S. Rational design of novel nanostructured arrays based on porous AAO templates for electrochemical energy storage and conversion. *Nano Energy* **2019**, *55*, 234–259. [[CrossRef](#)]
43. Callister, W.D.; Rethwisch, D.G. *Fundamentals of Materials Science and Engineering: An Integrated Approach*, 5th ed.; Wiley: New York, NY, USA, 2018; pp. 214–216. ISBN 978-1-119-17550-6.
44. Ge, J.; Ding, B.; Hou, S.; Luo, M.; Nam, D.; Duan, H.; Gao, H.; Lam, Y.C.; Li, H. Rapid fabrication of complex nanostructures using room-temperature ultrasonic nanoimprinting. *Nat. Commun.* **2021**, *12*, 3146. [[CrossRef](#)] [[PubMed](#)]
45. Dai, J.; Singh, J.; Yamamoto, N. Non-brittle Nanopore Deformation of Anodic Aluminum Oxide Membranes. *J. Am. Ceram. Soc.* **2017**, *101*, 2170–2180. [[CrossRef](#)]
46. Poinern, G.; Ali, N.; Fawcett, D. Progress in Nano-Engineered Anodic Aluminum Oxide Membrane Development. *Materials* **2011**, *4*, 487–526. [[CrossRef](#)] [[PubMed](#)]
47. DeAngelis, D.; Schulze, G. Performance of PZT8 Versus PZT4 Piezoceramic Materials in Ultrasonic Transducers. *Phys. Procedia* **2016**, *87*, 85–92. [[CrossRef](#)]
48. Jirout, T.; Jiroutová, D. Application of Theoretical and Experimental Findings for Optimization of Mixing Processes and Equipment. *Processes* **2020**, *8*, 955. [[CrossRef](#)]
49. Xavior, M.; Nishanth, D.; Kumar, N.; Jayapandiarajan, P. Synthesis and Testing of FGM made of ABS Plastic Material. *Mater. Today Proc.* **2020**, *22*, 1838–1844. [[CrossRef](#)]

50. Kozhukhova, A.E.; Preez, S.P.; Bessarabov, D.G. Preparation of anodized aluminium oxide at high temperatures using low purity aluminium (Al6082). *Surf. Coat. Technol.* **2019**, *378*, 124970. [[CrossRef](#)]
51. Ko, S.; Lee, D.; Jee, S.; Park, H.; Lee, K.; Hwang, W. Mechanical properties and residual stress in porous anodic alumina structures. *Thin Solid Film.* **2006**, *515*, 1932–1937. [[CrossRef](#)]
52. Vojkuvka, L.; Santos, A.; Pallarès, J.; Ferré-Borrulla, J.; Marsal, L.F.; Celis, J.P. On the mechanical properties of nanoporous anodized alumina by nanoindentation and sliding tests. *Surf. Coat. Technol.* **2012**, *206*, 2115–2124. [[CrossRef](#)]
53. Tsyntsar, N.; Kavas, B.; Sort, J.; Urgen, M.; Celis, J.P. Mechanical and frictional behaviour of nano-porous anodised aluminium. *Mater. Chem. Phys.* **2014**, *148*, 887–895. [[CrossRef](#)]

Article

Vibration-Assisted Synthesis of Nanoporous Anodic Aluminum Oxide (AAO) Membranes

Urte Cigane, Arvydas Palevicius *  and Giedrius Janusas 

Faculty of Mechanical Engineering and Design, Kaunas University of Technology, Studentu Str. 56, LT-51424 Kaunas, Lithuania

* Correspondence: arvydas.palevicius@ktu.lt

Abstract: In recent years, many research achievements in the field of anodic aluminum oxide (AAO) membranes can be observed. Nevertheless, it is still an interesting research topic due to its high versatility and applications in various fields, such as template-assisted methods, filtration, sensors, etc. Nowadays, miniaturization is an integral part of different technologies; therefore, research on micro- and nanosized elements is relevant in areas such as LEDs and OLEDs, solar cells, etc. To achieve an efficient mixing process of fluid flow in straight nanopores, acoustofluidic physics has attracted great interest in recent decades. Unfortunately, the renewal of the electrolyte concentration at the bottom of a pore is limited. Thus, excitation is used to improve fluid mixing along nanosized diameters. The effect of excitation by high-frequency vibrations on pore geometry is also investigated. In this study, theoretical simulations were performed. Using theoretical calculations, the acoustic pressure, acoustic velocity, and velocity magnitude were obtained at frequencies of 2, 20, and 40 kHz. Moreover, nanoporous AAO membranes were synthesized, and the influence of high-frequency vibrations on the geometry of the pores was determined. Using a high-frequency excitation of 20 kHz, the thickness of the AAO membrane increased by 17.8%. In addition, the thickness increased by 31.1% at 40 kHz and 33.3% at the resonant frequency of 40 kHz. Using high-frequency vibrations during the anodization process, the electrolyte inside the pores is mixed, and as a result, a higher oxide growth rate and a deeper structure can be achieved. On the other hand, to obtain pores of the same depth, the reaction can be performed in a shorter time.

Keywords: AAO nanoporous membrane; two-step anodization method; high-frequency excitation method



check for updates

Citation: Cigane, U.; Palevicius, A.; Janusas, G. Vibration-Assisted Synthesis of Nanoporous Anodic Aluminum Oxide (AAO) Membranes. *Micromachines* **2022**, *13*, 2236. <https://doi.org/10.3390/mi13122236>

Academic Editors: Wending Pan and Rui Cheng

Received: 23 November 2022

Accepted: 15 December 2022

Published: 16 December 2022

Publisher's Note: MDPI stays neutral with regard to jurisdictional claims in published maps and institutional affiliations.



Copyright: © 2022 by the authors. Licensee MDPI, Basel, Switzerland. This article is an open access article distributed under the terms and conditions of the Creative Commons Attribution (CC BY) license (<https://creativecommons.org/licenses/by/4.0/>).

1. Introduction

Porous anodic aluminum oxide (AAO) structures were first observed by Keller, Hunter, and Robinson in 1953 [1]. Then, a number of scientists, including Sir Nevill Francis Mott, who won the Nobel Prize in Physics in 1977, Hoar and Mott [2], and Dewald [3], proposed a mechanism for the formation of porous AAO. In 1990, Masuda, Tanaka, and Baba reported for the first time the fabrication process of highly ordered porous structured AAO membranes in oxalic acid [4]. Since then, new conditions have been discovered using different anodization regimes to obtain nanopores with different geometries. For example, anodization was performed using different types of acid electrolytes [5], changing experimental conditions such as the anodization temperature [6,7], the applied anodization potential [8], and the current [9], as well as the dependencies of the diameter of the pores and the distance between the pores, and the thickness of the AAO membranes on these parameters was discovered.

In recent years, researchers have made many achievements in the field of porous AAO membranes, so it is still an interesting research topic due to its great versatility and applications in various fields such as the fabrication of micro- and nanosized elements using the template-assistant approach [10–13], filtration [14–18], different types of sensors [19–21], tissue engineering [22], etc.

Moreover, looking at today's technologies and their development, miniaturization is an integral "economic driver" of today [23–27], and research related to micro- and nanosized elements is relevant in areas such as mini-LEDs and OLEDs [28], solar cells [29,30], electrotherapy and drug delivery [31], sensors [32], etc. The growing potential of these technologies encourages the study of microchannels, which differ from conventional channels in their channel diameter [33–36]. Since flow regimes in small fluid volumes are often laminar, fluid heat exchange is limited, and it is likely that the fluid temperature increases along the length of the microchannel [37]. Therefore, to achieve an efficient and rapid fluid flow mixing process in straight microchannels, acoustofluidic physics has gained much interest in recent decades [38,39]. Surface acoustic waves (SAW) apply the effects of ultrasonic waves and have received a lot of attention from researchers due to their noninvasive nature and the advantages of efficient fluidic control [40]. Researchers have shown that mixing efficiency of the hot and cold fluid laminar flows can be improved by using acoustic streaming [41].

In terms of AAO pore geometry, the peculiarity of the AAO structure is the pore width-to-length ratio. Synthesized AAO membranes have been reported with pore diameters in the range of tens to several hundreds of nanometers, and the length can reach several tens of micrometers [13]. Therefore, the renewal of fluid at the bottom of the pore during anodization is limited. Given these points, the application of acoustofluidics in the fabrication of porous AAO membranes during the anodization process could be used to overcome this limitation. Moreover, the effect of excitation by high-frequency vibrations used during the anodization process on the pore geometry has not yet been widely investigated, because high-frequency vibrations usually are used for treatment processes before or after the anodization [42,43].

Taking into account different theoretical models [44] that explain AAO formation and provide insight into oxide dissolution at the oxide/electrolyte interface and ion migration under high-field conditions, as well as based on changes in findings on temperature and pH along the nanopore, it is important to ensure the mixing process and renewal of fluid flow along the length of the pore with nano- and micro-sized length. Moreover, considering the wide application of micro- and nanomaterials in various fields and the current research related to better mechanical strength, brittleness, and other improved properties of porous AAO membranes [45,46], the problem related to the temperature and pH value differences of the electrolyte flow inside the pore during the anodization process is analyzed in this paper. As the problem is relevant, and further research is needed, the solution to ensure a more uniform flow temperature and pH value in the pore of the AAO membrane when AAO is fabricated by the two-step anodization process is presented.

Therefore, in this article, two techniques (high-frequency excitation and chemical anodization) are combined to study fluid mixing inside the pores and to study the changes in the geometry of the AAO pores using high-frequency excitation during the well-known two-step anodization process using 0.3 M oxalic acid at a constant temperature of 5 °C and a constant voltage at 60 V. The structure of the paper is as follows. The theoretical simulation method, boundary conditions, equations used, as well as experimental AAO membrane fabrication technology are presented in Section 2. The theoretical simulations and the experimental results are presented in Section 3. The results of the influence of vibrations on the fluid mixing inside the pore and the influence of vibrations on the geometry of AAO membrane pores are presented. Conclusions are drawn in Section 4.

2. Materials and Methods

2.1. Simulation Method and Conditions of Vibration Process

In this paper, the fluid flow inside nanopores was simulated using COMSOL Multiphysics 6.0 software. The numerical model consisted of two pores with a 105 nm diameter and an electrolyte container (part of the reactor volume). Two pores were chosen to determine the more realistic behavior of the electrolyte flow between the pores compared to the flow presented by a single pore. The model was meshed by finite tetrahedron elements

with fixed support constraint boundary conditions. The computational mesh for the pores and the boundary conditions of the numerical model are presented in Figure 1.

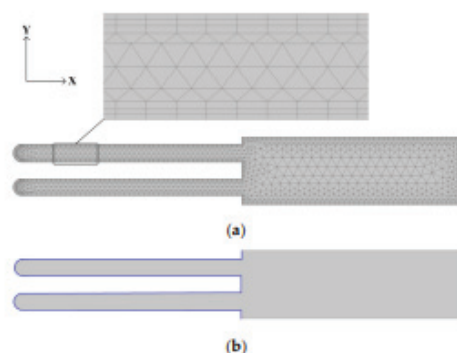


Figure 1. Simulation model. (a) Geometry and computational mesh for nanopores; (b) boundary conditions.

Thus, the walls of the pores were solid surfaces with no-slip and isothermal boundary conditions. Therefore, the properties of the boundary layer were applied around the perimeter, where 3 layers were stretched (Figure 1a). The model consisted of 2764 elements with 320 boundary elements. Additionally, velocity and isothermal fortifications were used in the area marked in blue (Figure 1b). The velocity boundary conditions in the y direction were constrained, and movements in the x direction were unconstrained (periodic oscillation was selected). The entire domain was continuous and selected as a Thermoviscous Acoustics Model in which the equilibrium pressure was 1 atm, and the temperature was 5 °C. The properties of the electrolyte fluid were selected from Material Libraries in COMSOL Multiphysics 6.0. The parameters of the simulation model are presented in Table 1.

Table 1. Parameters of the model of fluid flow simulation in nanopores.

Parameter	Symbol	Inscription	Value	Units
Frequency	f_0	2 [kHz]	2000	Hz
		20 [kHz]	20,000	
		40 [kHz]	40,000	
Ambient temperature	T_0	5 [degC]	278.15	K
Ambient pressure	p_0	1 [atm]	1.0133×10^5	Pa
Angular frequency	ω_0		12,566	Hz
		$2 \times \pi \times f_0$	1.257×10^5	
			2.513×10^5	
Mesh viscous penetration depth at f_0	$d_{\text{visc}0}$	$100 \text{ [}\mu\text{m]} \times \sqrt{\text{sqrt}(100 \text{ [Hz]}/f_0)}$	2.236×10^{-5}	m
			7.071×10^{-6}	
Speed of sound in water	c_0	1495.3 [m/s]	1495.3	m/s

Table 1. Cont.

Parameter	Symbol	Inscription	Value	Units
Wavelength	lam0	c0/f0	0.747650	m
			0.074765	
			0.037383	
Wave number	k0	$2 \times \pi / \text{lam0}$	8.4039	1/m
			84.039	
			168.08	
Channel cross section width	W	105 [nm]	10.5×10^{-8}	m
Channel cross-section height	H	1000 [nm]	1×10^{-6}	m
		5000 [nm]	5×10^{-6}	
		30,000 [nm]	30×10^{-6}	
		55,000 [nm]	55×10^{-6}	
Wall displacement	d0	1 [nm]	1×10^{-9}	m
		5 [nm]	5×10^{-9}	

Since an acid electrolyte is used during anodization, the thermophysical properties of water have been used in the simulation. The thermophysical properties of fluid (water) are shown in Table 2.

Table 2. Thermophysical properties of fluid (water).

Fluid	Density, kg/m ³	Dynamic Viscosity, Pa·s	Bulk Viscosity, Pa·s	Ratio of Specific Heats	Heat Capacity at Constant Pressure, J/(kg·K)	Thermal Conductivity, W/(m·K)	Speed of Sound, m/s
Water	1000	0.0018	0.005	1	4200	0.56	1400

In this study, two sets of governing equations were used to obtain the results. Based on the temporal and spatial scales, the acoustic velocity field was first calculated using the thermoviscous acoustics module in the frequency domain. Then, the streaming flow velocity field was calculated by applying the creeping flow module.

In the Thermoviscous Acoustics mathematical model, the following equations were used. Assuming small harmonic oscillations about the steady background properties, the dependent variables could be written as

$$p_t = p_1 + p_b \quad (1)$$

$$u_t = u_1 + u_b \quad (2)$$

$$T_t = T_1 + T_b \quad (3)$$

where p is the pressure, u is the velocity field, and T is the temperature. The prime variables (subscript 1) are the acoustic variables, and the variables accompanied by subscript b represent the background mean flow quantities.

In the Thermoviscous Acoustics interface, the continuity equation could be written as

$$p_t = p_1 + p_b \quad i\omega \rho_t + \nabla \times (\rho_0 u_t) = 0 \quad (4)$$

where ω is the frequency of actuation, ρ_0 is the equilibrium density, u_t is the acoustic velocity field, and ρ_t is the density at temperature T_t :

$$\rho_t = \rho_0 (\beta_T p_T - \alpha_p T_t) \quad (5)$$

$$\beta_T = (1/\rho_0) - (\gamma/c^2) \quad (6)$$

$$\alpha_p = (1/c) - ((c_p (\gamma - 1))/T_0)^{1/2} \quad (7)$$

where β_T is the isothermal compressibility coefficient, α_p is the coefficient of thermal expansion, c is the speed of sound in the fluid, and p_T is the equilibrium pressure. Equation (5) shows related variations in pressure, temperature, and density. The momentum equation could be written as

$$\sigma = -p_T I + \mu (\nabla u_t + (\nabla u_t)^T) - (2/3 \mu - \mu_B) (\nabla \times u_t) I \quad (8)$$

where μ is the dynamic viscosity, and μ_B is the bulk viscosity. The right side of the equation indicates the divergence of the stress tensor.

In the frequency domain, multiplication with $i\omega$ corresponds to differentiation with respect to time

$$i\omega \rho_0 u_t = \nabla - \sigma \quad (9)$$

Then, the energy conservation equation could be written as

$$\rho_0 C_p (i\omega T_t + u_t \times \nabla T_0) - \alpha_p T_0 (i\omega p_t + u_t \times \nabla p_0) = \nabla \times (k \nabla T_t) + Q \quad (10)$$

where C_p is the heat capacity at constant pressure, k is the thermal conductivity, α_p is the coefficient of thermal expansion (isobaric), and Q is a possible heat source.

Because creeping flow, also known as Stokes flow, could occur in the systems with small geometrical length scales, the following equations were used:

$$0 = \nabla \times [-p \ 2 I + K] + F \quad (11)$$

$$\rho \nabla \times u_2 = 0 \quad (12)$$

$$K = \mu (\nabla u_2 + (\nabla u_2)^T) \quad (13)$$

where ρ is density of the fluid, p is the fluid pressure field, u is velocity field of the fluid, and F is external force.

In the first study, frequencies of 2, 20, and 40 kHz were used. During the second study, the results obtained from the first simulation were used (each frequency was simulated separately).

2.2. Fabrication of AAO Nanoporous Membranes

AAO nanoporous membranes were fabricated using the two-step anodization process (Figure 2). A high-purity annealed aluminum foil (1050A, 99.5%) with a thickness of 0.5 mm was used for experiments. At first, aluminum foil was cut into 5 cm × 5 cm square specimens, which were annealed at 400 °C for 4 h under nitrogen ambient. Annealing was carried out in a conventional furnace. Then, the specimens were degreased in acetone and rinsed with distilled water. The prepared specimens were anodized in the electrochemical reactor. Anodization was performed at a voltage of 60 V and a temperature of 5 °C using 0.3 M oxalic acid (H₂C₂O₄) as the electrolyte. The first anodization step lasted 1 h. Then, the synthesized oxide layer was chemically etched in a mixture of 3.5% concentrated phosphoric acid (H₃PO₄) and 2% chromium anhydride (CrO₃) acid solution in water at 80 °C for 10 min. After being washed with distilled water, the specimens were placed in an electrochemical reactor, where the second step of anodization at 60 V and 5 °C temperature for 8 h was performed. Then, the aluminum layer from the AAO membrane was removed using a solution of a concentrated hydrochloric acid (HCl), copper chloride dihydrate (CuCl₂ × 2H₂O), and distilled water (1:0.3:1). Finally, the specimens were rinsed with distilled water and air-dried.

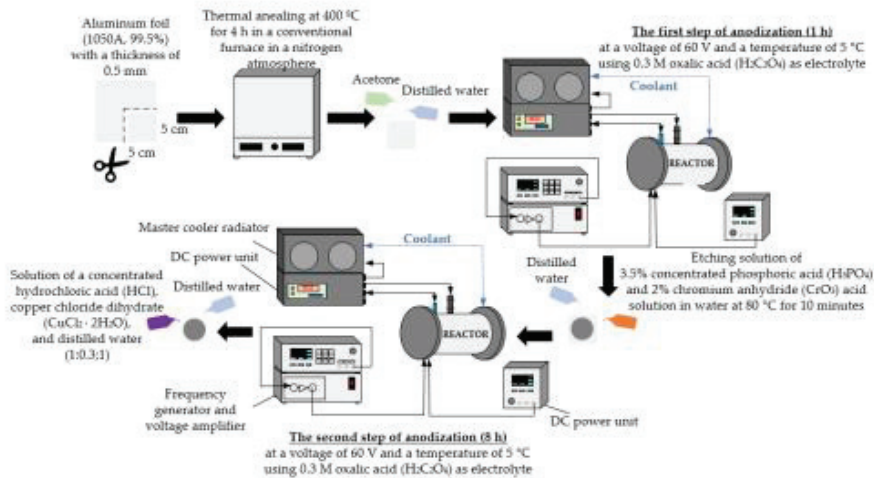


Figure 2. Illustration of the two-step anodization process.

Under the same anodization conditions, AAO membranes were fabricated using high-frequency excitation during the first and second steps of anodization. The high-frequency oscillations were generated using a piezoceramic ring, which was excited by the signal from the frequency generator and the voltage amplifier. A piezoceramic ring was installed inside the reactor.

3. Results and Discussion

3.1. Influence of Vibration on Fluid Flow Inside the Pores

In this section, the simulations performed and the results obtained are described in order to verify the effect of high-frequency vibrations on the mixing process of the fluid flow inside membrane pores.

First, a line was drawn through the center of the entire length of the pore, which allowed for the collection of finite element method plot values. Three parameters were analyzed: total acoustic pressure, total acoustic velocity, and velocity magnitude. The simulations were performed at different frequencies of 2, 20, and 40 kHz. Considering the growth of oxide during the electrochemical process and the deepening of the pores, the simulations were also performed at different depths (1, 5, 30, and 55 μm) to evaluate how the total acoustic pressure, the total acoustic velocity, and velocity magnitude change with the change in the depth of the pores. At 1 and 5 μm depth, data were recorded at 4–5 nm, and at 30 and 55 μm depth, data were recorded at 7–8 nm. To evaluate changes in fluid flow at different excitation frequency values and pore depths, and to process large amounts of data, the calculation of mean values was used. Therefore, the dependencies of the variation in the average values of acoustic pressure, acoustic velocity, and velocity magnitude were obtained. The dependencies of different parameters on frequency and depth are presented in Figure 3.

The acoustic pressure decreased (Figure 3a) in all cases as the pore deepened. The highest acoustic pressure values were obtained at the resonant high-frequency excitation of 40 kHz. When evaluating the acoustic velocity (Figure 3b), the obtained results showed that the velocity slightly increased with the depth of the pore. The maximum value of the acoustic velocity was obtained at the resonant frequency of 40 kHz. When evaluating the velocity magnitude (Figure 3c), the maximum average values of the fluid flow velocity were also obtained at the resonant frequency of 40 kHz.

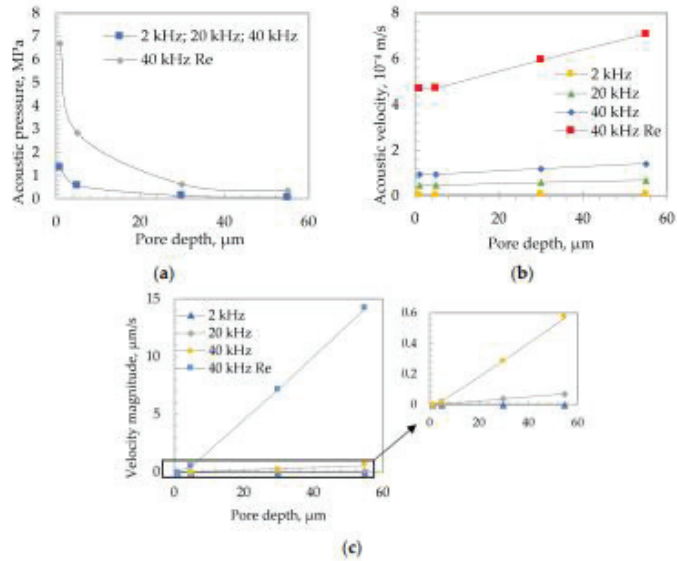


Figure 3. Comparative curves of different frequencies. (a) Acoustic pressure; (b) acoustic velocity; (c) velocity magnitude.

Since the highest values were obtained at the resonant frequency of 40 kHz, the variation in the velocity value inside the pore at different pore depths is analyzed below. Comparative velocity curves are shown in Figure 4.

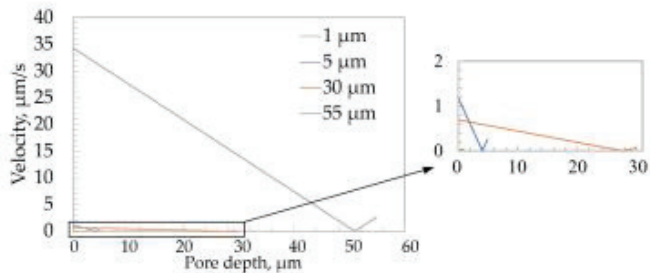


Figure 4. Comparative velocity curves of different pore depths.

When evaluating the velocity dependence along the length of the pore, the velocity decreased uniformly as the pore deepened. In all the cases, close to the bottom of the pore, the velocity values decreased to zero and started to rise steadily until the fluid flow approached the bottom of the pore. At the point at which the flow velocity was zero, a barrier zone of unmixed flow appeared. At a depth of 1 μm , there was no unmixed barrier fluid flow, so the electrolyte could be intensively refreshed all the time. At a resonant frequency of 40 kHz, the velocity contours of fluid flow at different pore depths are presented in Figure 5.

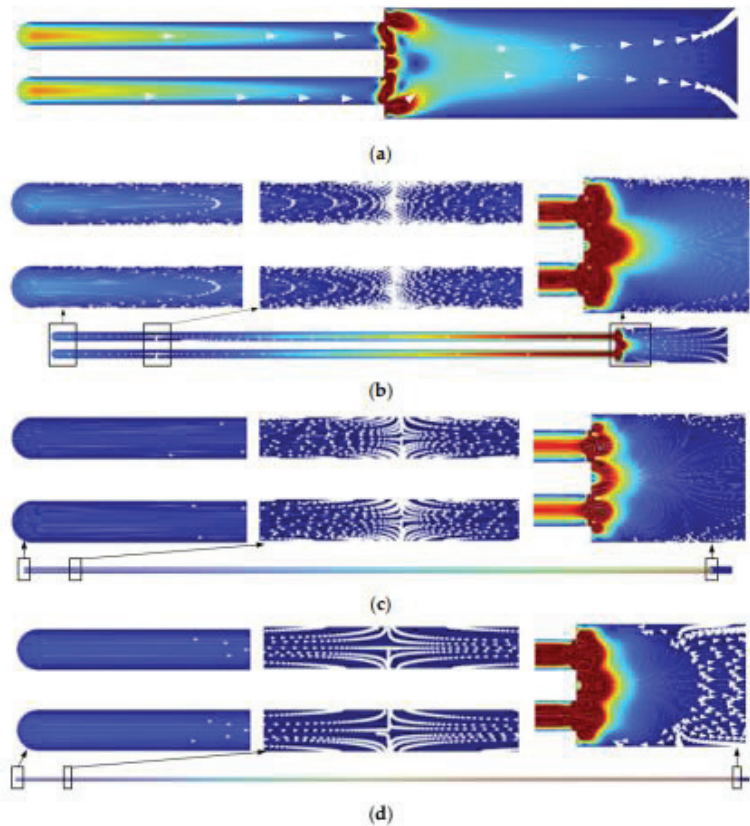


Figure 5. Fluid flow velocity contour at resonant frequency excitation of 40 kHz at different pore depths: (a) 1 μm ; (b) 5 μm ; (c) 30 μm ; (d) 55 μm .

As the pore depth increased, the speed and direction of the flow in the pore changed. At the beginning of the anodization process, when the depth of the pore was 1 μm , the electrolyte flowed throughout the length of the pore, and mixing also occurred at the bottom of the pore. As aluminum oxide formed, the pores became deeper. In the deeper pore, the barrier appeared, and the direction of fluid flow changed. Moreover, the results of the analysis showed that the highest speed was at the beginning of the pore. Inside the pore, the electrolyte flow rate was low (the mixing process was relatively slow) while the liquid outside (in the reactor) was intensively mixed. Such movement of the liquid during excitation was beneficial, because the electrolyte near the pore was intensively mixed with the entire reactor liquid, and the flow in the pore was constantly renewed. The results of the numerical simulations showed that mixing of the fluid flow inside the pore was ensured by using high-frequency excitation. Therefore, the electrolyte concentration inside the pore was also refreshed during the mixing process. Based on theoretical models of oxide growth, it was concluded that the pH value and the temperature change along the length of the pore. Therefore, high-frequency excitation during the anodization process could ensure a more uniform distribution of the electrolyte temperature and pH values along the entire length of the pores.

3.2. Influence of Vibration on Pore Geometry

After evaluating the theoretical fluid flow velocities and pressures inside the pore at different frequencies, experimental studies were carried out, during which it was possible to determine the effect of high-frequency vibrations on the pore geometry of AAO membrane. Since the most significant theoretical results were obtained at the frequency of 40 kHz, this frequency was further analyzed experimentally, and the frequency of 20 kHz was used for comparison.

Scanning electron microscopy (SEM) and energy dispersive spectroscopy (EDS) were used to determine the morphology and surface chemical composition of the nanopores of the AAO membranes. For analysis, the Hitachi S-3400N scanning electron microscope with an integrated Bruker energy dispersive X-ray spectroscopy (EDS) system was used. Using the “ImageJ” data-processing program, the diameters of the membrane pores, the distances between the pores, and the thickness of the obtained membranes were determined, and the results are presented in Table 3.

Table 3. Pore diameter, interpore distance, and thickness of AAO nanoporous membranes.

Parameter	Pore Diameter (nm)	Interpore Distance (nm)	Thickness (μm)
No excitation	104 ± 10	143 ± 10	45 ± 0.5
Excitation frequency 20 kHz	103 ± 10	140 ± 10	53 ± 0.5
Excitation frequency 40 kHz	105 ± 10	140 ± 10	59 ± 0.5
Resonant excitation frequency 40 kHz	105 ± 10	145 ± 10	60 ± 0.5

Using frequencies of 20 kHz and 40 kHz and the resonance frequency of 40 kHz, the pore diameters of the fabricated membrane were obtained. Respectively, they were 103 ± 10 nm, 105 ± 10 nm, and 105 ± 10 nm. Consequently, the interpore distances were 140 ± 10 nm, 140 ± 10 nm, and 145 ± 10 nm, and the thicknesses were 53 ± 0.5 μm , 59 ± 0.5 μm , and 60 ± 0.5 μm . It can be concluded that the pore diameter and the interpore distance remained unchanged under different anodization conditions. However, the thickness of the AAO membrane increased by 17.8% at 20 kHz. Furthermore, the thickness increased by 31.1% at 40 kHz and 33.3% at the resonant frequency of 40 kHz. The thickness of the AAO membrane was also measured using a microscope (Nikon Eclipse lv150, Tokyo, Japan). Images of the thickness of the AAO membrane are shown in Figure 6.

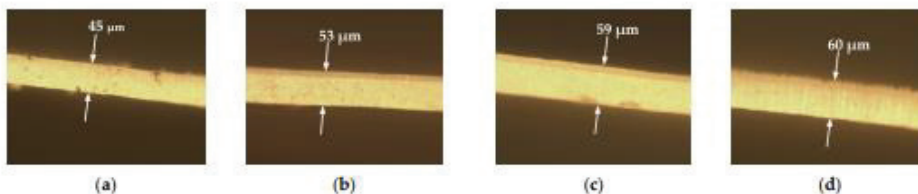


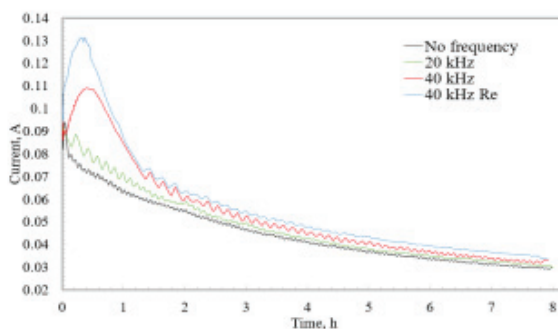
Figure 6. Images of the thickness of the AAO membrane when the membranes were fabricated under different anodization conditions: (a) no frequency excitation; (b) excitation at 20 kHz; (c) excitation at 40 kHz; (d) resonant frequency excitation at 40 kHz.

The chemical compositions of the nanoporous AAO membranes are shown in Table 4. Analysis of EDS showed that two elements (aluminum and oxygen) predominated. It confirmed the formation of Al_2O_3 . Due to amorphous aluminum oxide, two elements, sulfur and carbon, were identified as impurities. After the EDS analysis, it can be stated that the frequency did not affect the chemical composition of the membrane.

Table 4. Chemical composition of AAO nanoporous membranes.

		Element			
		Aluminum	Oxygen	Carbon	Sulfur
No excitation	Atomic concentration, at%	35.39	63.15	1.18	0.28
	Error, %	2.3	6.9	0.3	0.1
Excitation frequency 20 kHz	Atomic concentration, at%	31.92	64.78	2.90	0.41
	Error, %	2.3	7.9	0.6	0.1
Excitation frequency 40 kHz	Atomic concentration, at%	31.44	66.02	2.11	0.43
	Error, %	2.2	7.4	0.4	0.1
Resonant excitation frequency 40 kHz	Atomic concentration, at%	32.38	66.73	0.23	0.66
	Error, %	2.1	7.3	0.3	0.1

Based on the analysis and comparisons of the complex “current-time” (I-t) curves, valuable conclusions about the established self-organization regime and ion migration, as well as new insights about the self-ordering oxide formation under different anodization conditions, were provided. Thus, during the second step of the anodization process, the anodization current was measured and observed. Current-time curves are presented in Figure 7.

**Figure 7.** Current-time curves recorded during the second step of the anodization process.

In Figure 7, the curves of the current measurement in four different fabrication regimes were presented. The first curve, when anodization was performed without the use of high-frequency excitation, can be named the standard anodization curve. First, the curve was increased, and then the curve steadily decreased, revealing a slowing process. Slight current fluctuations were caused by changing the reactor temperature in the range of 4.5–6.0 °C. Using a high-frequency excitation of 20 kHz, it was possible to conclude from the increasing current curve that the anodization reactions intensified. This could be explained by faster ion migration. At a higher frequency of 40 kHz, in the first hour of anodization, the current was increased, which could be influenced by the increased frequency and the increased oscillating amplitude. At a resonant frequency of 40 kHz, the current was even more intense. As the current started to decrease, its value approached the standard current curve (when the frequency was not used), but the current remained slightly higher throughout the process. Such a change in the current could have been influenced by the liquid barrier that formed that is reviewed in the theoretical simulations. Although the refreshing process

was not as intensive as at the beginning of the anodization, the electrolyte concentration was still updated due to the high frequency.

The experimental results and the current curves discussed above lead to the conclusion that the rate of the reaction and the rate of oxide formation are directly dependent on the concentration of the electrolyte. By renewing the electrolyte inside the pore, higher growth rates and deeper structure can be achieved. On the other hand, to obtain a pore of the same depth, the reaction can be performed in a shorter time when high-frequency vibrations are used.

4. Conclusions

A well-known two-step anodization process was proposed in which the excitation by high-frequency vibrations was used to ensure mixing of the fluid flow inside nanopores, thus ensuring a uniform temperature and pH value along the entire length of the pore. Further, the influence of the high-frequency vibrations on the geometry of AAO membrane pores was determined. The obtained results of the theoretical calculations showed that fluid flow inside the pores could be mixed more efficiently when high-frequency vibrations were used. The highest acoustic pressure, acoustic velocity, and velocity magnitude were obtained when the high-frequency excitation was applied at a resonant frequency of 40 kHz. Further, fabricated AAO membranes under different frequency conditions showed that the membrane thickness increased. The thickness of the AAO membrane increased by 17.8% at 20 kHz. The thickness also increased by 31.1% at 40 kHz and 33.3% at the resonant frequency of 40 kHz. The obtained experimental results agreed with the theoretical ones, which showed that at a resonant frequency of 40 kHz, due to the best mixing of the liquid flow in the pore, the reaction speed was the most intense, and therefore, the AAO membrane thickness was the highest during the same fabrication time. Moreover, it could be concluded that the pore diameter and the interpore distance remained unchanged using a frequency at 20 kHz and 40 kHz. Furthermore, after EDS analysis, it could be stated that the frequency did not affect the chemical composition of the AAO membrane. Current–time curves led to the conclusion that the rate of reaction and the rate of oxide formation were directly dependent on the concentration of the electrolyte in the pore. By renewing the electrolyte inside the pore, higher growth rates and a deeper structure could be achieved. On the contrary, in order to obtain a pore of the same depth, the reaction could be performed in a shorter time when high frequency vibrations were used.

Author Contributions: Conceptualization, U.C.; methodology, U.C. and A.P.; investigation, U.C. and G.J.; calculation and analysis, U.C. and G.J.; formal analysis, U.C. and A.P.; writing—original draft preparation, U.C.; writing—review and editing, A.P. and G.J.; visualization, U.C.; validation, A.P. and G.J.; funding acquisition G.J. All authors have read and agreed to the published version of the manuscript.

Funding: This research was funded by grant No. 0.1.2.2-CPVA-K-703-03-0015, “Development of new technology for the formation of microstructures in functional materials”, from the European Regional Development Fund.

Institutional Review Board Statement: Not applicable.

Informed Consent Statement: Not applicable.

Data Availability Statement: Not applicable.

Conflicts of Interest: The authors declare no conflict of interest.

References

1. Keller, F.; Hunter, M.S.; Robinson, D.L. Structural Features of Oxide Coatings on Aluminum. *J. Electrochem. Soc.* **1953**, *100*, 411. [[CrossRef](#)]
2. Hoar, T.P.; Mott, N.F. A mechanism for the formation of porous anodic oxide films on aluminium. *J. Phys. Chem. Solids* **1959**, *9*, 97–99. [[CrossRef](#)]
3. Dewald, J.F. A Theory of the Kinetics of Formation of Anode Films at High Fields. *J. Electrochem. Soc.* **1955**, *102*, 1. [[CrossRef](#)]

4. Hideki, M.; Hideki, T.; Nobuyoshi, B. Preparation of Porous Material by Replacing Microstructure of Anodic Alumina Film with Metal. *Chem. Lett.* **1990**, *19*, 621–622. [\[CrossRef\]](#)
5. Domagalski, J.T.; Xifre-Perez, E.; Marsal, L.F. Recent Advances in Nanoporous Anodic Alumina: Principles, Engineering, and Applications. *Nanomaterials* **2021**, *11*, 430. [\[CrossRef\]](#)
6. Guo, F.; Cao, Y.; Wang, K.; Zhang, P.; Cui, Y.; Hu, Z.; Xie, Z. Effect of the Anodizing Temperature on Microstructure and Tribological Properties of 6061 Aluminum Alloy Anodic Oxide Films. *Coatings* **2022**, *12*, 314. [\[CrossRef\]](#)
7. Kozhukhova, A.E.; Preez, S.P.; Bessarabov, D.G. Preparation of anodized aluminium oxide at high temperatures using low purity aluminium (Al6082). *Surf. Coat. Technol.* **2019**, *378*, 124970. [\[CrossRef\]](#)
8. Chahrouh, K.M.; Ahmed, N.M.; Hashim, M.R.; Elfadill, N.G.; Maryam, W.; Ahmad, M.A.; Bououdina, M. Effects of the voltage and time of anodization on modulation of the pore dimensions of AAO films for nanomaterials synthesis. *Superlattices Microstruct.* **2015**, *88*, 489–500. [\[CrossRef\]](#)
9. Chung, I.C.; Chung, C.K.; Su, Y.K. Effect of current density and concentration on microstructure and corrosion behavior of 6061 Al alloy in sulfuric acid. *Surf. Coat. Technol.* **2017**, *313*, 299–306. [\[CrossRef\]](#)
10. Vorobjova, A.I.; Tishkevich, D.I.; Outkina, E.A.; Shimanovich, D.L.; Razanau, I.U.; Zubar, T.I.; Bondaruk, A.A.; Zheleznova, E.K.; Dong, M.; Aloraini, D.A.; et al. A Study of Ta₂O₅ Nanopillars with Ni Tips Prepared by Porous Anodic Alumina Through-Mask Anodization. *Nanomaterials* **2022**, *12*, 1344. [\[CrossRef\]](#)
11. Vorobjova, A.; Tishkevich, D.; Shimanovich, D.; Zubar, T.; Astapovich, K.; Kozlovskiy, A.; Zdorovets, M.; Zhaludkevich, A.; Lyakhov, D.; Michels, D.; et al. The influence of the synthesis conditions on the magnetic behaviour of the densely packed arrays of Ni nanowires in porous anodic alumina membranes. *RSC Adv.* **2021**, *11*, 3952–3962. [\[CrossRef\]](#) [\[PubMed\]](#)
12. Mijangos, C.; Hernández, R.; Martín, J. A review on the progress of polymer nanostructures with modulated morphologies and properties, using nanoporous AAO templates. *Prog. Polym. Sci.* **2016**, *54–55*, 148–182. [\[CrossRef\]](#)
13. Ruiz-Clavijo, A.; Caballero-Calero, O.; Martín-González, M. Revisiting anodic alumina templates: From fabrication to applications. *Nanoscale* **2021**, *13*, 2227–2265. [\[CrossRef\]](#)
14. Hun, C.W.; Chiu, Y.J.; Luo, Z.; Chen, C.C.; Chen, S.H. A New Technique for Batch Production of Tubular Anodic Aluminum Oxide Films for Filtering Applications. *Appl. Sci.* **2018**, *8*, 1055. [\[CrossRef\]](#)
15. Wen, F.Y.; Chen, P.S.; Liao, T.W.; Juang, Y.J. Microwell-assisted filtration with anodic aluminum oxide membrane for Raman analysis of algal cells. *Algal Res.* **2018**, *33*, 412–418. [\[CrossRef\]](#)
16. Chang, Y.J.; Yang, W.T.; Wu, J.C. Isolation and detection of exosomes via AAO membrane and QCM measurement. *Microelectron. Eng.* **2019**, *216*, 111094. [\[CrossRef\]](#)
17. Ma, Y.; Kaczynski, J.; Ranacher, C.; Roshanghias, A.; Zauner, M.; Abasahl, B. Nano-porous aluminum oxide membrane as filtration interface for optical gas sensor packaging. *Microelectron. Eng.* **2018**, *198*, 29–34. [\[CrossRef\]](#)
18. Aminullah; Kasi, A.K.; Kasi, J.K.; Bokhari, M. Fabrication of mechanically stable AAO membrane with improved fluid permeation properties. *Microelectron. Eng.* **2018**, *187–188*, 95–100. [\[CrossRef\]](#)
19. Peng, D.; Chen, J.; Jiao, L.; Liu, Y. A fast-responding semi-transparent pressure-sensitive paint based on through-hole anodized aluminum oxide membrane. *Sens. Actuators A Phys.* **2018**, *274*, 10–18. [\[CrossRef\]](#)
20. Mondal, S.; Kim, S.J.; Choi, C.G. Honeycomb-like MoS₂ Nanotube Array-Based Wearable Sensors for Noninvasive Detection of Human Skin Moisture. *ACS Appl. Mater. Interfaces* **2020**, *12*, 17029–17038. [\[CrossRef\]](#)
21. Podgolin, S.K.; Petukhov, D.I.; Dorofeev, S.G.; Eliseev, A.A. Anodic alumina membrane capacitive sensors for detection of vapors. *Talanta* **2020**, *219*, 121248. [\[CrossRef\]](#) [\[PubMed\]](#)
22. Davoodi, E.; Zhanmanesh, M.; Montazerian, H.; Milani, A.S.; Hoorfar, M. Nano-porous anodic alumina: Fundamentals and applications in tissue engineering. *J. Mater. Sci. Mater. Med.* **2020**, *31*, 60. [\[CrossRef\]](#) [\[PubMed\]](#)
23. Rodriguez-Saona, L.; Aykas, D.P.; Borba, K.R.; Urtubia, A. Miniaturization of optical sensors and their potential for high-throughput screening of foods. *Curr. Opin. Food Sci.* **2020**, *31*, 136–150. [\[CrossRef\]](#)
24. Wong, H.; Cernak, T. Reaction miniaturization in eco-friendly solvents. *Curr. Opin. Green Sustain. Chem.* **2018**, *11*, 91–98. [\[CrossRef\]](#)
25. Dick, H.B.; Schultz, T.; Gerste, R.D. Miniaturization in Glaucoma Monitoring and Treatment: A Review of New Technologies That Require a Minimal Surgical Approach. *Ophthalmol. Ther.* **2019**, *8*, 19–30. [\[CrossRef\]](#) [\[PubMed\]](#)
26. Kim, C. Evolution of Advanced Miniaturization for Active Implantable Medical Devices. In *Nano-Bio-Electronic, Photonic and MEMS Packaging*; Wong, C.P., Moon, K.S., Eds.; Springer: Cham, Switzerland, 2021; pp. 407–415. [\[CrossRef\]](#)
27. Yeo, S.H.; Ogawa, H.; Kahnfeld, D.; Schneider, R. Miniaturization perspectives of electrostatic propulsion for small spacecraft platforms. *Prog. Aerosp. Sci.* **2021**, *126*, 100742. [\[CrossRef\]](#)
28. Hsiang, E.L.; Yang, Z.; Yang, Q.; Lan, Y.F.; Wu, S.T. Prospects and challenges of mini-LED, OLED, and micro-LED displays. *J. Soc. Inf. Disp.* **2021**, *29*, 446–465. [\[CrossRef\]](#)
29. Albert, P.; Jaouad, A.; Hamon, G.; Volatier, M.; Valdivia, C.E.; Deshayes, Y.; Hinzer, K.; Béhou, L.; Aimez, V.; Darnon, M. Miniaturization of InGaP/InGaAs/Ge solar cells for micro-concentrator photovoltaics. *Prog. Photovolt. Res. Appl.* **2021**, *29*, 990–999. [\[CrossRef\]](#)
30. Liu, L.; Choi, S. Miniature microbial solar cells to power wireless sensor networks. *Biosens. Bioelectron.* **2021**, *177*, 112970. [\[CrossRef\]](#)

31. Huang, Y.; Li, H.; Hu, T.; Li, J.; Yiu, C.K.; Zhou, J.; Li, J.; Huang, X.; Yao, K.; Qiu, X.; et al. Implantable Electronic Medicine Enabled by Bioresorbable Microneedles for Wireless Electrotherapy and Drug Delivery. *Nano Lett.* **2022**, *22*, 5944–5953. [[CrossRef](#)]
32. Farrokhi, M.; Manavi, S.P.; Taheri, F. Non-invasive monitoring of pH and oxygen using miniaturized electrochemical sensors. *J. Transl. Med.* **2021**, *19*, 252. [[CrossRef](#)] [[PubMed](#)]
33. Liang, G.; Mudawar, I. Review of single-phase and two-phase nanofluid heat transfer in macro-channels and micro-channels. *Int. J. Heat Mass Transf.* **2019**, *136*, 324–354. [[CrossRef](#)]
34. Chamkha, A.J.; Molana, M.; Rahnama, A.; Ghadami, F. On the nanofluids applications in microchannels: A comprehensive review. *Powder Technol.* **2018**, *332*, 287–322. [[CrossRef](#)]
35. Wang, B.; Hu, Y.; He, Y.; Rodionov, N.; Zhu, J. Dynamic instabilities of flow boiling in micro-channels: A review. *Appl. Therm. Eng.* **2022**, *214*, 118773. [[CrossRef](#)]
36. Dixit, T.; Ghosh, I. Review of micro- and mini-channel heat sinks and heat exchangers for single phase fluids. *Renew. Sustain. Energy Rev.* **2015**, *41*, 1298–1311. [[CrossRef](#)]
37. Li, S.; Zhang, H.; Cheng, J.; Cai, W.; Li, X.; Wu, J.; Li, F. A Numerical Study on Heat Transfer Performance in a Straight Microchannel Heat Sink with Standing Surface Acoustic Waves. *Heat Transf. Eng.* **2021**, *43*, 371–387. [[CrossRef](#)]
38. Chen, Z.; Shen, L.; Zhao, X.; Chen, H.; Xiao, Y.; Zhang, Y.; Yang, X.; Zhang, J.; Wei, J.; Hao, N. Acoustofluidic micromixers: From rational design to lab-on-a-chip applications. *Appl. Mater. Today* **2022**, *26*, 101356. [[CrossRef](#)]
39. Hsu, J.C.; Chang, C.Y. Enhanced acoustofluidic mixing in a semicircular microchannel using plate mode coupling in a surface acoustic wave device. *Sens. Actuators A Phys.* **2022**, *336*, 113401. [[CrossRef](#)]
40. Maramizonouz, S.; Jia, C.; Rahmati, M.; Zheng, T.; Liu, Q.; Torun, H.; Wu, Q.; Fu, Y.Q. Acoustofluidic Patterning inside Capillary Tubes Using Standing Surface Acoustic Waves. *Int. J. Mech. Sci.* **2022**, *214*, 106893. [[CrossRef](#)]
41. Ding, X.; Li, P.; Lin, S.C.S.; Stratton, Z.S.; Nama, N.; Guo, F.; Slotcavage, D.; Mao, X.; Shi, J.; Costanzo, F.; et al. Surface acoustic wave microfluidics. *Lab Chip* **2013**, *13*, 3626–3649. [[CrossRef](#)]
42. Chien, Y.C.; Weng, H.C. Cost-effective technique to fabricate a tubular through-hole anodic aluminum oxide membrane using one-step anodization. *Microelectron. Eng.* **2021**, *247*, 111589. [[CrossRef](#)]
43. Montakhab, E.; Rashchi, F.; Sheibani, S. Modification and photocatalytic activity of open channel TiO₂ nanotubes array synthesized by anodization process. *Appl. Surf. Sci.* **2020**, *534*, 147581. [[CrossRef](#)]
44. Pashchanka, M. Conceptual Progress for Explaining and Predicting Self-Organization on Anodized Aluminum Surfaces. *Nanomaterials* **2021**, *11*, 2271. [[CrossRef](#)] [[PubMed](#)]
45. Sundararajan, M.; Devarajan, M.; Jaafar, M. Investigation of surface and mechanical properties of Anodic Aluminium Oxide (AAO) developed on Al substrate for an electronic package enclosure. *Surf. Coat. Technol.* **2020**, *401*, 126273. [[CrossRef](#)]
46. Dai, J.; Singh, J.; Yamamoto, N. Nonbrittle nanopore deformation of anodic aluminum oxide membranes. *J. Am. Ceram. Soc.* **2017**, *101*, 2170–2180. [[CrossRef](#)]

Article

A Free-Standing Chitosan Membrane Prepared by the Vibration-Assisted Solvent Casting Method

Urte Cigane ^{*}, Arvydas Palevicius ^{*} and Giedrius Janusas

Faculty of Mechanical Engineering and Design, Kaunas University of Technology, Studentu Street 56, 51424 Kaunas, Lithuania; giedrius.janusas@ktu.lt

^{*} Correspondence: urte.cigane@ktu.lt (U.C.); arvydas.palevicius@ktu.lt (A.P.)

Abstract: Much attention has been paid to the surface modification of artificial skin barriers for the treatment of skin tissue damage. Chitosan is one of the natural materials that could be characterized by its biocompatibility. A number of methods for the preparation of chitosan membranes have been described in scientific articles, including solvent casting methods. This study investigates an improved technology to produce chitosan membranes. Thus, chitosan membranes were prepared using a vibration-assisted solvent casting method. First, aqueous acetic acid was used to pretreat chitosan. Then, free-standing chitosan membranes were prepared by solvent casting on nanoporous anodized aluminum oxide (AAO) membrane templates, allowing for the solvent to evaporate. Using finite element methods, a study was obtained showing the influence of chitosan solutions of different concentrations on the fluid flow into nanopores using high-frequency excitation. The height of the nanopillars and the surface area of the chitosan membrane were also evaluated. In this study, the surface area of the chitosan membrane was found to increase by 15, 10 and 6 times compared to the original flat surface area. The newly produced nanopillared chitosan membranes will be applicable in the fabrication of skin barriers due to the longer nanopillars on their surface and the larger surface area.

Keywords: chitosan membrane; nanoporous AAO template; high-frequency excitation; two-step anodization method; solvent casting method; surface area



check for updates

Citation: Cigane, U.; Palevicius, A.; Janusas, G. A Free-Standing Chitosan Membrane Prepared by the Vibration-Assisted Solvent Casting Method. *Micromachines* **2023**, *14*, 1419. <https://doi.org/10.3390/mi14071419>

Academic Editor: Giovanna Tomaiuolo

Received: 16 June 2023

Revised: 5 July 2023

Accepted: 13 July 2023

Published: 14 July 2023



Copyright: © 2023 by the authors. Licensee MDPI, Basel, Switzerland. This article is an open access article distributed under the terms and conditions of the Creative Commons Attribution (CC BY) license (<https://creativecommons.org/licenses/by/4.0/>).

1. Introduction

Skin is a human organ that acts as a physical barrier against external damage [1]. However, injuries can easily deform the multilayered structure and complications such as infections, melanoma, or the formation of scar tissue may result from the wound [2]. To treat wounds, artificial skin barriers could be applied [3]. These barriers can support cellular activity in a moist environment, allow for the transport of gaseous species, and simultaneously prevent the transmission of pathogens [4].

To create artificial skin barriers, different films and membranes are being developed [5]. Unlike other materials, nanomaterials have unique physical (nanoscale size, high surface-to-volume ratio, diversity of morphology and structure, etc.), chemical (corrosion resistance, high reactivity, etc.), and biological properties (biocompatibility, low immunogenicity, etc.) which allow for nanomaterials to be widely used in tissue engineering [6]. With the increasing emphasis on environmental friendliness, nanomaterial templates are receiving a lot of attention and are considered one of the most promising techniques [7]. Moreover, the template allows for the structure to be reconstructed with the best possible reproducibility and plays the role of a skeleton, which can be used to develop various functions and adapt the created nanostructure in different areas [8,9]. In recent years, there has been a lot of interest in the potential application of nanopillars to membranes and films [10]. In fact, nanopillar surfaces have properties that make them more valuable than conventional planar surfaces in biological applications, such as medical therapy, tissue engineering,

and antibacterial agents [11–14]. The nanopillars have three effects on surface biological processes: increase the surface area, increase cell adhesion and growth, and increase the ability to penetrate the cell [15].

One of the possibilities to fabricate nanopillars is the template method. Nanomaterials templates can be made using a variety of methods (additive manufacturing (3D printing) [16,17], lithography [18]), but most of them are relatively complex and expensive compared to the anodization process, which can be characterized by high efficiency, simplicity, low cost, and the notable qualities of the obtained nanostructures [19]. The anodization process in the fabrication of anodic aluminum oxide (AAO) nanoporous membranes is superior because structural changes can be obtained by controlling the electrochemical process conditions (type of electrolyte, electrolyte concentration, temperature, anodization time, anodizing potential, current density, etc.) during the fabrication process [20,21]. Furthermore, AAO nanoporous membranes have exceptional properties, such as a high thermal stability, mechanical hardness, and chemical inertness [22]. The use of the nanoporous AAO membrane as a template has several advantages over other types of templates, such as a nanometer-sized diameter and straight micropore length, low cost, and thermal stability over a wide temperature range without loss of porous structure, even after processing above 1000 °C; in addition, porous alumina can be used with a barrier layer on one side and a main porous oxide layer on the other side, or base materials can be removed on both sides to obtain a self-sustaining nanohole structure that can be used as a template [23–25].

Research has shown that chitosan is a promising candidate for the development of biocompatible, bactericidal, and bio-adhesive skin barriers and is already widely used in commercial wound dressings [10,26–28], hemostatic dressings [29] or drug delivery systems for wound healing [30]. At present, many types of commercial products based on chitosan (OneStop™ Bandage Rx, Hemcon® Bandage PRO, HemCon ChitoDot®, ChitoGauze® XR PRO (Tricol Biomedical, Portland, OR, USA)) are available for wound care [31]. To improve its properties, various derivatives of chitosan can be produced [32]. For example, the combination of chitosan and gelatin not only produces a biomatrix that is more durable, but also allows for the controlled release of biological agents and protects the wound from contaminating molecules [33]. The antimicrobial activity of chitosan and its potential for osteogenesis in stem cell culture environments were also presented by researchers [34]. Due to the less transferable nanostructure on the chitosan membrane, there are few studies on the micro/nanopatterning of chitosan membranes and films; therefore, two methods are commonly used: low-pressure, low-temperature nanoimprinting and solvent casting [35]. However, the low-pressure, low-temperature nanoimprinting method required careful control of the viscosity and the use of a nanoimprinter; therefore, the solvent casting method is the easiest and most-used method to transfer the nanostructure onto the chitosan membrane when the polymer solution is poured onto the patterned template [36]. When the bottom of the pores of the AAO template is closed, it is difficult to ensure the flow of the solution into the nanopores, so different chitosan derivatives could be used for this purpose [37], or the AAO template could be modified with surface energy-reducing agents [34].

Because chitosan membranes with nanopillars are promising in the creation of barriers for skin protection, it is important to develop fabrication technologies that involve controlling the geometry of nanopillars. This study presents the fabrication of a chitosan membrane with nanopillars using the nanoporous AAO membrane as a template. Because the solvent casting method was performed without high-frequency excitation in previous studies, the novelty of this study is that a free-standing chitosan membrane was prepared using a vibration-assisted solvent casting method and the influence of high-frequency excitation on the geometry of the nanopillars is analyzed. Moreover, in this study, the velocity of the chitosan solution into the closed nanopore was calculated mathematically. Therefore, to control the geometry of the nanopillars and expand the application of templates in membrane production, free-standing nanopillared chitosan membranes were produced, using 1 wt%, 2 wt% and 3 wt% concentrations of chitosan solutions to determine the influence on

the formation of nanopillar using high-frequency excitation of 40 kHz for 5 s. Moreover, the effect of vibration on the surface area of the nanopillared chitosan membrane was also investigated. Furthermore, the velocity of the fluid flow into the nanopore, the height of the nanopillars, and the surface area of a single nanopillar were theoretically evaluated using COMSOL Multiphysics 6.0 software.

2. Materials and Methods

2.1. Fabrication of Nanoporous AAO Template

To control the geometry of the nanopillars and expand the application of templates in membrane fabrication, nanopillared chitosan membranes were fabricated using the nanoporous AAO templates. A facile and cost-effective two-step anodization process was used to fabricate the nanoporous AAO templates. The synthesis route of the nanoporous AAO template is shown in Figure 1.

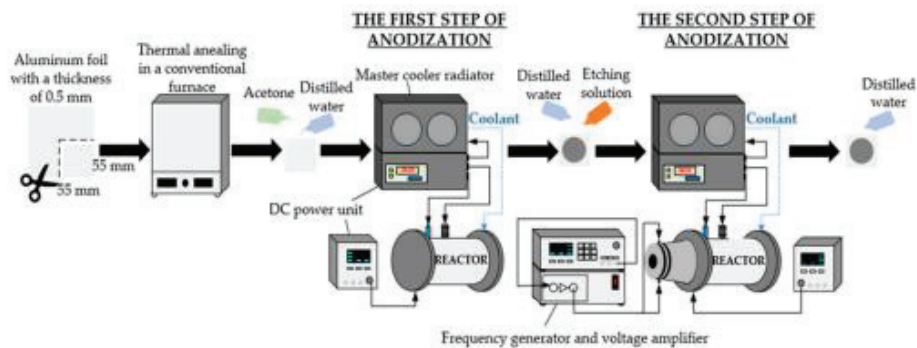


Figure 1. The synthesis route of nanoporous AAO template.

In this study, annealed aluminum foil of high purity (>99%) was used. First, the specimens of aluminum foil with a size of $55 \times 55 \times 0.5$ mm were annealed at 400°C for 4 h in a nitrogen environment in a conventional furnace. The samples were then cleaned with distilled water after being degreased with acetone. An electrochemical reactor was used to prepare the nanoporous AAO templates. The novel design of the electrochemical reactor is presented in Figure 2.

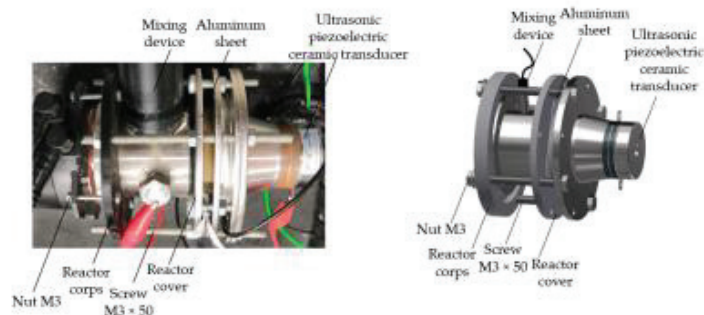


Figure 2. A novel design of the electrochemical reactor.

Using a 0.3 mol/L oxalic acid solution ($\text{H}_2\text{C}_2\text{O}_4$) as the electrolyte, the two-step anodization process was conducted at a voltage of 60 V and a temperature of 5 °C. The initial anodization process took one hour. A solution of 3.5% concentrated phosphoric acid (H_3PO_4) and 2% concentrated chromium anhydride (CrO_3) acid in water was used to etch the oxide layer. The chemical etching process was performed at 80 °C for 10 min. The second step of the anodization process was carried out in the electrochemical reactor at 60 V and 5 °C for 4 h after they had been cleaned with distilled water. During the second step of anodization, high-frequency excitation was used. More information on the anodization process using high-frequency excitation is given in [38]. Lastly, the produced nanoporous AAO templates were washed with distilled water and air-dried.

Additionally, using the Hitachi S-3400N (Hi-Tech Instruments, Bandar Bukit Puchong, Malaysia) scanning electron microscope (SEM), the geometry of the AAO pores was examined. By evaluating the pore diameters and interpore distances of the entire 45 mm diameter AAO membrane area and calculating the normal distribution of the pore diameters and interpore distances, the average values of the pore diameters and interpore distance were determined using the “ImageJ” data-processing program. Furthermore, the surface chemical composition of the AAO template was examined using Bruker Quad 5040 EDS energy dispersive X-ray spectroscopy.

2.2. Fabrication of Nanopillared Chitosan Membrane

1 wt%, 2 wt% and 3 wt% chitosan (high molecular weight, deacetylation degree >95%) were dissolved in 1 wt% acetic acid solution. The preparation procedure for the nanopillared chitosan membrane is shown in Figure 3.

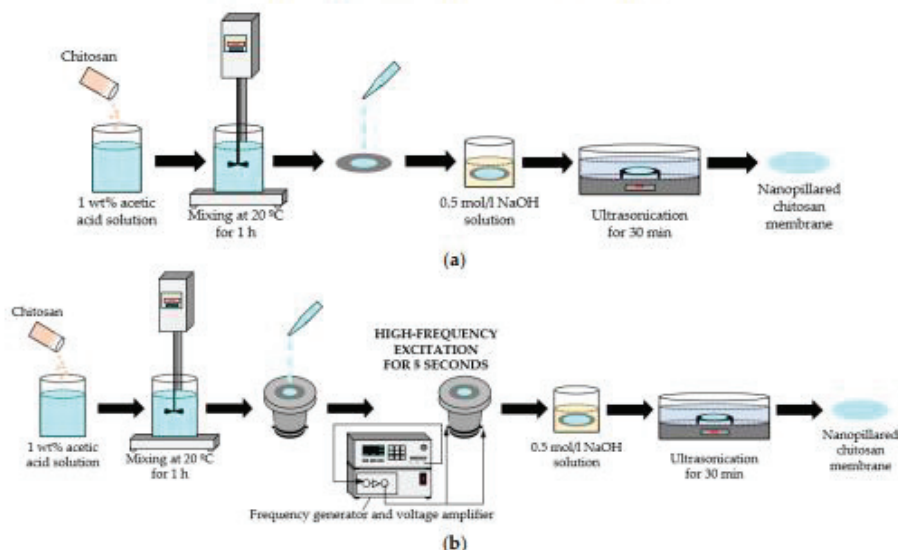


Figure 3. Fabrication of nanopillared chitosan membrane: (a) standard preparation procedure; (b) preparation procedure using high-frequency excitation.

The mixtures were stirred at 20 °C for 1 h, until the chitosan was completely dissolved. In the next step, the chitosan solution was added dropwise (casting temperature 20 °C) onto the prepared nanoporous AAO templates (diameter 45 mm) and dried at the temperature of 20 °C for 24 h. To dissolve the template, the samples were immersed in the 0.5 mol/L NaOH

solution. Finally, the nanopillared chitosan membranes were cleaned by ultrasonication in distilled water. The geometry of chitosan nanopillars was examined using SEM.

To determine the influence of vibration on the geometry of the nanopillars, after dropping chitosan onto the nanoporous AAO template, the chitosan, together with the AAO template, was vibrated at the frequency of 40 kHz for 5 s, and then all procedures were conducted as usual. The device for chitosan and AAO template vibrations is presented in Figure 4.

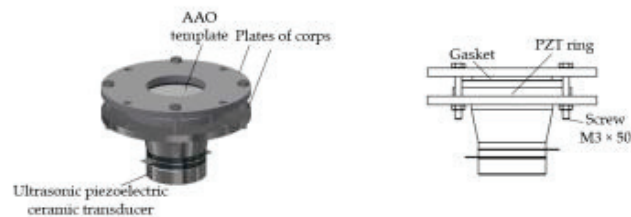


Figure 4. The device for the high-frequency excitation of chitosan solution and AAO template.

The structures of nanopillars are primarily responsible for their unique properties. Numerous vertically aligned nanopillars considerably increase the surface area of an original surface without altering the original substrate's size. Formula (1) could be used to determine the surface area (S) of the nanopillared surface [16]:

$$S = S_0 + n(2\pi rl) \quad (1)$$

where S_0 is the area of the original flat surface, r is the radius of each nanopillar, l is the height of the nanopillars, and n is the number of nanopillars on the flat surface.

2.3. Simulation Method and Conditions of Vibration Process

Due to recent advances in the production of microfluidic systems, acoustics are used to control microparticles, living cells, and other particles [39]. Using acoustics, an acoustic streaming flow is created in the microchannels, which also affects the particles with a viscous drag force [40]. The forces of viscous drag and acoustic radiation control the particle trajectories [41]. Due to the non-linear terms in the governing equations, the acoustic radiation force is the effect of the transfer of momentum from the acoustic field to the particles [42]. As a result, the acoustic radiation force acts as a net force on the particles [43].

Acoustic streaming is a term for the net time-averaged flow that results from harmonic disruption of the flow due to non-linear factors in the Navier–Stokes equations [44]. A second-order (nonlinear) acoustic effect is acoustic streaming [45]. The viscous drag force on the particles is influenced by the acoustic streaming and the balance between the acoustic radiation force and the viscous drag force (from the streaming flow) dominates the trajectory of the particles [46].

In this study, the theoretical model was a multiphysics task that included three main stages. The first stage was related to the determination of the first-order acoustic field in the domain, the second included the acoustic streaming flow in the domain, and the third stage was related to the flow of the fluid (also evaluating the streaming flow) inside the pore.

Firstly, the first-order acoustics field was solved by the Thermoviscous Acoustics and Frequency Domain interface in the model [47]. The acoustic boundary layer was determined, and the streaming flow in this layer was obtained. Then, the relevant source terms from the first-order fields were added to the Laminar flow interface to solve the second-order time-averaged net flow. Pressure Acoustics, Frequency Domain, and Thermoviscous Boundary Layer Impedance were used to account for the damping in the thin viscous boundary layers.

The steady-state streaming flow is described by the formulas:

$$0 = -\nabla \cdot (\rho_0 \mathbf{u}_2) - \nabla \cdot (\langle \rho_1 \mathbf{u}_1 \rangle) \quad (2)$$

$$0 = \nabla \cdot \sigma_2 - \nabla \cdot (\rho_0 \langle \mathbf{u}_1 \mathbf{u}_1^T \rangle) \quad (3)$$

where ρ is the density (kg/m^3), \mathbf{u} is the fluid velocity (m/s), T is the temperature (K), $\langle \dots \rangle$ is the time averaging and subscript 2 is the streaming flow variables.

Formula (4), governing the transport and reinitialization of ϕ , can be written as [48]:

$$\partial \phi / \partial t + \mathbf{u} \cdot \nabla \phi = \gamma \nabla \cdot (\varepsilon \nabla \phi - \phi (1 - \phi) (\nabla \phi / |\nabla \phi|)) \quad (4)$$

where ϕ is the isocontour (determines the position of the interface), t is the time (s), γ is the reinitialization parameter (m/s), which determines the amount of reinitialization, and ε is the reinitialization parameter (m), which determines the layer thickness surrounding the interface where ϕ goes from zero to one).

An interface thickness can be described by the following formula:

$$\varepsilon = h_c / 2 \quad (5)$$

where h_c is the characteristic mesh size in the area passed by the interface.

The parameter ϕ is also used to calculate the density and dynamic viscosity:

$$\rho = \rho_{ch} + (\rho_a - \rho_{ch}) \phi \quad (6)$$

$$\mu = \mu_{ch} + (\mu_a - \mu_{ch}) \phi \quad (7)$$

where ρ_{ch} , μ_{ch} , ρ_a , μ_a are the constants of density and viscosity of chitosan solution and air, respectively.

The incompressible Navier–Stokes equations, which include surface tension, regulate the transfer of mass and momentum in the Laminar Two-Phase Flow and Level Set interface:

$$\rho (\partial \mathbf{u} / \partial t + \mathbf{u} \cdot \nabla \mathbf{u}) = -\nabla p + \nabla \cdot \mu (\nabla \mathbf{u} + \nabla \mathbf{u}^T) + \rho \mathbf{g} + \mathbf{F}_{st} \quad (8)$$

$$\nabla \cdot \mathbf{u} = 0 \quad (9)$$

where p is the pressure (Pa), μ is the viscosity (Pa·s), $\rho \mathbf{g}$ is the gravity (m/s^2), \mathbf{F}_{st} is the surface tension force components.

The surface tension force can be described by the following formula:

$$\mathbf{F}_{st} = \nabla \cdot \mathbf{T} = \nabla \cdot [\sigma (\mathbf{I} + (-\mathbf{nn}^T))] \delta \quad (10)$$

where σ is the surface tension coefficient, \mathbf{I} is the identity of the matrix, \mathbf{n} is the interface unit normal, δ is a Dirac delta function (nonzero only at the fluid interface).

The interface normal could be calculated from the following formula:

$$\mathbf{n} = \nabla \phi / |\nabla \phi| \quad (11)$$

The parameter ϕ can be used to approximate the delta function:

$$\delta = 6 |\phi (1 - \phi)| |\nabla \phi| \quad (12)$$

In this study, COMSOL Multiphysics 6.0 software was used to simulate the behaviour of fluids in the nanopore. The deposition of the chitosan solution on the porous AAO structure and the flow of liquid into the pores was simulated using high frequencies. The mathematical model was composed of one pore with a diameter of 100 nm and a chitosan

reservoir. The model was meshed by free triangular elements with a boundary layer inside the structure. The finite element mesh is shown in Figure 5.

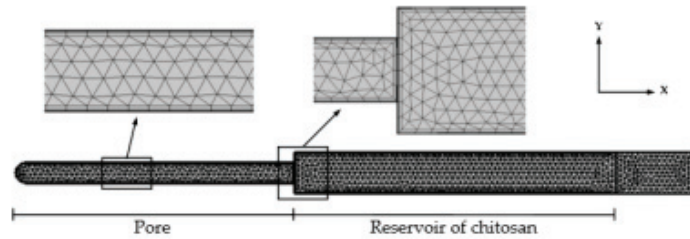


Figure 5. The finite element mesh of the simulation model.

The inner wall of the AAO nanopore was determined to be solid surfaces with no-slip and isothermal boundary conditions. The walls of the chitosan reservoir were determined to be a wetted wall with a Navier slip condition. The model was composed of 4213 domain elements and 453 boundary elements. Movement in the Y direction was constrained, and periodic movements occurred in the X direction. The main model parameters are presented in Table 1.

Table 1. The model parameters.

Parameter	Symbol	Inscription	Value
Frequency	f_0	40 [kHz]	40,000 Hz
Ambient temperature	T_0	20 [$^{\circ}$ C]	293.15 K
Ambient pressure	p_0	1 [atm]	1.0133×10^5 Pa
Study angular frequency	ω_0	$2 \times \pi \times f_0$	2.5132×10^5 Hz
Channel cross-section width	W	100 [nm]	1×10^{-7} m
Channel cross-section height	H	1000 [nm]	1×10^{-6} m
Wall displacement	d_0	100 [nm]	1×10^{-7} m
Time	t	4 [s]	4 s

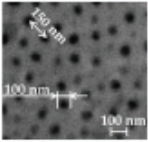
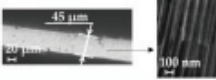
Thermoviscous acoustics, laminar flow, and level set physics were applied to the entire model. In the multiphysics discipline, the two-phase flow was selected. Here, the laminar flow was selected as the fluid flow and the level set as the moving interface. The temperature of the model was set at room temperature, at 20 $^{\circ}$ C.

3. Results and Discussion

3.1. Investigation of Porous AAO Template

In this section, the fabricated nanoporous AAO template is described. To produce nanopillared chitosan membranes, nine identical nanoporous AAO templates were fabricated. For the pore diameter, the distance between pores and thickness analysis, the “ImageJ” data-processing program was used. The average values of the pore diameters and interpore distance were obtained by evaluating the pore diameters and interpore distances of the entire 45 mm diameter AAO membrane area, and the normal distribution of pore diameters and interpore distances were calculated. The results of the geometry of the nanoporous AAO template are presented in Table 2.

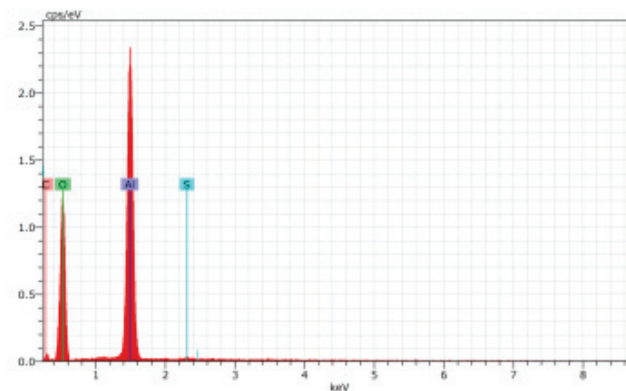
Table 2. Average pore diameter and interpore distance of porous AAO templates.

Parameter	Value	Image
Pore diameter, nm	100 ± 10	
Interpore distance, nm	150 ± 10	
Thickness, μm	45 ± 1	

To determine the chemical elements and their quantity in the porous AAO template, EDS analysis was used. The elements determined during EDS analysis are presented in Table 3 and Figure 6.

Table 3. Chemical composition of AAO template.

	Element			
	Aluminum	Oxygen	Carbon	Sulfur
Normalised concentration, wt%	44.90	53.38	1.24	0.48
Atomic concentration, at%	32.51	65.18	2.02	0.29
Error, %	2.4	7.8	0.5	0.1

**Figure 6.** The EDS curve of AAO template.

According to Table 3 and Figure 6, two elements (aluminum and oxygen) predominated. This confirmed the formation of Al_2O_3 . Sulfur and carbon were identified as impurities due to amorphous Al_2O_3 .

3.2. Theoretical Results of the Flow of Different Concentrations of Chitosan Solution into the AAO Nanopores

The results of the first and second simulations showed the distribution of acoustic velocity and streaming velocity. The acoustic velocity showed the propagation of the sound waves through the air in the pore and the chitosan solution. Affected by the streaming velocity, the chitosan solution gained enough energy to flow into the pore. The flow of

chitosan solutions of different concentrations into the pore was calculated during the last simulation, and the volume fraction of fluid was obtained. The resulting images of the simulations are presented in Figure 7.

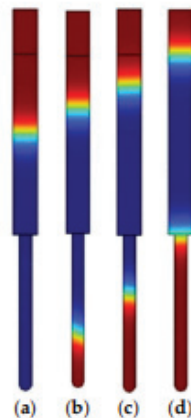


Figure 7. Flow of different concentrations of chitosan solution into the nanopore using the high-frequency excitation of 40 kHz in 4 s: (a) 1 wt% chitosan solution; (b) 2 wt% chitosan solution; (c) 3 wt% chitosan solution; (d) any concentration of chitosan solution without high-frequency excitation. The blue represents chitosan solution, and red represents the air.

The results related to the velocity, the height of the nanopillars, and the surface area of a single nanopillar are presented in Table 4.

Table 4. Simulation results of chitosan solution with concentrations of 1 wt%, 2 wt% and 3 wt%.

Parameter	1 wt%	2 wt%	3 wt%
Velocity, nm/s	250	169	94
Height of nanopillars, nm	1000	675	375
Surface area of a single nanopillar, μm^2	0.314	0.212	0.118

Using the high-frequency excitation of 40 kHz in 4 s, the velocity of the 1 wt% chitosan solution was 250 nm/s, while the velocity of the 2 wt% chitosan solution was 169 nm/s under the same conditions. The speed of the 3 wt% chitosan solution was the lowest and reached 94 nm/s. However, when high-frequency excitation was not used, the flow of the chitosan solution into the closed nanopore was not ensured and a flat surface was obtained. Using high-frequency excitation, the results showed that as the concentration of the solution decreased, the height of the nanopillars increased, which led to an increase in the surface area. When the concentration varied from 3 wt% to 1 wt%, the surface area of the single nanopillar increased more than twice under the same conditions. The results led to an increase in the surface area of the chitosan membrane compared to a flat chitosan membrane. Furthermore, by changing the concentration of the chitosan solution during production, the required surface area can be calculated and obtained according to the surface area shown in Formula (1).

3.3. Investigation of Nanopillared Chitosan Membrane

The nine free-standing chitosan membranes (three membranes of each concentration) were prepared by the vibration-assisted solvent casting method. Nanopillared chitosan membranes were experimentally prepared from different concentrations of chitosan solu-

tions to determine their influence on the formation of nanopillars using high-frequency excitation. SEM images of the nanoporous AAO templates, chitosan membranes, and nanopillars are presented in Figure 8.

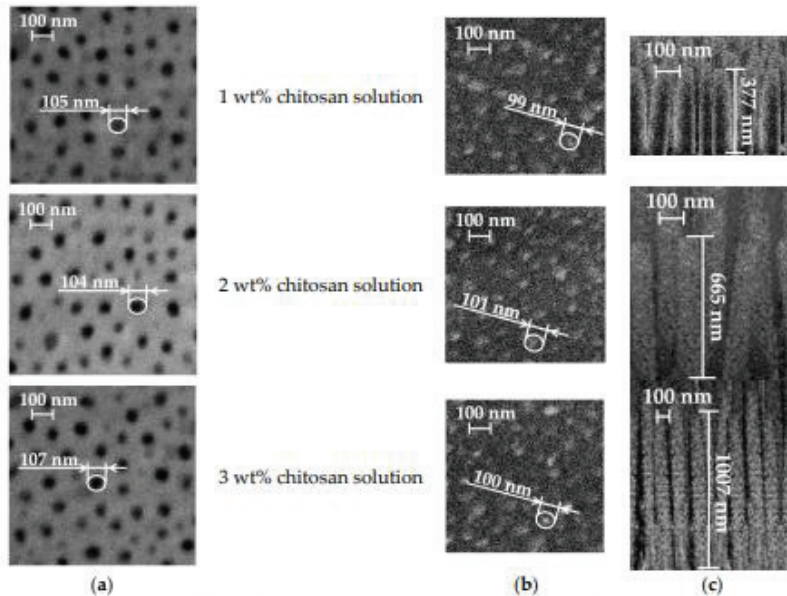


Figure 8. SEM images of: (a) nanoporous AAO template; (b) chitosan membrane; (c) nanopillar of chitosan membrane (cross-section).

The experimental results of chitosan membranes using 1 wt%, 2 wt%, and 3 wt% chitosan solutions are presented in Table 5.

Table 5. Experimental results of chitosan membrane.

Parameter	1 wt%	2 wt%	3 wt%
Diameter of nanopillars, nm	99 ± 10	101 ± 10	100 ± 10
Height of nanopillars, nm	1007 ± 10	665 ± 10	377 ± 10
Average surface area of a single nanopillar, μm^2	0.313	0.211	0.118
Calculated experimental velocity, nm/s	201	133	75
Calculated surface area, cm^2	15.05	10.28	6.26

In all cases where a high-frequency excitation of 40 kHz was used during the solvent casting method, nanopillared chitosan membranes were obtained. Depending on the concentration of the prepared chitosan solution, nanopillars of different heights were obtained. It can be assumed that the diameter of the nanopillars did not depend on the concentration, and the obtained nanopillar diameters were 100 ± 10 nm in all cases. However, changes in the height of the nanopillars were observed.

To obtain the height of nanopillars as in the theoretical calculations, high frequency was applied for 5 s. Experimental liquid flow velocities were obtained, at 201 nm/s, 133 nm/s and 75 nm/s, respectively, for concentrations of 1 wt%, 2 wt% and 3 wt%. With the experimental velocities of chitosan solutions into the pore and the concentration of the chitosan solution, the heights of the nanopillars could be controlled by high-frequency

excitation. It was experimentally found that high-frequency excitation ensured fluid flow into the nanoporous AAO template, and the heights of the nanopillars could be controlled by changing the concentration of the chitosan solution.

As a result of the changing height of the nanopillars, the surface area of the membrane changed, and the research contributes to the wider application of chitosan membranes as an artificial skin barrier. To develop artificial skin barriers, surface area calculations were performed for the free-standing chitosan membrane with a size of 10×10 mm (Figure 9).

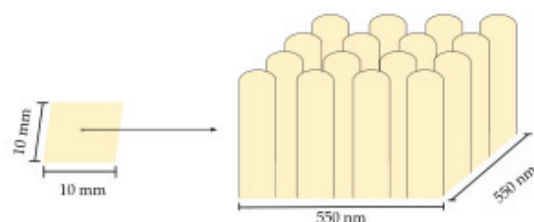


Figure 9. Free-standing chitosan membrane.

According to Formula (1), the surface areas were calculated when the height of the nanopillars was 377, 665 and 1007 nm. In all cases, the area of the original flat surface was 1 cm^2 , the number of nanopillars was $4.4 \cdot 10^9$, and the radius of each nanopillar was 50 nm. Based on the experimental data, the values of the calculated surface area are given in Table 5. Compared to the original flat surface area, the surface area of the nanopillared chitosan membrane could be increased by 6, 10, and 15 times when chitosan solution with different concentrations was poured onto the nanoporous AAO template using a high-frequency excitation of 40 kHz for 5 s.

4. Conclusions

In this study, free-standing nanopillared chitosan membrane was fabricated using the improved solvent casting method on the nanoporous AAO template. The high-frequency excitation of 40 kHz was used during the solvent casting method to improve the flow of liquid into the nanopore. Nanopillared chitosan membranes were successfully fabricated using 1 wt%, 2 wt% and 3 wt% solutions of chitosan in acetic acid. SEM images confirmed the formation of AAO nanopores and chitosan nanopillars. Three types of chitosan membranes were experimentally obtained when the height of the nanopillars was 1007, 665, and 377 nm. From the obtained heights of the nanopillars, according to the surface area formula, the surface areas of the free-standing nanopillared chitosan membranes (with a size of 10×10 mm) were calculated, which were 15.05, 10.28 and 6.26 cm^2 . Compared to the flat membrane surface, the nanopillared surface area was increased by 15, 10, and 6 times. Furthermore, the experimental velocities of chitosan solution into the pore were 201, 133 and 75 nm/s , determined at concentrations of 1 wt%, 2 wt% and 3 wt% chitosan solution, respectively. The experimentally determined liquid flow velocities into the nanopore make it possible to form nanopillars of the desired height, which leads to precise control of the surface area. Due to the easily controlled surface area, these studies contribute to the development of artificial skin barriers for commercial use.

Author Contributions: Conceptualization, U.C.; methodology and investigation U.C. and A.P.; calculation and analysis, U.C. and G.J.; visualization, U.C.; writing—original draft preparation, U.C.; writing—review and editing, A.P. and G.J. All authors have read and agreed to the published version of the manuscript.

Funding: This research received no external funding.

Institutional Review Board Statement: Not applicable.

Informed Consent Statement: Not applicable.

Data Availability Statement: Data sharing is not applicable.

Conflicts of Interest: The authors declare no conflict of interest.

References

- Harris-Tryon, T.A.; Grice, E.A. Microbiota and maintenance of skin barrier function. *Science* **2022**, *376*, 940–945. [CrossRef]
- Zhang, A.; Wang, J.; Wang, B. Bio-thermo-viscoelastic behavior in multilayer skin tissue. *J. Therm. Stress.* **2022**, *45*, 559–575. [CrossRef]
- Priya, S.; Rath, S.N. Chapter 5—Artificial skin: Current advanced methods of fabrication and development. In *Natural Polymers in Wound Healing and Repair*; Sah, M.K., Kasoju, N., Mano, J.F., Eds.; Elsevier: Amsterdam, Netherlands, 2022; pp. 103–128. [CrossRef]
- Peng, W.; Li, D.; Dai, K.; Wang, Y.; Song, P.; Li, H.; Tang, P.; Zhang, Z.; Li, Z.; Zhou, Y.; et al. Recent progress of collagen, chitosan, alginate and other hydrogels in skin repair and wound dressing applications. *Int. J. Biol. Macromol.* **2022**, *208*, 400–408. [CrossRef]
- Ray, P.; Chakraborty, R.; Banik, O.; Banoth, E.; Kumar, P. Surface Engineering of a Bioartificial Membrane for Its Application in Bioengineering Devices. *ACS Omega* **2023**, *8*, 3606–3629. [CrossRef]
- Zheng, X.; Zhang, P.; Fu, Z.; Meng, S.; Dai, L.; Yang, H. Applications of nanomaterials in tissue engineering. *RSC Adv.* **2021**, *11*, 19041. [CrossRef]
- Rane, A.V.; Kanny, K.; Abitha, V.K.; Thomas, S. Chapter 5—Methods for Synthesis of Nanoparticles and Fabrication of Nanocomposites. In *Synthesis of Inorganic Nanomaterials*; Bhagyaraj, S.M., Oluwafemi, O.S., Kalarikkal, N., Thomas, S., Eds.; Elsevier: Amsterdam, Netherlands, 2018; pp. 121–139. [CrossRef]
- Xie, Y.; Kocaepe, D.; Chen, C.; Kocaepe, Y. Review of Research on Template Methods in Preparation of Nanomaterials. *J. Nanomater.* **2016**, *2016*, 2302595. [CrossRef]
- Dixon, D.T.; Gomillion, C.T. Conductive Scaffolds for Bone Tissue Engineering: Current State and Future Outlook. *J. Funct. Biomater.* **2022**, *13*, 1. [CrossRef] [PubMed]
- Lin, H.T.; Venault, A.; Chang, Y. Zwitterionized chitosan based soft membranes for diabetic wound healing. *J. Membr. Sci.* **2019**, *591*, 117319. [CrossRef]
- Han, W.; Ren, J.; Xuan, H.; Ge, L. Controllable degradation rates, antibacterial, free-standing and highly transparent films based on polylactic acid and chitosan. *Colloids Surf. A Physicochem. Eng. Asp.* **2018**, *541*, 128–136. [CrossRef]
- Jiang, Y.; Deng, Y.; Tu, Y.; Ay, B.; Sun, X.; Li, Y.; Wang, X.; Chen, X.; Zhang, L. Chitosan-based asymmetric topological membranes with cell-like features for healthcare applications. *J. Mater. Chem. B* **2019**, *7*, 2634–2642. [CrossRef] [PubMed]
- Jenkins, J.; Mantell, J.; Neal, C.; Gholinia, A.; Verkade, P.; Nobbs, A.H.; Su, B. Antibacterial effects of nanopillar surfaces are mediated by cell impedance, penetration and induction of oxidative stress. *Nat. Commun.* **2020**, *11*, 1626. [CrossRef] [PubMed]
- Valiei, A.; Lin, N.; McKay, G.; Nguyen, D.; Moraes, C.; Hill, R.J.; Tufenkji, N. Surface Wettability Is a Key Feature in the Mechano-Bactericidal Activity of Nanopillars. *ACS Appl. Mater. Interfaces* **2022**, *14*, 27564–27574. [CrossRef] [PubMed]
- Gudur, A.; Ji, H.F. Bio-Applications of Nanopillars. *Front. Nanosci. Nanotechnol.* **2016**, *2*, 1–10. [CrossRef]
- Ngo, T.D.; Kashani, A.; Imbalzano, G.; Nguyen, K.T.Q.; Hui, D. Additive manufacturing (3D printing): A review of materials, methods, applications and challenges. *Compos. Part B Eng.* **2018**, *143*, 172–196. [CrossRef]
- Velu, R.; Calais, T.; Jayakumar, A.; Raspall, F. A Comprehensive Review on Bio-Nanomaterials for Medical Implants and Feasibility Studies on Fabrication of Such Implants by Additive Manufacturing Technique. *Materials* **2020**, *13*, 92. [CrossRef] [PubMed]
- Vakalopoulou, E.; Rath, T.; Warchomicka, F.G.; Carraro, F.; Falcaro, P.; Amenitsch, H.; Trimmel, G. Honeycomb-structured copper indium sulfide thin films obtained via a nanosphere colloidal lithography method. *Mater. Adv.* **2022**, *3*, 2884. [CrossRef]
- Yu, H.M.; Lee, J. Fabrication of nanomaterials using anodic aluminum oxide and their properties. *Curr. Appl. Phys.* **2011**, *11*, S339–S345. [CrossRef]
- Lee, W.; Park, S.J. Porous Anodic Aluminum Oxide: Anodization and Templated Synthesis of Functional Nanostructures. *Chem. Rev.* **2014**, *114*, 7487–7556. [CrossRef]
- Poinern, G.E.J.; Ali, N.; Fawcett, D. Progress in Nano-Engineered Anodic Aluminum Oxide Membrane Development. *Materials* **2011**, *4*, 487–526. [CrossRef]
- Noormohammadi, M.; Arani, Z.S.; Ramazani, A.; Kashi, M.A.; Abbasimofrad, S. Super-fast fabrication of self-ordered nanoporous anodic alumina membranes by ultra-hard anodization. *Electrochim. Acta* **2020**, *354*, 136766. [CrossRef]
- Ruiz-Clavijo, A.; Caballero-Calero, O.; Martín-González, M. Revisiting anodic alumina templates: From fabrication to applications. *Nanoscale* **2021**, *13*, 2227–2265. [CrossRef]
- Manzano, C.V.; Martín, J.; Martín-González, M.S. Ultra-narrow 12 nm pore diameter self-ordered anodic alumina templates. *Microporous Mesoporous Mater.* **2014**, *184*, 177–183. [CrossRef]
- Resende, P.M.; Martín-González, M. Sub-10 nm porous alumina templates to produce sub-10 nm nanowires. *Microporous Mesoporous Mater.* **2019**, *284*, 198–204. [CrossRef]
- Augustine, R.; Rehman, S.R.U.; Ahmed, R.; Zahid, A.A.; Sharifi, M.; Falahati, M.; Hasan, A. Electrospun chitosan membranes containing bioactive and therapeutic agents for enhanced wound healing. *Int. J. Biol. Macromol.* **2020**, *156*, 153–170. [CrossRef]

27. Genesi, B.P.; Barbosa, R.M.; Severino, P.; Rodas, A.C.D.; Yoshida, C.M.P.; Mathor, M.B.; Lopes, P.S.; Viseras, C.; Souto, E.B.; Silva, C.F. Aloe vera and copaiba oleoresin-loaded chitosan films for wound dressings: Microbial permeation, cytotoxicity, and in vivo proof of concept. *Int. J. Pharm.* **2023**, *634*, 122648. [CrossRef]
28. Ji, M.; Li, J.; Wang, Y.; Li, F.; Man, J.; Li, J.; Zhang, C.; Peng, S.; Wang, S. Advances in chitosan-based wound dressings: Modifications, fabrications, applications and prospects. *Carbohydr. Polym.* **2022**, *297*, 120058. [CrossRef]
29. Hamed, H.; Moradi, S.; Hudson, S.M.; Tonelli, A.E.; King, M.W. Chitosan based bioadhesives for biomedical applications: A review. *Carbohydr. Polym.* **2022**, *282*, 119100. [CrossRef]
30. Liu, H.; Wang, C.; Li, C.; Qin, Y.; Wang, Z.; Yang, F.; Li, Z.; Wang, J. A functional chitosan-based hydrogel as a wound dressing and drug delivery system in the treatment of wound healing. *RSC Adv.* **2018**, *8*, 7533. [CrossRef]
31. Tricol Biomedical Inc. Available online: <https://tricolbiomedical.com/product-category/trauma/> (accessed on 2 July 2023).
32. Tang, W.; Wang, J.; Hou, H.; Li, Y.; Wang, J.; Fu, J.; Lu, L.; Gao, D.; Liu, Z.; Zhao, F.; et al. Review: Application of chitosan and its derivatives in medical materials. *Int. J. Biol. Macromol.* **2023**, *240*, 124398. [CrossRef] [PubMed]
33. Herliana, H.; Yusuf, H.Y.; Laviana, A.; Wandawa, G.; Cahyanto, A. Characterization and Analysis of Chitosan-Gelatin Composite-Based Biomaterial Effectivity as Local Hemostatic Agent: A Systematic Review. *Polymers* **2023**, *15*, 575. [CrossRef]
34. Altuntas, S.; Dhaliwal, H.K.; Bassous, N.J.; Radwan, A.E.; Alpaslan, P.; Webster, T.; Buyukserin, F.; Amiji, M. Nanopillared Chitosan/Gelatin Films: A Biomimetic Approach for Improved Osteogenesis. *ACS Biomater. Sci. Eng.* **2019**, *5*, 4311–4322. [CrossRef]
35. De Masi, A.; Tonazzini, I.; Masciullo, C.; Mezzena, R.; Chiellini, F.; Puppi, D.; Cecchini, M. Chitosan films for regenerative medicine: Fabrication methods and mechanical characterization of nanostructured chitosan films. *Biophys. Rev.* **2019**, *11*, 807–815. [CrossRef] [PubMed]
36. Sung, C.Y.; Yang, C.Y.; Chen, W.S.; Wang, Y.K.; Yeh, J.A.; Cheng, C.M. Probing neural cell behaviors through micro-/nano-patterned chitosan substrates. *Biofabrication* **2015**, *7*, 045007. [CrossRef] [PubMed]
37. Altuntas, S.; Dhaliwal, H.K.; Radwan, A.E.; Amiji, M.; Buyukserin, F. Local epidermal growth factor delivery using nanopillared chitosan-gelatin films for melanogenesis and wound healing. *Biomater. Sci.* **2023**, *11*, 181–194. [CrossRef]
38. Cigane, U.; Palevicius, A.; Janusas, G. Vibration-Assisted Synthesis of Nanoporous Anodic Aluminum Oxide (AAO) Membranes. *Micromachines* **2022**, *13*, 2236. [CrossRef]
39. Lei, J.; Cheng, F.; Li, K. Numerical Simulation of Boundary-Driven Acoustic Streaming in Microfluidic Channels with Circular Cross-Sections. *Micromachines* **2020**, *11*, 240. [CrossRef] [PubMed]
40. Peng, T.; Zhou, M.; Yuan, S.; Fan, C.; Jiang, B. Numerical investigation of particle deflection in tilted-angle standing surface acoustic wave microfluidic devices. *Appl. Math. Model.* **2022**, *101*, 517–532. [CrossRef]
41. Qiao, Y.; Zhang, X.; Gong, M.; Wang, H.; Liu, X. Acoustic radiation force and motion of a free cylinder in a viscous fluid with a boundary defined by a plane wave incident at an arbitrary angle. *J. Appl. Phys.* **2020**, *128*, 044902. [CrossRef]
42. Wang, Q.; Riaud, A.; Zhou, J.; Gong, Z.; Baudoin, M. Acoustic Radiation Force on Small Spheres Due to Transient Acoustic Fields. *Phys. Rev. Appl.* **2021**, *15*, 044034. [CrossRef]
43. Basch, T.; Pavlic, A.; Dual, J. Acoustic radiation force acting on a heavy particle in a standing wave can be dominated by the acoustic microstreaming. *Phys. Rev. E* **2019**, *100*, 061102. [CrossRef]
44. Luo, J.; Zhou, Q.; Jin, T. Numerical simulation of nonlinear phenomena in a standing-wave thermoacoustic engine with gas-liquid coupling oscillation. *Appl. Therm. Eng.* **2022**, *207*, 118131. [CrossRef]
45. Das, P.K.; Snider, A.D.; Bhethanabotla, V.R. Acoustic streaming in second-order fluids. *Phys. Fluids* **2020**, *32*, 123103. [CrossRef]
46. Rubio, L.D.; Collins, M.; Sen, A.; Aranson, I.S. Ultrasound Manipulation and Extrusion of Active Nanorods. *Small* **2023**, *2300028*. [CrossRef] [PubMed]
47. COMSOL AB. *Acoustic Streaming in a Microchannel Cross Section*, COMSOL Multiphysics® v. 6.1; COMSOL AB: Stockholm, Sweden, 2023; pp. 2–24.
48. COMSOL AB. *Rising Bubble*, COMSOL Multiphysics® v. 6.1; COMSOL AB: Stockholm, Sweden, 2023; pp. 2–14.

Disclaimer/Publisher's Note: The statements, opinions and data contained in all publications are solely those of the individual author(s) and contributor(s) and not of MDPI and/or the editor(s). MDPI and/or the editor(s) disclaim responsibility for any injury to people or property resulting from any ideas, methods, instructions or products referred to in the content.

CURRICULUM VITAE

Urtė Ciganė

urte.cigane@ktu.edu

Education:

- 2014 – 2018 Bachelor of Engineering Sciences, Kaunas University of Technology, study programme Chemical Technology and Engineering.
- 2018 – 2020 Master of Business Management, Kaunas University of Technology, study programme Innovation Management and Entrepreneurship.
- 2020 – 2024 PhD studies in Mechanical Engineering, Kaunas University of Technology, topic: Development and investigation of technology for the nanostructured membranes fabrication applied in bioengineering.

Work experience:

- 2015 – 2016 Characterization and synthesis of organic semiconductors at KTU Department of Polymer Chemistry and Technology.
- 2016 – 2017 Project of scientific cooperation between Lithuania, Latvia and Taiwan, programme *New materials and technologies for very-high color rendering and high sunlight spectrum resemblance OLED lighting sources*. KTU Department of Polymer Chemistry and Technology, Organic Semiconductor Laboratory (Position: Chief Technician of the Project).
- 2016 – 2017 Project of scientific group *New Structure Hole Transporting for Enlargement Efficiency of Organic Light Emitting Diodes (OLEDSEMI)*. KTU Department of Polymer Chemistry and Technology, Organic Semiconductor Laboratory (Position: Project Technician).
- 2017 – 2018 Project of scientific group *New Structure Electroactive Materials for Efficient Phosphorescent Organic Light Emitting Diodes (E-MATERIALS)*. KTU Department of Polymer Chemistry and Technology, Organic Semiconductor Laboratory (Position: Chief Technician of the Project).
- 2019 – 2020 Project *Formation, investigation and application of structured nano-composites for nano/micro bioparticles analysis and manipulation*. KTU Department of Mechanical Engineering (Position: laboratory assistant).
- 2020 – 2023 Project *Development of new technologies for the formation of microstructures in functional materials*. KTU Department of Mechanical Engineering (Position: Project Junior Researcher).

ARTICLES IN PEER-REVIEWED SCIENTIFIC PUBLICATIONS

In journals indexed in the Web of Science with Impact Factor (JCR SCIE), when IF/AIF > 0.25

Foreign publishers

- [A1] **Ciganė, Urtė**; Palevičius, Arvydas; Janušas, Giedrius. Review of nanomembranes: materials, fabrications and applications in tissue engineering (bone and skin) and drug delivery systems // *Journal of Materials Science*. New York: Springer. ISSN 0022-2461. eISSN 1573-4803. 2021, vol. 56, iss. 24, p. 13479-13498. DOI: 10.1007/s10853-021-06164-x. [Science Citation Index Expanded (Web of Science); Scopus] [IF: 4.682; AIF: 6.504; IF/AIF: 0.719; Q2 (2021, InCites JCR SCIE)]
- [A2] **Cigane, Urte**; Palevicius, Arvydas; Jurenas, Vytautas; Pilkauskas, Kestutis; Janusas, Giedrius. Development and analysis of electrochemical reactor with vibrating functional element for AAO nanoporous membranes fabrication // *Sensors*. Basel: MDPI. ISSN 1424-8220. 2022, vol. 22, iss. 22, art. no. 8856, p. 1-14. DOI: 10.3390/s22228856. [Science Citation Index Expanded (Web of Science); Scopus; MEDLINE] [IF: 3,900; AIF: 4,333; IF/AIF: 0,900; Q2 (2022, InCites JCR SCIE)]
- [A3] **Cigane, Urte**; Palevicius, Arvydas; Janusas, Giedrius. Vibration-assisted synthesis of nanoporous anodic aluminum oxide (AAO) membranes // *Micromachines*. Basel: MDPI. ISSN 2072-666X. 2022, vol. 13, iss. 12, art. no. 2236, p. 1-13. DOI: 10.3390/mi13122236. [Science Citation Index Expanded (Web of Science); Scopus; MEDLINE] [IF: 3,400; AIF: 5,700; IF/AIF: 0,596; Q2 (2022, InCites JCR SCIE)]
- [A4] **Cigane, Urte**; Palevicius, Arvydas; Janusas, Giedrius. A free-standing chitosan membrane prepared by the vibration-assisted solvent casting method // *Micromachines*. Basel: MDPI. ISSN 2072-666X. 2023, vol. 14, iss. 7, art. no. 1419, p. 1-13. DOI: 10.3390/mi14071419. [Science Citation Index Expanded (Web of Science); Scopus; MEDLINE] [IF: 3,400; AIF: 5,700; IF/AIF: 0,596; Q2 (2022, InCites JCR SCIE)]

In peer-reviewed scientific publications refereed in other international databases

Foreign publishers

- [B1] **Cigane, Urte**; Palevicius, Arvydas. Electrochemical reactor with an ultrasonic piezoelectric ceramic transducer for manufacturing nanoporous aluminum oxide membrane // 2022 IEEE 18th international conference on the perspective technologies and methods in MEMS design (MEMSTECH), Polyana, Ukraine, September 7-11, 2022: proceedings. Piscataway, NJ: IEEE, 2022. ISBN 9798350396812. eISBN 9798350396805. ISSN 2573-5357. eISSN 2573-5373. p. 7-10. DOI: 10.1109/MEMSTECH55132.2022.10002918. [Scopus]

- [B2] **Ciganė, Urtė**; Palevičius, Arvydas. Design of electrochemical reactor for manufacturing aluminum oxide nanoporous membrane // 2021 IEEE XVII international conference on the perspective technologies and methods in MEMS design (MEMSTECH), Polyana, May 12–16, 2021: proceedings. Piscataway, NJ: IEEE, 2021. ISBN 9781665424110. eISBN 9781665424103. ISSN 2573-5357. p. 50-53. DOI: 10.1109/MEMSTECH53091.2021.9467913. [Scopus; INSPEC]

In other peer-reviewed scientific publications

Lithuanian publishers

- [B3] **Cigane, Urte**; Naginevicius, Vytenis. The effect of applied vibrations on structural features and wettability of nanopores of anodic alumina oxide formed by twostep anodization process // *Mechanika 2023: proceedings of the 27th international scientific conference*, 26 May 2023, Kaunas University of Technology, Lithuania: proceedings. Kaunas: Kaunas University of Technology. ISSN 2783-5677. 2023, p. 92-95.

PRESENTATION OF RESEARCH RESULTS AT CONFERENCES

Other conference presentation abstracts and non-peer reviewed conference papers

- [C1] **Cigane, Urte**; Palevicius, Arvydas. Study of the Effect of Vibration on Fluid Flow in Aluminum Oxide Nanopores // *Open Readings 2023: 66th international conference for students of physics and natural sciences*, April 18–21, 2023, Vilnius, Lithuania: annual abstract book / editors: M. Keršys, Š. Mickus. Vilnius: Vilnius University Press, 2023. ISBN 9786090708835. p. 207.
- [C2] **Cigane, U.**; Palevicius, A.; Janusas, G. Vibration Application for Porous AAO Membrane Synthesis // *Chemistry and Chemical Technology: international conference CCT-2023*, March 10, 2023, Vilnius: conference book. Vilnius: Vilnius University Press, 2023, P 016. ISBN 9786090708330. p. 53.
- [C3] **Cigane, Urte**; Palevicius, Arvydas. Effects of the Voltage and Temperature of Anodization on Pore Geometry of Anodic Aluminum Oxide (AAO) membranes // *Advanced composites and applications: 81st international scientific conference of the University of Latvia*, February 16, 2023: book of abstracts. Riga: University of Latvia. 2023, p. 16.
- [C4] **Cigane, Urte**; Palevicius, Arvydas. Analysis of AAO Membranes Manufactured by Applying Vibration in Electrochemical Reactor // *IRWBM 2022: 3rd International Research Workshop in Biomechanical Microsystems 2022*: October 21, 2022, Kaunas University of Technology, Lithuania: program and abstracts. Kaunas: Kaunas University of Technology. 2022, p. 13.
- [C5] **Ciganė, Urtė**; Palevičius, Arvydas; Janušas, Giedrius. Vibro-Electrochemical Reactor for the Fabrication of AAO Nanoporous Membranes // *Technorama 2022: Code: innovation: catalogue*. Kaunas: KTU. 2022, p. 47–48.

- [C6] **Cigane, Urte**; Palevicius, Arvydas. Development of an Electrochemical Reactor for the Fabrication of Nanoporous AAO Membranes // Open Readings 2022: 65th International Conference for Students of Physics and Natural Sciences, March 15–18: abstract book / editors: Š. Mickus, S. Pūkienė, L. Naimovičius. Vilnius: Vilnius University Press. 2022, P2-8, p. 169.
- [C7] **Ciganė, Urtė**. Review of Recent Research on Nanomembranes in Bioengineering // IRWBM 2021: 2nd International Research Workshop in Biomechanical Microsystems 2021: October 22, 2021, Kaunas University of Technology, Lithuania: Program and Abstracts. Kaunas: Kaunas University of Technology. 2021, p. 15.
- [C8] **Ciganė, Urtė**; Palevičius, Arvydas. Research and Development of Innovative Functional Nanomembranes in Bioengineering // Open Readings 2021: 64th International Conference for Students of Physics and Natural Sciences, March 16–19, Vilnius, Lithuania: Abstract Book / editors: Š. Mickus, R. Platakytė, S. Pūkienė. Vilnius: Vilnius University Press, 2021, P2-27. ISBN 9786090705902. p. 196.

ACKNOWLEDGMENTS

I would like to acknowledge the enthusiastic and encouraging supervision of Prof. Dr. Hab. Arvydas Palevičius who has provided invaluable counseling on the thesis and has shown immense confidence in me. Your motivation, encouragement, and support have been very valuable and inspiring. I am glad I had the opportunity to work with you.

I would like to thank Prof. Dr. Vytautas Jūrėnas for his support, professional comments, and valuable remarks.

I owe a special thanks to Prof. Dr. Giedrius Janušas for his technical support, guidance, and advice to achieve the experimental goals. It was a pleasure to work with you on projects.

I am also grateful for Dr. Joris Vėžys, Dr. Tomas Simonaitis, PhD student Ieva Markūnienė for contributing to the measurements and Dr. Simona Tučkutė for contributing to the SEM studies.

I would like to thank the Research Council of Lithuania and Kaunas University of Technology for providing the funding and giving me the opportunity to attend conferences.

My gratitude extends to all the staff of the Faculty of Mechanical Engineering and Design and Doctoral School for their help during my studies.

Finally, I would like to thank my family, who has always been by my side, encouraged and supported me. I dedicate this little achievement to my children.

APPENDIX

Appendix 1. Copy of the Protocol 2023-06-22 No. ST16-T009-12

**MECHANIKOS INŽINERIJOS MOKSLO KRYPTIES
KAUNO TECHNOLOGIJOS UNIVERSITETO IR
VYTAUTO DIDŽIOJO UNIVERSITETO ŽŪA
BENDROS DOKTORANTŪROS KOMITETO
POSĖDŽIO PROTOKOLAS**

2023-06-22 Nr. ST16-T009-12

Kaunas

Posėdis įvyko 2023-06-22, 10:00 val., 109 kab.

Posėdžio pirmininkas – prof., habil. dr. Vytautas Ostaševičius

Posėdžio sekretorius – prof., dr. Regita Bendikienė

Dalyvavo:

prof., habil. dr. Arvydas Palevičius
prof., dr. Vytenis Jankauskas
prof., dr. Juozas Padgurskas
prof., vyr. m. d. dr. Vytautas Jūrėnas
prof., dr. Rimvydas Gaidys
prof., dr. Giedrius Janušas
vyr. m. d., dr. Gintautas Dundulis
vyr. m. d., dr. Rolanas Daukševičius

Posėdyje dalyvavo 10 narių iš 11 narių (kvorumas – 2/3).

DARBOTVARKĖ:

1. Mechanikos inžinerijos mokslo krypties 1-o kurso doktorantų atestacija už 2022/2023 m. m. pavasario semestrą.
2. Mechanikos inžinerijos mokslo krypties 2-o kurso doktorantų atestacija už 2022/2023 m. m. pavasario semestrą.
3. Mechanikos inžinerijos mokslo krypties 3-o kurso doktorantų atestacija už 2022/2023 m. m. pavasario semestrą.
4. Mechanikos inžinerijos mokslo krypties 4-o kurso doktorantų atestacija už 2022/2023 m. m. pavasario semestrą.

<...>

3. SVARSTYTA. III-o kurso KTU doktorantų: Pauliaus Skėrio, Tomo Vaitkūno, Justo Cigano, Vaidoto Gudžiūno, Urtės Ciganės individualūs studijų planai ir daktaro disertacijos rengimo etapai.

Doktorantai pristatė parengtas skaidres apie atliktus darbus per 2022/2023 m. m. pavasario semestrą ir planus kitiems metams, atsakė į užduotus klausimus.

Doktorantė Urtė Ciganė pateikė prašymą dėl jos publikacijos „Review of nanomembranes: materials, fabrications and applications in tissue engineering (bone and skin) and drug delivery systems“ paskelbta 2021 gegužės 20 dieną Springer leidyklos „Journal of Materials Science“ žurnale (Nuoroda į publikaciją: <https://link.springer.com/article/10.1007/s10853-021-06164-x>), kuris priskiriamas kvartilui Q2 (Cituojamumo rodiklis IF= 4,682) pripažinimo tinkama ir kad galėtų ją naudoti kaip vieną iš publikacijų rašant disertaciją mokslinių straipsnių pagrindu.

NUTARTA:

3.1. Pritarti, jog publikacija „Review of nanomembranes: materials, fabrications and applications in tissue engineering (bone and skin) and drug delivery systems“ paskelbta 2021 gegužės 20 dieną Springer leidyklos „Journal of Materials Science“ žurnale, kuris priskiriamas kvartilui Q2 (Cituojamumo rodiklis IF= 4,682, publikacijos kopija priede) yra tinkama ir gali būti naudojama kaip viena iš publikacijų rašant disertaciją mokslinių straipsnių pagrindu (kaip tai nurodyta Kauno technologijos universiteto Senato 2020 m. lapkričio 30 d. nutarimo Nr. V3-S-37 KTU mokslo doktorantūros reglamento 61 p.).

<...>

Posėdžio pirmininkas

Vytautas Ostaševičius

Posėdžio sekretorius

Regita Bendikienė

Išrašas tikras:
Mechanikos inžinerijos mokslo krypties
KTU ir VDU ŽŪA bendros doktorantūros
komiteto sekretorė

2023-10-23

prof., dr. Regita Bendikienė

Appendix 2. Copy of the Protocol 2023-09-22 No. ST16-T009-14

**MECHANIKOS INŽINERIJOS MOKSLO KRYPTIES
KAUNO TECHNOLOGIJOS UNIVERSITETO IR
VYTAUTO DIDŽIOJO UNIVERSITETO ŽŪA
BENDROS DOKTORANTŪROS KOMITETO
ELEKTRONINIO POSĖDŽIO PROTOKOLAS**

**2023-09-22 Nr. ST16-T009-14
Kaunas**

Elektroninis posėdis vyko nuo 2023-09-18 12:00 val. iki 2023-09-22 12:00 val.

Posėdžio pirmininkas – prof., habil. dr. Vytautas Ostaševičius

Posėdžio sekretorius – doc., dr. Regita Bendikienė

Dalyvavo: prof., habil. dr. Rimvydas Barauskas
prof., habil. dr. Arvydas Palevičius
prof., dr. Rimvydas Gaidys
prof., dr. Vytenis Jankauskas
prof., dr. Juozas Padgurskas
prof., vyr. m. d. dr. Vytautas Jūrėnas
prof., dr. Giedrius Janušas
vyr. m. d., dr. Gintautas Dundulis
vyr. m. d., dr. Rolanas Daukševičius

Elektroniniu būdu praveistame posėdyje dalyvavo 11 narių iš 11 (kvorumas – 2/3).

ELEKTRONINIAM BALSAVIMUI PATEIKTAS KLAUSIMAS.

IV kurso doktorantės Urtės Ciganės pateiktas prašymas apsvarstyti ir pripažinti tinkamomis jos publikacijas, kad galėtų jas naudoti kaip vienas iš publikacijų rašant disertaciją mokslinių straipsnių pagrindu.

SVARSTYTA. Doktorantės Urtės Ciganės pateiktas prašymas dėl jos publikacijų pripažinimo tinkamomis, kad galėtų jas naudoti kaip vienas iš publikacijų rašant disertaciją mokslinių straipsnių pagrindu.

Doktorantė Urtė Ciganė pateikė prašymą dėl jos publikacijų:

1. Cigane, Urte; Palevicius, Arvydas; Jurenas, Vytautas; Pilkauskas, Kestutis; Janusas, Giedrius.
Development and analysis of electrochemical reactor with vibrating functional element for AAO

nanoporous membranes fabrication // Sensors. Basel : MDPI. ISSN 1424-8220. 2022, vol. 22, iss. 22, art. no. 8856, p. 1-14. Impact factor 3,900, Q2.

2. Cigane, Urte; Palevicius, Arvydas; Janusas, Giedrius. Vibration-assisted synthesis of nanoporous anodic aluminum oxide (AAO) membranes // Micromachines. Basel : MDPI. ISSN 2072-666X. 2022, vol. 13, iss. 12, art. no. 2236, p. 1-13. Impact factor 3,400, Q2.

3. Cigane, Urte; Palevicius, Arvydas; Janusas, Giedrius. A free-standing chitosan membrane prepared by the vibration-assisted solvent casting method // Micromachines. Basel : MDPI. ISSN 2072-666X. 2023, vol. 14, iss. 7, art. no. 1419, p. 1-13. Impact factor 3,400, Q2.

pripažinimo tinkamomis, kad galėtų jas naudoti kaip vienas iš publikacijų rašant disertaciją mokslinių straipsnių pagrindu.

Dėl doktorantės prašymo balsuota el. būdu.

Elektroninio balsavimo rezultatai: pritariu – 11, nepritariu – 0, susilaikau – 0.

NUTARTA. Pritarti, jog publikacijos:

1. Cigane, Urte; Palevicius, Arvydas; Jurenas, Vytautas; Pilkauskas, Kestutis; Janusas, Giedrius. Development and analysis of electrochemical reactor with vibrating functional element for AAO nanoporous membranes fabrication // Sensors. Basel : MDPI. ISSN 1424-8220. 2022, vol. 22, iss. 22, art. no. 8856, p. 1-14. Impact factor 3,900, Q2.

2. Cigane, Urte; Palevicius, Arvydas; Janusas, Giedrius. Vibration-assisted synthesis of nanoporous anodic aluminum oxide (AAO) membranes // Micromachines. Basel : MDPI. ISSN 2072-666X. 2022, vol. 13, iss. 12, art. no. 2236, p. 1-13. Impact factor 3,400, Q2.

3. Cigane, Urte; Palevicius, Arvydas; Janusas, Giedrius. A free-standing chitosan membrane prepared by the vibration-assisted solvent casting method // Micromachines. Basel : MDPI. ISSN 2072-666X. 2023, vol. 14, iss. 7, art. no. 1419, p. 1-13. Impact factor 3,400, Q2.

yra tinkamos ir gali būti naudojamos kaip vienos iš publikacijų, rašant disertaciją mokslinių straipsnių pagrindu (kaip tai nurodyta Kauno technologijos universiteto Senato 2020 m. lapkričio 30 d. nutarimo Nr. V3-S-38 KTU mokslo doktorantūros reglamento VII skyriaus, 63 dalyje).

Posėdžio pirmininkas



Vytautas Ostaševičius

Posėdžio sekretorius



Regita Bendikienė

UDK 620.3+66.081.6+615.46](043.3)

SL344. 2024-03-25, 15 leidyb. apsk. 1. Tiražas 14 egz. Užsakymas 41.
Išleido Kauno technologijos universitetas, K. Donelaičio g. 73, 44249 Kaunas
Spausdino leidyklos „Technologija“ spaustuvė, Studentų g. 54, 51424 Kaunas

